Journal of the
OPTICAL SOCIETY
of AMERICA

VOLUME 37, NUMBER 8 AUGUST, 1947

Transmission Measurements with the Beckman Quartz Spectrophotometer

KASSON S. GIBSON AND MARGARET M. BALCOM
National Bureau of Standards, Washington 25, D. C.

(Received March 31, 1947)

The Beckman quartz photoelectric spectrophotometer, covering the wave-length range from about 200 to 1200 millimicrons is proving of great utility in spectral transmission and absorption measurements. Essential features of the instrument are described, including a constant-temperature inclosure (for samples) designed and constructed at the Bureau. Various instrumental characteristics are noted and possible errors discussed, particularly those that may be present in the measurement of polarizing samples. Wave-length calibrations are shown for two instruments. A detailed over-all check of the reliability of data obtained on the Beckman spectrophotometer by means of glass standards of spectral transmittance shows it to give results over the wave-length range from 390 to 750 mμ fully as reliable as those obtained with our other spectrophotometers, if various precautions are taken.

TABLE OF CONTENTS

1. Introduction
2. Description and Operation of the Instrument
   Constant-Temperature Inclosure
   Multiple Reflections
   Stray Spectral Energy
   Measurement of Fluorescent Samples
3. Other Instrumental Characteristics
   Spectral-Response Curves
   Polarization Effects
   Spectral Purity Data
4. Wave-Length Calibration
5. Check of the Photometric Scale
6. Conclusions

1. INTRODUCTION

IN a standardization and testing institution such as the National Bureau of Standards it is essential that every means be taken to insure accuracy of results. It is further desirable that many different methods and instruments be available to handle the wide variety of testing submitted.

This is true in spectrophotometry as in other fields. Spectrophotometers are subject to many annoying and hard to detect errors. One can have a good instrument, make a careful wave-length calibration, reduce stray light to negligible proportions, reduce the slit widths or use homogeneous radiant energy, test the photometric scale, and control the temperature of the instrument or the sample. In this and other ways one may believe that the results obtainable over the better part of the appropriate wave-length range are highly accurate. One may also do this with other instruments of different type, covering the wave-length range in which he is interested.

One may then carefully measure the spectral transmittance[1] of a glass on each instrument but

[1] The terms *spectral transmittance* (T) and *spectral transmittancy* (T_s) are used as defined in the OSA Colorimetry Committee Report (J. Opt. Soc. Am. **34**, 183 (1944)). *Spectral transmittance* (pp. 184, 188) is thus the ratio of transmitted to incident radiant flux, evaluated for a particular wave-length of incident energy. In the present paper

find that the results do not agree to the expected extent. One may or may not have the time or otherwise be able to eliminate the discrepancy. For this reason it is advisable to have several different types of instruments on hand, especially if one is issuing spectrophotometric standards to other laboratories to check the performance of their instruments, or is otherwise interested in finding with the greatest certainty the true values of transmittance at the specified wave-lengths.

With respect to the wide variety of work submitted, transmission values may range from unity down to a few hundredths of one percent (for example, welding glasses or filters for viewing searchlights), and these values may be desired to two or three significant figures. Also, the wave-length ranges of all spectrophotometers are limited and values obtained near the ends of these ranges are usually of lowered reliability. Furthermore, most spectrophotometers are designed primarily for special purposes and will handle adequately only a limited variety of testing.

For reasons such as these the Photometry and Colorimetry Section of the National Bureau of Standards maintains several types of spectrophotometer which have been developed or purchased over a period of years. The development or operation of these have been described in numerous publications listed in NBS letter circulars LC 398, 628, and 789, and reference to some of these is made later in the paper.

Two of the Beckman quartz spectrophotometers have been obtained by the Photometry and Colorimetry Section, one in 1943 and one in 1945. These were not obtained for the purpose of "testing" the instruments but to assist in the heavy standardization and testing work of the section during war times. Complete study of the instruments has accordingly not been made, but sufficient information on their calibration and operation has been obtained to be of interest and value to others, as was true earlier with the General Electric recording spectrophotometer.[2]

The scope of the present paper is limited mostly to transmission measurements, although much of the information obtained is equally useful in reflection work. Furthermore, only the optics of the measurements are considered as little study has been made of the electrical circuits of the Beckman spectrophotometer. A few of the points noted were briefly considered in a recent publication.[3]

FIG. 1. Optics of the Beckman spectrophotometer. This is a reproduction of Fig. 3 of the paper by Cary and Beckman published in J. Opt. Soc. Am. **31**, 682 (1941).

2. DESCRIPTION AND OPERATION OF THE INSTRUMENT

The Beckman spectrophotometer has been discussed in some detail in a paper by Cary and Beckman.[4] In that paper questions of design, stray radiant energy, photo-tube sensitivity, electrical circuits, and slit widths are considered and illustrated. Figure 1 of the present paper is a reproduction of Fig. 3 of the paper by Cary and Beckman.

Radiant energy from an incandescent lamp or other illuminant, *A*, is focused on the slit, *D*, by means of the concave mirror, *B*, and the plane mirror, *C*. The beam entering the slit is collimated by the mirror, *E*, and passes through the quartz prism to the reflecting surface, *F*. After reflection at *F* the beam returns along nearly the same path to the same slit, *D*, where it emerges slightly above the entrance beam and the mirror, *C*. After passage through the sample or sample compartment, *G*, the beam is incident on the phototube, *H*.

it is often abbreviated simply to transmittance. *Spectral transmittancy* (p. 189) is the ratio of the transmittance of a solution to that of the solvent in equivalent thickness, again evaluated for a particular wave-length. It can be measured if the solution and solvent are placed in identical absorption cells.

Consistent with the above, the word *transmission* has been discontinued as a specific term, along with many other words ending in *ion*. As an adjective, however, the word is often useful when it is desired *not* to be specific. For example, in the present paper, the word transmission is used where the statement being made would apply both to the measurement of transmittance and to the measurement of transmittancy.

[2] Kasson S. Gibson and Harry J. Keegan, "Calibration and operation of the General Electric recording spectrophotometer of the National Bureau of Standards," J. Opt. Soc. Am. **28**, 372 (1938).

[3] Kasson S. Gibson, "Spectrophotometers," Proc. A.S.T.M. **44**, 725 (1944).

[4] H. H. Cary and Arnold O. Beckman, "A quartz photoelectric spectrophotometer," J. Opt. Soc. Am. **31**, 682 (1941).

Two photo-tubes are supplied installed in the instrument; either may be inserted in the beam at will. One is a "caesium oxide" photo-tube ("red sensitive") for use primarily in the range from 620 mμ to 1200 mμ. The other is a special "caesium antimony" photo-tube ("blue sensitive") for use primarily below 620 mμ. If incandescent lamp and common glass photo-tube are used, this range terminates at about 320 mμ. If the tube has an envelope of Corning 9740 glass, and if a hydrogen lamp with a window of the same type of glass is used as source (all supplied with the instrument when desired), the range extends to about 210 mμ.

The photometric scale is based on electrical rather than optical principles. The photoelectric current from the irradiated cell produces across the photo-tube load resistor a voltage drop which is balanced by a potentiometer. While this null setting is being made any imbalance is amplified electronically and is indicated by a milliammeter on the instrument. Accuracy of the photometric scale depends among other things on conformity of the photo-tube load resister to Ohm's law, and on the linearity of the irradiation-current relationship. Since vacuum photo-tubes are used, the relation should hold closely. We are informed that linearity is still further assured by the use of a frame-type anode in the photo-tubes.

In general, three readings are necessary to make a transmission determination at any wave-length: (1) The zero reading, in which the beam is blocked from the photo-tube by an "off" shutter and the galvanometer is brought to balance by a "dark-current" adjustor, (2) the 100 percent reading, in which the beam falls on the photo-tube after passing through the transmission standard (blank beam, solvent cell, or standard glass) and the milliammeter is brought to balance by adjusting the slit width or the "sensitivity" adjustor, and (3) the transmission reading, in which the unknown or test sample is placed in the beam and the galvanometer is brought to balance by turning the potentiometer dial carrying the "transmission" or "density"[5] scale. The 100 percent reading may be made either by setting the dial to 100.0 or, more conveniently, by setting a selector switch to "check." This switch is then set to "1" for the transmission reading, or to "0.1" if it is desired to read transmission values between zero and 0.10 on a "×10" scale. Unless the transmission values are low (below 0.10), the zero reading does not usually have to be checked at every wave-length.

[5] The words "transmission" and "density" are engraved on the dial on which the scales are carried. By density in this case is meant the negative logarithm of transmittance or transmittancy.

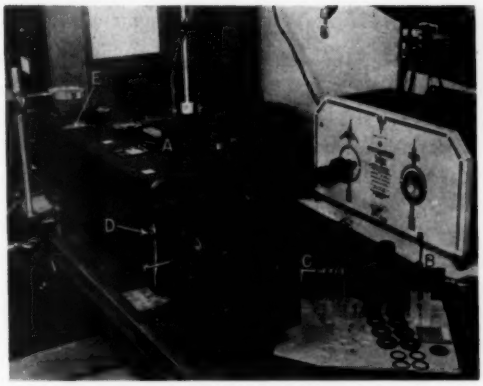

FIG. 2. The Beckman spectrophotometer and various auxiliary equipment as installed and used in the Photometry and Colorimetry Section of the National Bureau of Standards. See text for explanation.

The instrument is designed primarily to measure the transmittancy T_s (or $-\log_{10}T_s$) of solutions relative to solvent in a 1-cm thickness, and a holder is supplied for carrying the 1-cm cells furnished with the instrument, as well as shorter cells which are also available. To measure the transmittance of glasses, it was necessary to construct a special holder which would fit into the shifting platform. The glass can thus be readily moved in and out of the beam. Samples up to about 2 inches square can be accommodated.

To handle solutions up to 10 cm in thickness the manufacturers supply an alternative sample chamber which may be placed between the instrument slit and the photo-tube compartment. They also supply absorption cells of 2, 5, and 10-cm length with adjustable holder. This auxiliary equipment was purchased with the first Beckman spectrophotometer, but for reasons of convenience the carrier has been replaced by a constant-temperature inclosure of our own design, which will accommodate the absorption cells used with our König-Martens and Gibson spectrophotometers.

Constant-Temperature Inclosure

This constant-temperature inclosure is somewhat similar to those used on these other spectrophotometers. The outside dimensions were necessarily smaller, however, since it had to fit light-tight into the sample chamber which is supplied with the Beckman instrument.

A photograph of this holder is shown in Fig. 2, along with various other accessories related to the instrument or the measurements. The temperature of the holder, *A*, is kept constant at 25°C or other desired temperature by means of water pumped through it from a constant-temperature bath. The temperature of the water in the holder is indicated by the thermometer shown, the bulb of which is placed inside between the two cell compartments.

The absorption cell parts are shown beside the instrument. These cells are 1, 2, 4, or 10 cm in length. They have been described in detail in previous publications.[6] Inside, they consist of glass tubes with separate glass or quartz end plates held on by the brass caps. The cells are thus easily taken apart for cleaning.

The diameter of the openings in the constant-temperature inclosure is about 30 mm, just large enough to hold the absorption cells shown and also the glass standards of spectral transmittance which the National Bureau of Standards issues. Other samples such as 2-inch squares of glass or plastic can be mounted on the outside of the holder, resting on the platform and held in place by a spring finger.

This means of temperature control is considered adequate for the purpose. This purpose is primarily to hold the samples at some specified temperature within room-temperature range. In Washington these room temperatures may vary from less than 20°C in the winter to about 35°C in the summer, and such variations may have important effects on transmission values. An additional reason for the temperature control is that the lamp sources on the Beckman spectrophotometer are closely adjacent to the sample compartment, and without the control the whole inclosure (with samples) slowly heats up during extended measurements.

While this means of temperature control is primarily for maintenance at 25°C, it is also considered adequate for maintaining the absorption cells and 30-mm glass standards at temperatures from about 25°C up to 55°C, and has often been so used.

Certain other points of interest may be noted in Fig. 2. At *B* is the holder for glass samples to which reference has already been made, used when temperature control of the sample is unnecessary. At *C* is the 4-compartment solution-cell holder supplied with the instrument. At *D* is the slide carrying the stray-energy filter, supplied with the instrument.

At *E* is an auxiliary indicator line which the authors have added above the wave-length scale of the instrument. The use of a single indicator line, as installed in the instrument, results in parallax and consequent uncertainties of wave-length setting larger than desired. A slide rule indicator glass fits nicely into the space, and was cemented onto the instrument glass with the black line up. The two fine lines thus presented greatly increase the precision of wave-length settings.

Multiple Reflections

Certain other points regarding the instrument and its operation may be noted. On the first instrument both slits were covered with plane quartz plates to keep out dust and fumes. However, the normal divergence of the exit beam prevented accurate measurements with 10-cm cells, the beam hitting the sides of the cell near the far end. To remedy this the authors had the quartz plate over the exit slit changed to a lens of 30-cm focal length which rendered the beam more or less "parallel" and made it possible to use cell lengths up to 10 cm. On the second instrument the quartz plate over the exit slit had been replaced by this type of lens when received.

On both instruments the authors have placed this lens in the sliding piece carrying the stray-energy filter, so that it can be moved in or out at will, and have left no plate or lens over the exit slit. This is to avoid the slight multiple-reflection error obtained with the quartz plate or lens in use when a glass sample is measured relative to a

[6] K. S. Gibson, H. J. McNicholas, E. P. T. Tyndall, M. K. Frehafer, and W. E. Mathewson, "The spectral transmissive properties of dyes . . . ," Nat. Bur. Stand. Sci. Paper No. 440 (1922). Also described in RP 30, reference below.

blank beam. For a non-absorbing glass sample of index 1.7, the error in T, by measurement, amounts to about one percent, the value obtained being too high. When solutions are measured relative to solvents in similar cells, or when one glass is measured relative to another, this effect is usually of negligible importance.

Further troubles originating in the quartz plates are discussed below.

Stray Spectral Energy

Stray light can readily be perceived by looking directly into the exit slit of the instrument at a region of low luminosity—for example, below 450 or above 700 mμ. Likewise, in the spectral regions to which the photo-tubes are relatively insensitive, stray energy from the rest of the spectrum may be present in important amounts. It should be noted that, with the usual type of caesium-oxide photo-tube, the response obtained from 1200 to 2000 mμ on the Beckman spectrophotometer is produced almost entirely by stray energy. Enormous errors may be obtained if the instrument is used at scale settings nominally in this region.

One stray-energy filter is supplied with each instrument, as already indicated. This is a dense purple glass transmitting the ultraviolet freely and absorbing the visible strongly and, as recommended, should always be used when measurements with the incandescent source are being made below 400 mμ. A similar (blue) filter for the region from 400 to 500 mμ is advantageous for some work. In this region erroneous values of transmittance from 0.001 to 0.005 may be obtained with non-fluorescent yellow selenium glasses whose true transmittance is known to be 0.

This example shows that the importance of stray energy depends not only on the spectral region but also on the type of glass or solution being measured. This is further mentioned below in connection with the measurements made on the cobalt blue spectrophotometric standard. Additional slides have been purchased for holding stray-energy filters of varying type which may be inserted at will in the instruments.

To avoid multiple-reflection errors the stray-energy filter should be mounted with surfaces inclined somewhat to the plane of the sample being measured.

Measurement of Fluorescent Samples

In spectrophotometers where the radiant energy is dispersed before incidence upon the sample, an error of measurement may occur with fluorescent samples. For example, if energy of wave-length 550 mμ excites reddish fluorescence, this fluorescent energy is incident directly upon the photo-tube and adds to the photo-current excited by the normally transmitted or reflected energy at 550 mμ. The magnitude of this error depends on the ratio of fluorescent to incident energy and on the relative sensitivity of the photo-tube to the incident and the fluorescent energy.

The error is apparently never very large in transmission measurements because the fluorescent energy is emitted throughout the whole spherical solid angle and only a small fraction of it is incident upon the photo-tube. If of importance, it can be reduced by placing the sample as far from the photo-cell as possible and by use of selective filters which transmit the incident energy freely and absorb the fluorescent energy strongly. The error is of much greater importance in the spectral reflection measurement of diffusing samples because here the angle of the fluorescent energy accepted for measurement bears the same ratio to the full hemispherical angle as does the reflected spectral energy itself.

3. OTHER INSTRUMENTAL CHARACTERISTICS

A matter of interest and importance in the use of any spectrophotometer is the relative spectral response of the receptor and the spectral purity of the radiant energy transmitted by the exit slit under normal working conditions. The former is of importance in connection with study or elimination of errors resulting from stray energy, and the latter is of importance (along with other factors) in any consideration of the absolute accuracy of spectral-transmission measurements.

Information on both of these points is given in the paper by Cary and Beckman. In their Fig. 4 the relative photo-currents for nominal band widths of 3 millimicrons are illustrated, and in their Fig. 9 are given the minimum spectral band widths which permit scale readings to 0.1

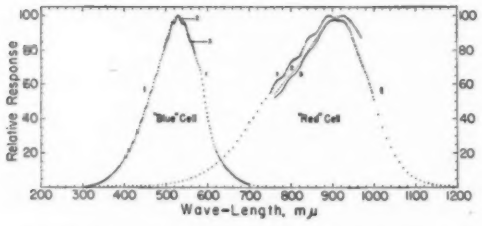

FIG. 3. Spectral-response curves of photo-tubes in a Beckman spectrophotometer. These are as obtained, relative to 100.0 at the respective maxima, for constant mechanical slit widths, and with no corrections for energy distribution of source, dispersion of spectrometer, or other factors affecting the selectivity. For explanation, see text.

percent. For our purposes it was desired to know the relative spectral response of each photo-tube when the slits are kept at a constant mechanical width, and to determine the spectral band widths transmitted by the exit slit over the whole wave-length range under normal working conditions; the latter amounts to a check of Cary and Beckman's Fig. 9 for our instruments.

Spectral-Response Curves

The relative response curves were obtained for each photo-tube with the incandescent illuminant in normal operation. With the selector dial set at "1" the slits were adjusted to give a reading of 100.0 at the wave-length of maximum response for each cell. Readings on the photometric scale were then made at the various wave-lengths through the spectrum, continual check (and slight adjustment if necessary) being made to keep all readings truly relative to 100.0 at the respective wave-lengths of maximum response. When the relative response fell to about 10.0 the selector dial was changed to "1" and the readings made to one more decimal place. The results are shown in Fig. 3. Readings were taken at every 2 or 10 millimicrons as shown. The data for the blue-sensitive photo-tube were obtained with our first instrument, those for the red-sensitive photo-tube with our second instrument. Data obtained with different photo-tubes are of course somewhat different but those shown are considered typical. It may be repeated that these data are for constant mechanical slit width and are not corrected for dispersion of the prism or other selectivity within the instrument or for energy distribution of source.

Polarization Effects

It may be noted that some of the curves of Fig. 3 are smooth and typical of the response curves ordinarily obtained with photo-tubes of these kinds with incandescent illuminant and prismatic dispersion. Others of the curves, however, are characterized by ripples superposed on the response curves. This is shown by curves 1 and 3 of Fig. 3.

The primary factor causing these ripples is the quartz plate over the entrance slit. This plate on both instruments was found to be cut with its faces parallel to the optic axis of the quartz crystal.[7] When such a plate is placed between polarizing elements and oriented so that its axis is not parallel with that of either of the polarizing elements, the spectrum contains a number of dark bands regularly spaced throughout. The conspicuousness of these bands depends on the degree of polarization of the polarizing elements, and on the deviation of the optic axis of the quartz plate from the polarization planes of these elements, which is greatest if at 45° to both of these planes.

The explanation of the effect is given by R. W. Wood. When plane polarized light is passed through a doubly refracting crystalline plate cut parallel to the axis, "it is resolved into two components vibrating at right angles to each other which traverse the plate with different velocities and consequently emerge with a phase-difference depending on the thickness of the plate. . . . Owing to dispersion the phase-difference of the emergent components depends not only on the thickness of the crystal plate but also on the wave-length of the light, consequently if white light is employed the state of polarization of the transmitted light varies as we pass along the spectrum, and if a plate of moderate thickness is used and the light is passed through a Nicol and into a spectroscope, the spectrum will be found to be furrowed by dark bands which represent the wave-lengths quenched by the Nicol."[8]

In the present instance the polarizing elements appear to be (1) the incandescent filament itself

[7] Determinations made by F. P. Phelps of the Bureau's Polarimetry Section, from whom the authors have received helpful advice in this connection.

[8] R. W. Wood, *Physical Optics* (The Macmillan Company, New York, 1934), p. 349, third edition.

(which may give up to 20 percent polarization),[9] modified possibly by elliptical polarization by the two mirrors, on one side of the quartz plate, and (2) the refracting surface of the dispersing prism, on the other side.

The ripples in the sensitivity curves are not apparent if (1) the quartz plate is oriented with its axis at 0° or 90° to the polarizing plane of the dispersing prism, (2) the plate is removed from the instrument, (3) if a quartz plate cut perpendicular to the axis is used over the entrance slits, or (4) if a glass plate is used over the entrance slit. The quartz lens or plate in the upper beam (regardless of how it is cut) has no appreciable effect on the sensitivity curve at any orientation; in this case the quartz is not between polarizing elements.

The band effect can readily be seen if the quartz plate (faces cut parallel to optic axis) is taken out of the instrument and examined between polarizing elements with a hand spectroscope. One of the polarizing elements may be the sky or a bare tungsten filament. The filament of the incandescent source of the Beckman spectrophotometer is thus demonstrated to be giving off partially polarized light. The dispersing prism of the hand spectroscope is the second polarizing element. Of course, the effect is far more pronounced if the polarizing elements are two polaroids or Nicols.

With reference to Fig. 3, again, curves 1 were obtained soon after the receipt of the respective instruments. In both cases the entrance quartz plate had not been disturbed before the data were taken and it would appear from the magnitudes of the ripples that each plate had been mounted with its axis approximately at 45° to the polarizing planes of the dispersing prism and lamp filament. The other curves of Fig. 3 were obtained later, curves 2 with the entrance quartz plate removed, curves 3 with it reinserted at the 45° position. It may be noted, in passing, that curves 1 and 3 ("blue" cell), which check closely, were obtained with different photo-tubes; curves 1 and 3 ("red" cell), which show change of sensitivity, were obtained with the same photo-tube 14 months apart.

It was at first thought that the ripples shown in Fig. 3 were of no particular importance. However, when measurement of the spectral transmittance of polarizing materials was attempted, it was found that the ripples were caused by some polarization phenomena and could no longer be ignored. Accordingly, the effect was investigated as partially described above. It is unnecessary to consider all of the data obtained, but it seems very worth while to point out some of the results obtainable if due precautions are not taken.

For example, in Fig. 4, top, is shown (1) the "transmittance" curve obtained on a polarizing goggle inserted in the carrier of the Beckman spectrophotometer at random orientation[10] and with the entrance plate of the instrument at unknown orientation. From 570 to 600 mμ are shown also (2) the maximum and minimum values of "transmittance" obtained by turning the goggle in its own plane (90° apart) and (3) the corresponding values obtained on the Gibson photoelectric spectrophotometer (with a Hilger constant-deviation glass prism). Similar ripples have been noted in the transmission curves of polarizing materials obtained by others using Beckman quartz spectrophotometers.

The effect was studied at some length by

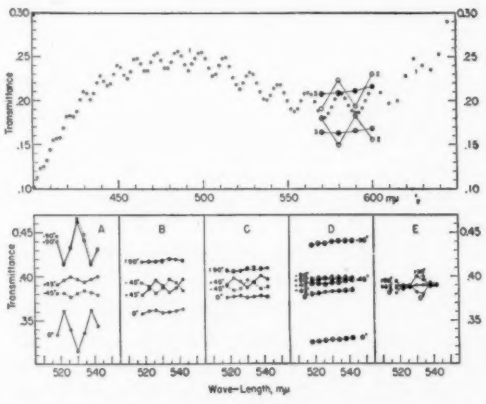

FIG. 4. Effect on the measured "transmittance" of polarizing materials caused by a quartz plate cut with optic axis parallel to surfaces when placed before entrance or exit slit at various orientations. For explanation, see text.

[9] A. G. Worthing, "Deviation from Lambert's law and polarization of light emitted by incandescent tungsten, tantalum, and molybdenum and changes in the optical constants of tungsten with temperature," J. Opt. Soc. Am. 13, 635 (1926).

[10] The shape and size of the sample did not permit orientation at 45°.

measuring the "transmittance" of a polaroid sample, these measurements more or less parallel in time to those from which the sensitivity curves were obtained, as described above. Some of the data are presented in the lower half of Fig. 4.

In A the quartz plate over the entrance slit is placed with its optic axis at 45° to the slit and no plate or lens is over the exit slit. The angles shown beside the five curves in A refer to various orientations of the polaroid. In the 0° position the electric vector of the radiant energy transmitted by the polaroid is in the vertical plane parallel to the slits and the refracting faces of the dispersing prism. At +45° and −45° the polaroid is turned at 45° from the 0° position. At +90° and −90° the polaroid is turned, respectively, at right angles from the 0° position.

In B and C, Fig. 4, the quartz entrance plate has been turned so that the optic axis is, respectively, horizontal and vertical, the angles on the graphs indicating the same respective orientations of the polaroid as before. No plate or lens is over the exit slit.

In D, Fig. 4, the quartz entrance plate has been removed and there is no plate or lens over the exit slit. For comparison are shown (the large crossed circles) the corresponding values obtained on the Gibson glass-prism spectrophotometer.

In E, Fig. 4, the quartz plate is still removed from the entrance slit but has been inserted over the exit slit at the 45° position. Data were also obtained with the quartz plate over the exit slit oriented at 0° and 90°. At 0° the curves obtained were similar to the Beckman (small circle) curves of Fig. 4, D, with about the same total spread. At 90° the curves were similar to those of Fig. 4, C, but with a total spread of only 0.02.

Various comments may be made regarding the data of Figs. 3 and 4.

1. The conditions causing the ripples of Fig. 3 are the same as those causing the worst distortions, Fig. 4, A, during measurement of the transmittance of polarizing samples. It is probable that the entrance quartz plate was close to the 45° position when the data shown in the top half of Fig. 4 were obtained.

2. Complete elimination of the trouble is effected by removing both quartz plates (or plate and lens) over the entrance and exit slits, Figs. 3 and 4, D.

3. Residual effects not apparent in the sensitivity curves may be found (by means of the polaroid) under other than 45° orientation of the entrance quartz plate (cut parallel to the optic axis). Such residual effects are shown in Fig. 4, B and C, and in other data not shown. In this connection, however, it should be pointed out that the angles indicated in Fig. 4 were rather crudely determined, particularly the angles at which the quartz plate was oriented. They are subject to an uncertainty of at least ±5°. It was not investigated whether or not, for example, the "ripples" of Fig. 4, B and C, would be eliminated by more exact 0° and 90° positioning.

4. With both quartz plates removed, the errors possible in the measurement of a polarizing sample at random orientation appear much less than on a glass-prism instrument. Note in Fig. 4, D, the total spread of about 0.02 on the Beckman as contrasted with the spread of about 0.11 on the Gibson instrument. This is undoubtedly largely brought about by the difference in the angle at which the radiant energy enters and leaves the respective quartz and glass prisms at 530 mμ on the two instruments.

The authors showed many of these results to Mr. Cary[4] in November 1946 and were told that the entrance plates and the exit lens or plate were cut from wastage material remaining from construction of the quartz dispersing prisms, and that the optic axis in these plates may be parallel or perpendicular to the faces or at angles in between. Accordingly, other users of the Beckman may or may not have been bothered by the effects shown in Figs. 3 and 4. Since in the past these plates have thus been cut at various angles to the optic axis and apparently inserted at random, it seems well to state the following conclusions in the matter:

1. The authors have had no trouble and detected no errors related to this effect except in the measurement of polarizing materials.

2. To avoid important errors in the measurement of polarizing materials, they have removed the entrance quartz plate and use the exit quartz lens only when necessary or desirable to collimate the beam (as when measuring thick samples).

3. One can readily study the effect on his own instrument by carrying out measurements similar to those shown in the lower half of Fig. 4. By

measuring the transmittance of a polarizing sample at various orientations over a short range of wave-lengths, the effect can be quickly found if present.

Spectral Purity Data

The spectral purity—that is, the extent of spectrum transmitted by the slits as normally used—was obtained as follows. For any given set of conditions (source, filter, photo-tube), with the "sensitivity" dial set three turns counter-clockwise from extreme (as recommended in the instructions), and with the selector switch set at "check" (equivalent to 100.0 on the "1" scale), the slit widths, necessary to obtain a balance of the galvanometer, were determined in millimeters. The mechanical slit widths so determined were then multiplied by the values of mμ/mm supplied by the manufacturer.

The results are shown in Fig. 5. These values were obtained on our first instrument. Values obtained on the second instrument are somewhat greater but otherwise similar. In either case the values are comparable with those illustrated by Cary and Beckman in their Fig. 9.

These slit widths are in general smaller, in some cases much smaller, than are usually practicable with commercial instruments and comprise one of the major advantages of the Beckman spectrophotometer for certain types of work. It is pointed out by the makers of the instrument that still smaller slit widths may be used if the 100 percent reading is made with the selector switch set at ".1" instead of at "check." The sensitivity is, of course, decreased under this condition.

The narrowness of the slits minimizes the fact, for much work, that the operator of the instrument is limited in his freedom to set the slits at any desired width; in normal operation they will vary as shown in Fig. 5. For most materials, for example, essentially the same result will be obtained whether the slits have widths equivalent to 1 mμ or 2 mμ. However, with many of the rare-earth glasses or solutions, this is not true. While, in general, the narrower the slits the more nearly will the measured transmission value approach the true transmission value, even on the Beckman instrument the slits are not narrow enough to make such further change negligible with these

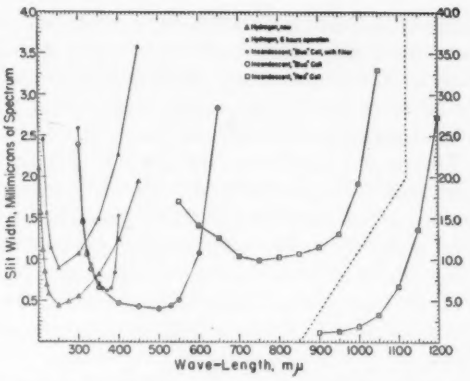

FIG. 5. Approximate amounts of spectrum transmitted by the slits of a Beckman spectrophotometer under normal conditions of operation.

materials. This is of considerable importance in chemical analytical work. In such work, in comparing results on different instruments or in analytical work on one's own instrument, it may be more important that the results be obtained at known slit widths than that these widths be as narrow as possible.

4. WAVE-LENGTH CALIBRATION

The wave-length scale of the Beckman spectrophotometer is direct-reading in millimicrons. Because of the variable dispersion incident to all prism spectrophotometers, this results in greatly varying lengths of the intervals on the scale representing any given number of millimicrons as the spectrum is traversed from the ultraviolet through the visible and into the infra-red. On the Beckman spectrophotometer the smallest scale division is equal to 0.5 mμ from 200 to 300 mμ, 1 mμ from 300 to 400 mμ, 2 mμ from 400 to 600 mμ, and 5 mμ from 600 to 2000 mμ. (However, as pointed out elsewhere, the sensitivity of the photo-tube does not permit reliable measurement above 1200 mμ, approximately.)

On a direct-reading spectrophotometer two types of wave-length check should be considered if one desires to obtain the greatest accuracy with the instrument. On the Beckman instrument one of these relates to adjustment of the internal screw (reached from the left end of the instrument) which rotates the collimating mirror and enables the whole wave-length scale to be brought into approximately correct adjustment. Such a

check or adjustment should be made when the instrument is received and as often thereafter as may be found necessary or desirable. On our instruments the Hg green line (546.1 mμ) has proved very satisfactory for this check.

The second check on the wave-length scale relates to the small residual errors that may be present when the best average adjustment has been made by means of the adjustment screw. These errors cannot easily be eliminated and, if they are large enough to be of importance, they should be allowed for in setting the wave-length scale.

Four light sources have been used in the wave-length calibration of our instruments. These are (1) the quartz-mercury lamp supplied with the Beckman spectrophotometer if desired, (2) the hydrogen arc also supplied if desired with the instrument, (3) a helium lamp (vacuum tube), and (4) a similar neon lamp.

A calibration technique was employed which gave scale corrections always on the basis of correct adjustment (zero error) at 546.1 mμ. In effect, settings with this Hg reference line were made before and after the settings with each of the numerous other lines of the various sources, 10 settings being made on each. Any deviations of the settings on the reference line from the correct value of 546.1 were allowed for in determining the deviations for the other line. In making this allowance the relative variable dispersion of the prism (as represented by the millimicrons per millimeter slit width curve supplied by the makers) was taken into account.

The scale corrections thus obtained are shown in Fig. 6 for the two instruments. It will be noted that the mercury green line at 546.1 (the "reference" point) has zero correction in both plots.

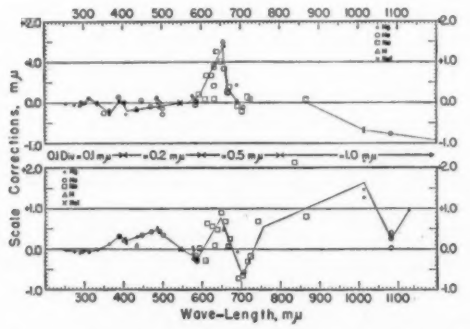

FIG. 6. Residual wave-length corrections found on two Beckman spectrophotometers after adjustment of each instrument to have zero correction at 546.1 millimicrons.

In studying these correction curves the millimicron equivalent of 0.1 scale division should be noted; this is shown between the two correction curves. This equivalent is also important as affecting the precision of the settings; note particularly the difference in precision above and below 600 mμ.

These data are published with the thought that they may serve to inform others of the magnitudes of the wave-length errors to be expected on the Beckman spectrophotometers. They are so small that they may probably be neglected in most work for which the instruments are used. They are likewise so small that they can be determined only by the most careful work and after installation of the auxiliary indicator line over the wave-length scale (see above) to eliminate parallax. On the other hand, these errors are large enough to be important in much of our work, particularly when standardization is being done.

Whether or not one makes the detailed check illustrated in Fig. 6, it may be emphasized that check should often be made on some reference line to insure that gross wave-length errors have not developed, for one reason or another.

5. CHECK OF THE PHOTOMETRIC SCALE

A check of the photometric scale of a spectrophotometer, independent of all other sources of error, is difficult or impossible to make on most spectrophotometers. Useful for this purpose would be a series of samples whose respective transmittances do not vary with wave-length, which will not displace the beam, and for which the transmittances can be independently determined with high accuracy. No such glasses or other materials are available, however.

On a visual spectrophotometer such a check is possible by means of rapidly rotating sectors. If such sectors are properly made, the fraction of the total opening relative to 360°—that is, the effective transmittance of the sector—can be measured on a circular dividing engine with uncertainties only in the fifth decimal place. Of course, the use of such rotating sectors is based on the validity of Talbot's law. Throughout the

spectrum, no certain deviations from this relation are known, however. As a matter of fact, average values obtained over a period of years in measuring the "transmittances" of accurately calibrated rotating sectors on the NBS König-Martens spectrophotometer, prove both the validity of Talbot's law at various wave-lengths and the reliability of the instrument over most of the photometric scale, or else there is a remarkable balancing of errors.

On photoelectric spectrophotometers, however, at least the ones considered in this paper, the use of rotating sectors to check the reliability of the photometric scale is either impossible or attended with too much uncertainty for one reason or another.

Accordingly, shortly after the advent of commercial photoelectric spectrophotometers the National Bureau of Standards instituted the service of issuing glass standards of spectral transmittance.[11] To date, about 80 of these filters have been issued with accompanying certificates.

Three of the four types of filter used for this purpose are of moderate selectivity, covering a large part of the transmittance range from 0.00 to 0.90 at various wave-lengths. A single filter thus covers a considerable part of the transmittance scale. In one sense these are inferior to strictly neutral filters in that a deviation from the true value may be due to other causes than inaccuracy of the photometric scale. On the other hand, they are superior to the neutral filters in detecting stray light, slit width, and gross wave-length errors.

One of the four types of filter used for these spectrophotometric standards is a fairly dense cobalt-blue glass, designated as Corning G55A. (This glass is also known as Corning Signal Purple, present catalog designation 5551.) The 30-mm disks, cut from the original roundel, were recently exhausted and it became necessary to prepare new samples from a new roundel. This of course required an extensive series of measurements in order that values of transmittance might be determined with satisfactory certainty. (After basic values are thus determined for selected disks from a given roundel, values of spectral transmittance for other disks cut from this roundel can be determined with much less labor, as noted below.)

About the time that these measurements were necessitated, the second Beckman spectrophotometer was received. It was decided that an excellent opportunity was thus presented for (1) making a fairly thorough check of the reliability of transmittance measurements made on the Beckman spectrophotometer as it was received from the manufacturer, and (2) if no consistent errors appeared to be present in the Beckman data thus obtained, increasing the over-all reliability of the basic spectral-transmittance values for the new glass disks. Only three things were done to the second Beckman instrument for these measurements—the quartz lens over the exit slit was removed to eliminate multiple-reflection errors, a careful check of the wave-length calibration was made after installation of the second indicator line, and the temperature-control sample holder constructed at this Bureau was used, all as noted above.

Corresponding work with the first Beckman spectrophotometer received in 1943 had not been done for two reasons: (1) The urgency of other work made it impossible to devote the necessary time for such measurements as long as the original supply of spectrophotometric standards held out, and (2) trouble was experienced in readings obtained with the caesium-oxide phototube, particularly at low transmissions, in that there was excessive and erratic "creep" of the galvanometer needle and one could seldom get a definite and trustworthy reading at these low transmittances. Changing photo-tubes did not remedy the trouble. Similar trouble was not experienced with the caesium-antimony phototube, nor with either photo-tube circuit on the new instrument.

Among the many disks cut from the second G55A roundel, designated as G55A β, were two which were identical in spectral transmittance, and a third which was also identical over part of the range. The identity of these spectral transmittances was established within about 0.1 percent of the transmittance by comparative measurements on the Beckman spectrophotometer.

[11] K. S. Gibson, Geraldine K. Walker, and Mabel E. Brown, "Filters for testing the reliability of spectrophotometers," J. Opt. Soc. Am. **24**, 58 (1934).

Measurements were accordingly made on each of these two (or three) glasses by each of the authors, on the Beckman, the König-Martens visual,[12] and the Gibson photoelectric[13] spectrophotometers, and at the various wave-lengths in the visible spectrum indicated in Table I. The temperature of the sample was kept at 25°C for all the measurements, so that this source of variation or uncertainty was eliminated.[14]

In Table I are given for each of the three instruments, at each of the respective wave-lengths, the number of determinations of transmittance made, the average value of the transmittance so measured, and the average deviation

TABLE I. Values of transmittance as measured with the Beckman, König-Martens, and Gibson spectrophotometers. Sample: Corning G55A β of 3-mm thickness. Temperature: 25°C.

Wave-length in milli-microns	Source	Stray-light filter	Beckman			König-Martens			Gibson			Adopted values of transmittance	Computed huge error (=4.9 × Prob. Er.)
			Number of detmns.	Average transmittance	Average deviation	Number of detmns.	Average transmittance	Average deviation	Number of detmns.	Average transmittance	Average deviation		
390	Incan.	Yes	4	8949	0012		—		4	8976	0019	} 895	0032
	Incan.	No	4	8909	0011		—			—			
404.7	Hg	No	4	8824	0016		—			—		} 884	0040
	Incan.	No	4	8809	0016		—			—			
	Incan.	Yes		—			—		4	8890	0010		
435.8	Hg	No	4	8059	0009		—			—		} 806	0016
	Incan.	No	4	8045	0015		—		4	8075	0005		
	Hg	Yes		—		5	8043	0011		—			
471.3	Incan.	No	4	6114	0021		—		4	6182	0008	} 612	0058
	Incan.	Yes		—		4	6064	0009		—			
491.6	Incan.	No	4	3406	0021		—		4	3466	0012	} 344	0033
	Incan.	Yes		—		4	3438	0018		—			
501.6	Incan.	No	4	2430	0028		—		4	2480	0010	} 245	0030
	He	No		—		4	2435	0007		—			
520	Incan.	No	6	0905	0008		—		6	0901	0014	} 091	0010
	Incan.	Yes		—		6	0916	0007		—			
540	Incan.	No	6	0305	0006	6	*0310	00017	6	0308	0006	0308	00045
546.1	Hg	No	4	0335	0001	4	*03355	00006		—		} 0335	00021
	Incan.	No	4	0332	0004		—		4	0337	0004		
560	Incan.	No	6	0646	0004	6	*0630	00018	6	0642	0005	064	00074
578	Hg	No	4	0271	0003	4	*02723	00015	(4)	(0284)	(0004)	} 0273	00044
	Incan.	No	4	0281	0002		—			—			
600	Incan.	No	(6)**	(0075)	(0001)	7	*00743	00012		—		} 0074	00020
	Incan.	Yes	(2)	(0072)	(0002)		—			—			
620	Incan.	No	(6*b*)	(0106)	(0002)	7	*01003	00011		—		} 0100	00021
	Incan.	No	(6*r*)	(0130)	(0007)		—			—			
	Incan.	Yes	(2*b*)	(0096)	(0004)		—			—			
	Incan.	Yes	(2*r*)	(0100)	(0002)		—			—			
640	Incan.	No	(2*b*)	(0084)	(0001)		—			—		} 0074	00022
	Incan.	No	(4*r*)	(0100)	(0006)		—			—			
	Incan.	Yes	(2*b*)	(0070)	(0003)	5	*00743	00010		—			
	Incan.	Yes	(2*r*)	(0081)	(0007)		—			—			
667.8	Incan.	No	4	0338	0006		—		(4)	(0371)	(0011)	} 034	0011
	Incan.	Yes		—		4	*0337	0008		—			
680	Incan.	No	4	136	003		—		4	137	006	14	008
690	Incan.	No	4	342	007		—		4	345	012	} 34	015
	Incan.	Yes		—		(4)	(321)	(009)		—			
706.5	Incan.	No	4	7136	0047		—		4	7110	0015	713	0056
720	Incan.	No	4	8449	0014		—		4	8455	0018	845	0024
750	Incan.	No	4	9015	0010		—		4	9016	0014	901	0018

* Rotating sector used in blank beam.
** Values in parentheses were not used in deriving the adopted values of transmittance nor in computing the huge errors.

[12] H. J. McNicholas, "Equipment for routine spectral transmission and reflection measurements," J. Research Bur. Stand. 1, 793 (1928), RP 30.
[13] K. S. Gibson, "Direct-reading photoelectric measurement of spectral transmission," Rev. Sci. Inst. 7, 693 (1923).
[14] The General Electric recording spectrophotometers were not used in this standardization of the G55A β glass because (1) no temperature control has been devised for use on these spectrophotometers, and (2) the slit widths are undesirably large for this type of work.

of each determination from the average value. On the Beckman and Gibson spectrophotometers, each determination consists of two or more readings with separate wave-length settings. On the König-Martens spectrophotometer a determination is derived from 20 photometric settings, 10 with the sample in each beam. At the left of the table and in the footnotes are indicated certain experimental conditions pertinent to the determinations. At the right are given the basic values of transmittance adopted from these measurements for the NBS standard glass, together with the "huge error" (4.9 times the probable error)[15] as computed from the deviations of the several separate determinations from this adopted value. Eight or more determinations always entered into the computation of this huge error.

In a consideration of the data of Table I, the following points should be noted:

1. The König-Martens and Gibson spectrophotometers were used in the usual routine manner.

2. Since part of the purpose of these measurements was a test of the Beckman instrument, measurements were made at all wave-lengths on it. On the other two instruments measurements were not made at those wave-lengths where long experience has indicated that they are relatively unreliable. This obviously applies to the violet and red ends of the spectrum with the König-Martens visual spectrophotometer. For this type of glass with the Gibson spectrophotometer it applies to the region from 600 to 660 mμ where the transmittance is extremely low and stray energy renders the values relatively unreliable; this stray-energy error is believed to affect also the values for this glass measured on this instrument at 578 and 667.8 mμ.

3. The same sort of error is apparent in the data obtained with the Beckman spectrophotometer in the region of very low transmittance with this glass, though apparently to a less extent. In both instruments this is the region in which the "blue-sensitive" and the "red-sensitive" photo-tubes give about the same response —near 590 mμ on the Gibson, and near 625 mμ on the Beckman. Normally in either case the photo-tube giving the greatest response is used in the measurements. For most types of sample, either instrument, with the appropriate photo-tube, will give as accurate results through this region as at other regions. With this glass, however, for which the transmittance being measured is very low and for which the transmittance is high at those spectral regions in which the photo-tube is much more sensitive, the freely transmitted stray energy from these regions may produce an important error. On the Beckman spectrophotometer this was checked by the use of stray-energy filters—Corning 2424 with the "blue-sensitive" photo-tube from 600 to 640 mμ and a Corning medium Aklo with the "red-sensitive" photo-tube from 620 to 640 mμ. It can be seen that the measured transmittance is lowered and on the average comes close to the values obtained with the König-Martens spectrophotometer.

4. The three instruments for which data are given in Table I differ in the number of decimal places which can be obtained in the transmittance, T.

(1) Values of T on the Gibson spectrophotometer can be read to only 0.001 or at most 0.000_5. However, this reading is definite since a vernier is provided on the reading scale of the rotating sector. For low transmittances the number of significant figures is limited, therefore, and the fourth decimals given in the table result simply from the averaging.

(2) On the Beckman instrument, values of T can be read to 0.001 by estimating tenths of a division, or on the same dial to 0.0001 for values of transmittance less than 0.11 if the selector dial is set to "0.1." This greatly facilitates making the reading but otherwise there appears to be little gain in the use of the magnified scale. Slight and erratic "creeping" of the galvanometer often makes it uncertain when the best reading is obtained. The authors have been able to obtain the precision indicated by the average deviations shown in Table I for these low values only by consistent checking of the "off" reading, bringing the transmittance reading to such a value that the galvanometer position is identical for the two juxtaposed readings.

(3) On the König-Martens spectrophotometer,

[15] Mansfield Merriman, *A Textbook on the Method of Least Squares* (John Wiley and Sons, Inc., New York, 1911), eighth edition revised, p. 205. Peter's approximation formula was used to compute probable errors.

TABLE II. Comparison of average transmittances obtained with the Beckman spectrophotometer with those adopted from extensive measurements on the Beckman, König-Martens, and Gibson Spectrophotometers.* Samples: Jena BG 14 (green) and Corning HT yellow C, each of 2-mm thickness. Temperature: 25°C.

Wave-length in millimicrons	Adopted transmittance		Deviation of average Beckman value from adopted transmittance	
	Jena BG 14	Corning HT yellow C	Jena BG 14	Corning HT yellow C
390	0.862	0.025	0.000	+0.001
404.7	.877	.020	.000	−.001
420		.019		.000
435.8	.893	.0240	.000	+.0003
471.3	.894	.081	+.001	.000
501.6	.859	.208	+.001	−.001
520		.316		+.001
530	.760	.379	−.001	−.001
546.1	.671	.479	+.001	−.001
560	.585	.557	−.002	+.002
578	.473	.636	−.001	.000
587.6		.668		.000
600	.350	.699	−.001	.000
620	.256	.731	+.001	.000
640	.187	.747	+.001	+.002
660		.754		.000
667.8	.122		.000	
690		.755		−.001
710	.074		+.001	
720		.748		−.001
750	.057	.730	.000	−.001
800	.051	.693	.000	.000
850	.057		.000	
900	.072	.631	+.001	+.001
950	.094		.000	
1000	.124	.600	+.001	.000

* Measurements by Lois A. Peterson.

the photometric settings are read to tenths of a degree (by vernier if desired), and transmittances computed by the cot×tan relation. The normal number of significant figures is three for transmittances greater than 0.10, although four are often kept temporarily. When the "10 percent" sector ($T=0.09945$) is used in the blank beam, the same number of significant figures is obtained, but the uncertainty as represented by the average deviation has been moved to the fourth decimal place. With the "1 percent" sector ($T=0.00883$) there is another displacement of the significant figures, but the lowered brightness may still result in slight uncertainty in the fourth decimal.

5. The precision or reproducibility of readings of the Beckman spectrophotometer, as judged by the average deviations, is comparable to that of the other instruments, except that the König-Martens is better than either the Beckman or Gibson instruments at the low values of T, as already discussed. It should be noted that each of the four to six determinations at each wave-length on the various spectrophotometers was made on a different day, this work extending off and on over a period of weeks. The reproducibility of either photoelectric instrument at any one time and wave-length setting is in general superior to that indicated in Table I. The Beckman is the most rapid of the three instruments, being somewhat superior in this respect to the Gibson and greatly superior, of course, to the König-Martens (visual).

6. No error in the photometric scale of the Beckman spectrophotometer can be demonstrated by the data of Table I. The following details may be noted:

(1) The consistent differences between results by the Beckman and the Gibson spectrophotometers at the shortest wave-lengths are not representative of results always obtained on these instruments at these wave-lengths. For example, see below in connection with the results of Table II.

(2) Except at 390 and 404.7 mμ the average value at each wave-length obtained on the Beckman either lies between the values obtained on the other instruments or agrees closely with one of them. This holds even at the low values at 620 and 640 mμ when the stray-energy filters are used.

(3) The use of the mercury (Hg) source at the four wave-lengths noted has proved very satisfactory. After a short warming-up period the lamp becomes steady. The slit widths are larger than with the incandescent source, but this is of no consequence since the light is homogeneous. It may be noted that in every case the values obtained with the Hg source are closer to the finally adopted values than those obtained at the same wave-lengths with the incandescent source. The values obtained with the Hg source are not subject to wave-length error, nor to as great a stray-energy error.

(4) At all but the lowest transmittances, the values obtained on the Beckman instrument differ from the finally adopted values by amounts that (1) are less than the uncertainties of the adopted values, and (2) do not exceed 1 percent of the value.

7. The adopted values and huge errors shown

in the table are similar to those certified on the C55A standards of spectral transmittance issued by the National Bureau of Standards, except that in the certificates the huge errors are designated by the term "uncertainty" and are reported to the same number of decimal places as the transmittance itself.

In further confirmation of the reliability of the photometric scale of the Beckman spectrophotometer are results obtained more recently by Lois A. Peterson of the Photometry and Colorimetry Section, with two others of the NBS standards of spectral transmittance, a Jena green glass and a Corning yellow glass. The same spectrophotometers were used as for the work on the blue-glass standard just described, and the number of determinations, the uncertainties, and the various other factors entering into the measurements were all comparable with those listed above. No stray-energy filter was used on the Beckman except at 390 mμ.

The results are shown in Table II, in which are given for each standard, (1) the adopted (usually the average) values obtained as a result of the extensive measurements on the three spectrophotometers (except that the visual determinations do not extend beyond 435.8 and 667.8 mμ), and (2) the deviations of the average Beckman values from these adopted values. Examination of these data shows that there is no consistent deviation of the spectral transmittances obtained on the Beckman spectrophotometer from those obtained on the other instruments.

In addition to the general over-all reliability of the Beckman spectrophotometer demonstrated above, special note may be made of the precision and reliability with which two nearly identical samples may be spectrophotometrically compared. In this case the "100 percent" reading is taken with a standard sample in the beam (instead of with the beam blank or with a solvent cell in the beam), and the only condition that has been changed to obtain balance is that the slits have been widened. Of course the lower the transmittance the wider must the slits be for balance, but since this width will vary inversely as the square root of the transmittance they will be only about 10 times the normal width when the transmittance is as low as 0.01.

For comparing two nearly identical samples such widths are not at all excessive. As a result, if accurately calibrated standards are available, such as the three glasses to which reference has been made above, the spectral transmittance of other similar glasses may be determined in a very short time with an accuracy comparable to that of the standard, even for the very low transmittances. In other words the comparison can be made with uncertainties of but 0.1 or 0.2 percent of the transmittance regardless of whether this is near 0.9 or 0.01.

An additional important feature of these narrow slits is that low transmittances can be determined by a "step-down" procedure, in which for example a glass transmitting 10 percent may be measured and used as standard for a glass transmitting 1 percent, that in turn for a glass transmitting 0.1 percent, and so on. On the Beckman the slits do not become excessively large in this procedure.

6. CONCLUSIONS

On the basis of measurements made mostly on a Beckman spectrophotometer received in the Photometry and Colorimetry Section of the National Bureau of Standards in 1945, it appears that the instrument is capable of precise and accurate measurement of spectral transmittance or transmittancy. This conclusion is based on measurements of the spectral transmittance of certain glass standards on the Beckman, the König-Martens, and the Gibson spectrophotometers. The measurements were limited to the spectral range from 390 to 750 mμ, but there seems no reason to doubt the reliability of transmission data obtained on the Beckman instrument at wave-lengths beyond this range—to approximately 1000 mμ in the infra-red, and to either 320 or 210 mμ in the ultraviolet, depending on the source and photo-tube used in the instrument.

On all three instruments the glass samples were kept at 25°C, being mounted in temperature-control boxes constructed at the National Bureau of Standards. The general statement of reliability given above is also dependent on careful check of the wave-length scale and on adjustment or correction of any errors greater than about 0.1 mμ. Furthermore, it applies only

to values of transmittance from 1.00 to about 0.02. Below 0.02 there is no demonstrated error in the photometric scale, but the authors have not always been able to obtain definite reproducible results for values in this region. If the $-\log_{10}T$ scale is used, large uncertainties may thus be present if values of the order of $-\log_{10}T = 2.0$ are being measured. Where possible it would be preferable to adjust solutions so that absorbancies greater than 1.0 or 1.5 need not be measured.

The slit widths normally used on the Beckman spectrophotometer are believed to be less than those on any other commercial spectrophotometer. For spectral-transmission measurements these widths normally are such as to transmit from 0.5 to 1.5 mμ of spectrum within the range 220–950 mμ when the appropriate source and photo-tube are used. This feature of the instrument serves three useful purposes. It enables the spectral transmission of samples having high selectivity to be determined with an accuracy unattainable with instruments having wider slits. It makes possible the precise and accurate comparison of nearly identical samples, even those having high absorption, without the use of slits unduly wide. It makes possible the reliable determination of very low transmittances by a "step-down" procedure using samples of intermediate transmittance.

As with any spectrophotometer the wave-length calibration should be carefully checked when the instrument is received and as often thereafter as may be found necessary. The mercury green line at 546.1 mμ has proved to be a good reference line for adjustment purposes. When this wave-length is correctly adjusted, errors in the rest of the scale exceeding 0.5 mμ were not found on either of our instruments, except above 600 mμ, where the dispersion is relatively small.

As with any single-dispersion spectrophotometer stray-energy errors will usually be present in the regions of low spectral response. The filter supplied by the makers of the Beckman instrument should always be used in the region from 320 to 400 mμ with incandescent source. Other filters may be desirable for certain types of transmission or for other special reasons. Multiple-reflection effects should be considered if errors less than one percent are considered important.

The instrument is subject to error if a fluorescent sample is measured. The magnitude of this error will depend on the ratio of fluorescent to incident energy and on the interrelation of the photo-cell sensitivity and the wave-length regions of excitation and fluorescence. If the fluorescent energy is in the visible region, it can be detected by placing the sample in the beam and viewing it from above as the wave-length is varied through the ultraviolet and visible regions. One can thus be fore-warned. If the fluorescence is in the ultraviolet, such error would be difficult to detect without special equipment for the purpose. The error can be much greater in reflection than in transmission measurements.

Care should be taken in the measurement of the transmittance of polarizing materials. Two effects may be noted. As with all prism instruments the energy transmitted by the dispersing prism becomes partially polarized. As a result, the value of transmittance obtained will depend on the orientation of the polarizing sample being measured. A second, and more serious effect may arise if the quartz plate over the entrance slit (and to a much less extent the quartz plate or lens over the exit slit) is cut with the optic axis parallel to the surfaces of the plate. Serious distortions of the transmittance curve may result as shown in Fig. 4 of the present paper.

In conclusion, therefore, we would state that spectral-transmission measurements of high reliability are obtainable on the Beckman quartz spectrophotometer. To obtain such results, however, one must take various precautions. The instrument is convenient and rapid to use and covers a wave-length range not heretofore readily available in a single instrument.

JOURNAL OF THE OPTICAL SOCIETY OF AMERICA VOLUME 37, NUMBER 8 AUGUST, 1947

The Spectrographic Analysis of Ferro-Silicon

J. H. COULLIETTE
Industrial Research Institute, University of Chattanooga, Chattanooga, Tennessee
(Received March 19, 1947)

A method has been devised for the spectrographic analysis of materials consisting of two or more principal components. One of the components is selected as a reference element. The ratios of the concentrations of the various component elements to the concentrations of the reference element in a set of standard samples are computed. These concentration ratios are plotted against spectral line intensity ratios to form the working curves. Having determined the intensity ratios for an unknown sample, its composition is readily computed from a set of simple equations.

Complete details of the application of the method to the analysis of ferro-silicon are given. Use of this method eliminates the necessity for adding a standardizing material to the sample or making approximations to correct for reference element dilution.

THE problem of the spectrographic analysis of materials consisting of more than one major component has been the source of some difficulty. M. F. Hasler, C. E. Harvey, and H. W. Dietert[1] proposed a method for approximating the amount of iron present in stainless steel in order to use iron as an internal standard. C. B. Post, D. G. Schoffstall, and G. Hurley[2] described the use of a dilution factor, evaluated for the type of steel, to compensate for the decrease in intensity of the iron lines caused by the diminished iron concentration in a variety of highly alloyed steels. The present author[3] developed the procedure of plotting the ratio of line intensities *versus* the ratio of concentrations for the determination of nickel and chromium in stainless steels. J. R. Churchill and R. G. Russell[4] have applied this method of plotting the ratio of line intensities *versus* the ratio of concentrations to the analysis of aluminous ores and have appropriately named the method, "the mutual standard method." C. H. Corliss[5] has used the method for the analysis of high speed tool steels. This method of plotting the ratio of line intensities *versus* the ratio of concentrations will hereinafter be designated as the mutual standard method.

Ferro-silicon is an alloy of iron and silicon prepared by fusing iron and silica in the presence of carbon in an electric furnace. It is of considerable importance in the manufacture of steel and cast iron. The complete analysis of ferro-silicon by wet chemical methods is a tedious process, requiring approximately one-hundred man hours for the determination of some fourteen elements. Consequently, analysis of ferro-silicon for manufacturing control has in the past been limited in most cases to the determination of silicon, or of silicon and aluminum. The manufacture of special high quality steels could be more effectively controlled if a complete analysis of the ferro-silicon were available. A method has been

TABLE I. Chemical analysis of FeSi samples used as spectrographic standards.

Sample number	Si	Fe	Al	Mn	Ni	Cr	Ti	Ca	Cu	Sn	Zr	CPS
5–565	78.68	18.25	1.45	.115	.048	.67	.142	.178	.025	—	.020	.422
5–604	48.65	48.32	1.05	.347	.173	.661	.14	—	.065	.003	—	.591
5–628	61.18	36.67	1.25	.267	.039	.058	.079	.15	.129	.003	.022	.153
5–643	49.93	48.35	.93	.31	.125	.08	.105	.04	.10	.001	.010	.019
5–644	49.73	48.36	.82	.50	.02	.034	.048	.173	.20	.008	—	.107
5–711	67.16	31.25	.265						.15	.002		

[1] M. F. Hasler, C. E. Harvey, and H. W. Dietert, Ind. Eng. Chem. Anal. Ed. **15**, 102 (1943).
[2] C. B. Post, D. G. Schoffstall, and G. Hurley, Ind. Eng. Chem. Anal. Ed. **17**, 412 (1945).
[3] J. H. Coulliette, Ind. Eng. Chem. Anal. Ed. **16**, 653 (1944).
[4] J. R. Churchill and R. G. Russell, Ind. Eng. Chem. Anal. Ed. **17**, 24 (1945).
[5] C. H. Corliss, J. Opt. Soc. Am. **36**, 357(A) (1946).

TABLE II. Concentration ratios for FeSi samples used as spectrographic standards.

Sample number	Si/Fe	Al/Fe	Mn/Fe	Ni/Fe	Cr/Fe	Ti/Fe	Ca/Fe	Cu/Fe	Sn/Fe	Zr/Fe
5–565	4.31	.0794	.0063	.0026	.0367	.0078	.0097	.0014		.0011
5–604	1.01	.0217	.0072	.0036	.0137	.0029	—	.0014	.000062	—
5–628	1.667	.0341	.0073	.0011	.0016	.0022	.0055	.0047	.000082	.0006
5–643	1.02	.0192	.0064	.0026	.0016	.0022	.0008	.0021	.000021	.00021
5–644	1.03	.0169	.0104	.0004	.0007	.0010	.0036	.0042	.00016	—
5–711	2.15	.0085						.0048		

worked out whereby the determination of the metallic constituents of ferro-silicon can be made spectrographically for three samples in approximately one hour.

SAMPLING

In order to obtain a representative sample, the procedure recommended by the American Society for Testing Materials[6] should be followed. The components of ferro-silicon exhibit a strong tendency to segregate. The sample should be ground in an agate or Boramic mortar until it will pass a 200-mesh sieve.

The powdered ferro-silicon was prepared for excitation by mixing thirty parts of high purity graphite powder with seventy parts by weight of ferro-silicon. The mixing was most readily accomplished by shaking with six or eight $\frac{1}{4}''$ steel balls in a one-ounce glass bottle for five minutes. The mixture was briquetted in a $\frac{1}{4}''$ pellet press under a pressure of 200,000 p.s.i. The graphite serves as a binder, a buffer, and as a mold lubricant, and gives conductivity to this briquet. The briquetted sample in a suitable holder served as the lower electrode of the analytical gap. The upper electrode consisted of a $\frac{1}{4}''$ graphite rod turned to a conical point with a hemispherical tip of $\frac{1}{8}''$ radius.

TABLE III.

Element	Wave-length	Iron wave-length	Excitation
Al	3082.15	3083.74	Spark
Ca	3968.5	3969.26	Spark
Cu	3273.96	3286.73	Spark
Cr	4254.34	4260.48	A. C. Arc
Mg	2802.69	2806.98	Spark
Mo	3170.34	3178.0	A. C. Arc
Mn	2933.06	2941.34	Spark
Ni	3492.9	3495.3	A. C. Arc
Si	3905.53	3815.84	Spark
Sn	3175.02	3178.0	A. C. Arc
Ti	3372.8	3370.78	Spark

[6] ASTM E-31, ASTM Methods of Chemical Analysis of Metals (1943).

EXCITATION

The laboratory equipment included the high voltage spark unit, and a.c. arc unit, spectrograph, and projection-comparator densitometer supplied by Applied Research Laboratories. The discharge circuit of the high voltage spark unit was set at the rated power of 4/3 kva, i.e., capacitance 0.007 micro farad and included an inductance of 0.32 millihenry. The a.c. arc unit was operated at 2.5 kv and 2.5 amperes. The slit of the spectrograph was adjusted to a width of 50 microns. Eastman spectrum analysis No. 1 film was used. The film was developed for three minutes in Eastman D19 developer solution, and fixed in Eastman rapid x-ray fixing solution at 70°F. The wash water for films was maintained at 70°F by a thermostatic mixing valve.

In order to obtain a series of samples for use as calibration standards, the analytical records and sample stock of the Southern Ferro-Alloys Company over a period of several years were examined. Six samples having compositions covering the normal range of the material were selected. Complete chemical analyses of these samples were supplied by the laboratory staff of the Southern Ferro-Alloys Company. These analyses are shown in Table I.

Since silicon has only a few lines available for measurement, the excitation conditions are largely dependent upon the silicon line selected. Iron was chosen as the reference element. The ratio of the concentration of each element to the concentration of iron was calculated. The values of these concentration ratios for the standard samples are shown in Table II. The low concentrations of some of the elements also limited the

number of spectral lines available for measurement. The spectral lines chosen and the type of excitation are listed in Table III.

The characteristic curve for the film emulsion was obtained by means of the four-step rotating sector having transmission ratios 1:2:4:8. The curves (Fig. 1) were plotted on a calculating board having sliding logarithmic scales, and used for converting transmissions to intensity ratios. The working curves were prepared by plotting the spectral line intensity ratios obtained from the standard samples against the concentration ratios calculated for these samples. Typical working curves are shown in Fig. 2. It will be noted that these curves are prepared in the same manner as those for the familiar internal standard method with the exception that concentrations are replaced by concentration ratios.

The concentration ratios (A = (percent Si/percent Fe), B = (percent Al/percent Fe), C = (percent Mn/percent Fe), etc.) for the various elements in the sample being analyzed are derived from the spectral line intensities and the working curves. Obviously, any of the various calculating devices used for converting spectral line intensities into concentrations in the internal standard method can be used for determining the concentration ratios in the mutual standard method.

The concentrations in the mutual standard method are calculated by solution of the set of equations:

$$\text{percent Fe} = \frac{100 - \text{CPS}}{1 + A + B + C + \cdots}, \qquad (1)$$

$$\text{percent Si} = A \times \text{percent Fe}, \qquad (2)$$

$$\text{percent Al} = B \times \text{percent Fe}. \qquad (3)$$

The quantity CPS represents the percentage of carbon, phosphorus, sulphur and any other elements not included in the set of equations. For precise determinations the quantity CPS must be determined by chemical methods. However, approximate values can be assumed from experience. Since the value of CPS is usually small, the error introduced by such assumption will not be great. A glance at a typical set of concentration ratios (Table II) shows that the silicon/iron ratio is the predominant one, which should be determined with special care. It has been found convenient to make three single exposures and two stepped

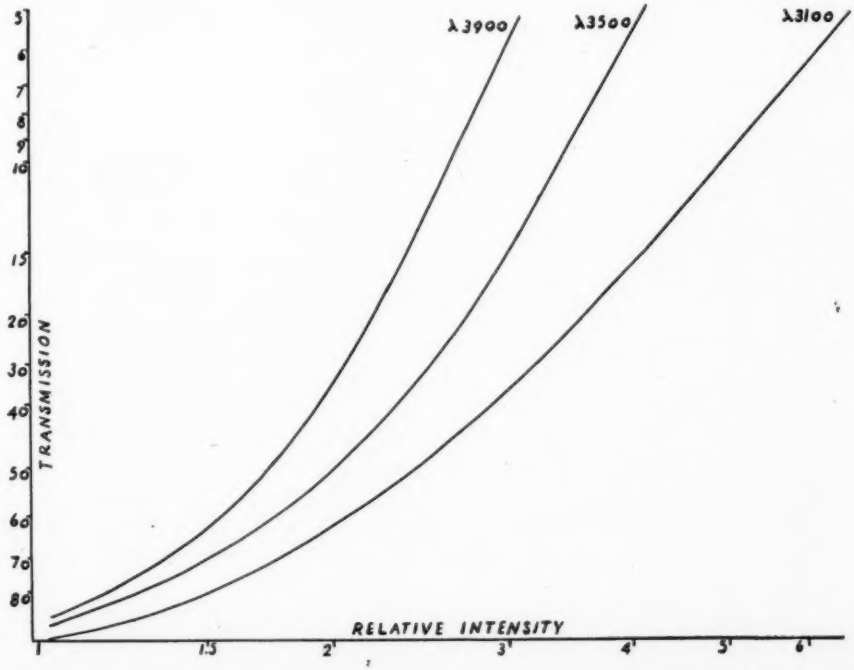

FIG. 1.

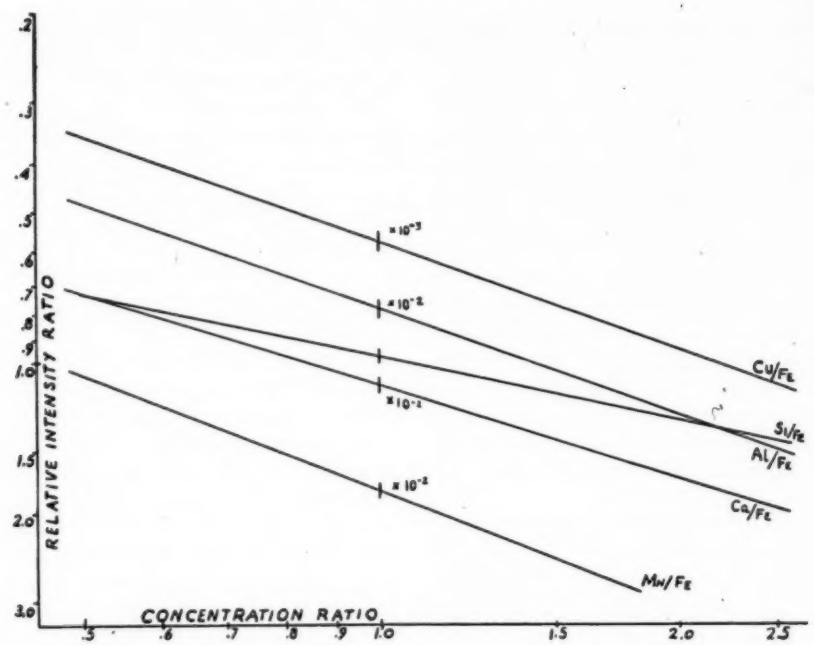

FIG. 2.

sector exposures for each sample. One exposure through the stepped sector is made with the spark, and the exposure is adjusted to give a film density suitable for measurement of the silicon line on the step of the lowest transmission. The single exposures are made with the rotating sector set for one-eighth transmission, and the same exposure time as for the stepped sector. The second stepped sector exposure is made with the a.c. arc excitation. By this means each film gives four determinations of the silicon/iron ratio and at least one determination for each of the minor elements. A photoelectric exposure control circuit, activating the spectrograph shutter, greatly facilitates the making of spectrograms having densities suitable for measurement.

TABLE IV. Line intensity ratios.

Si 3905/Fe 3815			Ca 3969/Fe 3815	
−80 Mesh	−200 Mesh		−80 Mesh	−200 Mesh
1.01	.953		.711	.633
.986	.965		.672	.650
1.00	.970		.734	.680
.978	.965		.685	.655
1.01	.974		.847	.620
.982	.953		.755	.627
1.03	.995		.752	.637
.985	.990		.677	.668
.982	.970		.635	.658
.970	.972		.682	.703
.972	.953		.725	.625
.975	.977		.667	.663
.983	.953		.662	.632
.957	.985		.712	.612
.972	.968		.645	.638
.972	.973		.680	.650
.965	.960		.756	.622
962	.970		.665	.638
.995	.972		.753	.730
.980	.970		.827	.672
.980	.980		.665	.667
.965	.971		.715	.667
.990	.990		.607	.645
.970	.980		.685	.735
.972	.967		.720	.622
.982	.971	Mean	.665	.650
.013	.009	a. d.	.051	.026
.073	.042	Spread	.240	.123

The effect of the particle size upon the analysis was investigated by making a series of twenty-five determinations upon two portions of the same sample, one portion being ground to pass on 80-mesh sieve, and the second being ground to pass a 200-mesh sieve.

Table IV shows the comparison of the spectral line intensity ratios obtained for the major constituents, silicon/iron; and for a minor constituent, calcium/iron. Similar results were obtained for the other minor constituents. It is apparent that the smaller particle size is desirable for high reproducibility.

The reproducibility of line intensity ratios is indicated by the data obtained in the study of the effect of particle size. The precision obtained is of the same order of magnitude as that generally obtained in spectrographic analyses. The accuracy of the final values for concentrations is somewhat lower because of the mutual dependence of the values obtained. The comparison of a large number of complete chemical analyses with corresponding spectrographic analyses has been precluded by the enormous amount of chemical laboratory time that would be required. However, a large number of comparable determinations of silicon and aluminum have been made. The comparison of the values for silicon and aluminum in a group of sixteen samples is shown in Table V. These indicate that the differences to be expected are of the order of 2 percent.

TABLE V. Comparison of chemical and spectrographic determinations of silicon and aluminum in ferro-silicon.

Sample number	Chem Si	Spectro Si	Chem Al	Spectro Al
2643	64.2	64.8	.34	.35
2778	64.6	64.2	.38	.37
2870	64.0	64.5	.35	.36
2913	64.5	63.5	.34	.34
3049	64.1	64.1	.34	.34
3080	63.9	63.8	.37	.32
3406	66.3	67.5	.30	.31
3573	64.6	64.4	.40	.38
3838	68.2	66.0	.33	.31
3882	63.8	63.5	.31	.31
3909	64.0	64.7	.31	.31
3948	64.0	65.0	.27	.25
4017	63.6	64.2	.31	.27
4318	65.4	64.1	.36	.42
5631	66.3	64.2	.30	.29
5641	65.8	65.3	.32	.31
	a.d. = 0.77		a.d. = 0.015	

ACKNOWLEDGMENTS

The work described above was sponsored by the Southern-Ferro Alloys Company of Chattanooga, Tennessee, under the direction of Mr. John Kruesi. The chemical analyses were performed by Mr. H. P. McCormack and Mr. Thomas J. McIntosh.

The Effect of Alkali and Alkaline Earth Salts on the Spectrographic Determination of Strontium*

E. FAST** AND J. RUD NIELSEN
Department of Physics, University of Oklahoma, Norman, Oklahoma

(Received April 14, 1947)

In connection with an attempt to develop a method of quantitative spectrographic analysis of oil-field waters a detailed investigation has been made of the determination of strontium in the presence of alkali and other alkaline earth salts. The dried salts, together with a powdered graphite buffer and titanium as internal standard, were placed in cupped water-cooled graphite electrodes of a high voltage a.c. arc regulated by a variable inductance in the primary circuit. The spectrum was photographed with a Hilger E 1 quartz spectrograph, and the intensities of Sr 3380.7A, Ti 3383.8A, and Ti 3387.8A were determined by a means of a step sector and a Dietert densitometer. With constant amounts of $SrCl_2$ and TiO_2 and various amounts of NaCl, KCl, $CaCl_2$, $BaCl_2$, or $MgCl_2$, exposures were made at different times after the arc was started, and the intensities were determined. In all cases the intensity ratios between strontium and titanium lines were most constant during the period from 2 to 10 minutes after the arc was started. Hence, the weighted averages of the intensity ratios observed during this period have been studied as functions of the amount and composition of the extraneous salts. With NaCl added, the intensity ratio Sr 3380.7/Ti 3383.8 has a maximum value twice as great as when no extraneous element is present, with $MgCl_2$ sixteen times as great. When an alkaline earth is added, the concentration of the extraneous substance giving the maximum value of the Sr/Ti intensity ratio decreases with atomic weight. Alkalis show the opposite behavior. When the total concentration of $CaCl_2$+NaCl is kept constant a maximum of Sr 3380.7/Ti 3383.8 is found for a certain ratio of $CaCl_2$ to NaCl. On the other hand, when various mixtures of KCl and NaCl are added a minimum value of this intensity ratio is obtained for a certain ratio of KCl to NaCl. In neither case are the effects of the extraneous substances additive.

INTRODUCTION

THE use of an "internal standard" in spectrographic analysis is based on the assumption that fluctuations in the source and in the photographic processing affect equally the chosen spectral line of the element to be determined and the line of the standard element, so that the intensity ratio for the line pair is a function only of the concentration of the element to be determined. However, in general this assumption is not accurately valid. The intensity ratio is found to depend markedly also upon the concentrations of other ("extraneous") elements present in the sample. This fact greatly complicates spectrographic analysis, except when the concentrations of the extraneous elements vary but little from sample to sample.

The effect of extraneous elements is usually reported in connection with the description of new applications of spectrographic analysis. Thus, Hultgren[1] found that sodium causes an increase in the intensity of Cu, Ag, Tl, and Cd lines when a spark-in-flame is used as source. Scott and Mitchell[2] reported erratic variations in intensity ratios caused by varying amounts of alkalis, alkaline earths, and phosphates in soil extracts. Duffendack, Wiley, and Owens[3] investigated the effects of extraneous elements in urine analysis, and Brody and Ewing[4] studied the influence of Na and K upon the determination of Cu, Al, Mn, Fe, Sn, and Pb in food and feces when Bi is used as an internal standard. Mitchell and Robertson[5] found the presence of Al to lower the values obtained for Ca, Sr, and Mn in the analysis of soils. Helz[6] observed that certain Sr lines are enhanced when Na_2O and K_2O are present in cement. Thurston[7] found Si to de-

* Presented at the meeting of the Optical Society of America, February 20–22, New York, New York. This work is based on parts of a thesis presented by E. Fast to the faculty of the Graduate College of the University of Oklahoma in partial fulfillment of the requirements for the degree of Doctor of Philosophy.

** Present address: Phillips Petroleum Company, Bartlesville, Oklahoma.

[1] R. Hultgren, J. Am. Chem. Soc. **54**, 2320 (1932).
[2] R. O. Scott and R. L. Mitchell, J. Soc. Chem. Ind. **62**, 4–8 (1943).
[3] O. S. Duffendack, F. H. Wiley, and J. S. Owens, Ind. Eng. Chem. Anal. Ed. **7**, 410 (1935).
[4] J. K. Brody and D. T. Ewing, Ind. Eng. Chem. Anal. Ed. **17**, 627 (1945).
[5] R. L. Mitchell and I. M. Robertson, J. Soc. Chem. Ind. **55**, 269 (1936).
[6] A. W. Helz, J. Research Nat. Bur. Stand. **34**, 129 (1945).
[7] M. N. Thurston, J. Soc. Chem. Ind. **61**, 144 (1942).

crease the intensities of lines of several of the metallic elements present in plant tissues. Other observations have been reported by Parks,[8] Duffendack, Thomson, Lee, and Koppius,[9] and by McCarth, Scribner, Lawrenz, and Hopkins.[10]

A few investigations have been made with the effect of extraneous elements as their main object. Thus, Brode and co-workers[11–13] carried out a series of investigations and observed that line intensities tend to increase when volatile extraneous substances are present, whereas they are depressed by easily excited extraneous elements. Langstroth and Newbound[14] made a detailed study of the effect of KCl, LiCl, $CaCl_2$, H_3BO_3, and NH_4Cl on the intensities of lines of Cd, Mg, and Pb. Langstroth and McRae,[15] using a single spark discharge, investigated the effect of extraneous elements of varying ionization potentials upon the intensity ratio for the chosen line pair in different parts of the discharge.

The effect of extraneous elements has been found to depend on the excitation conditions in the source. Thus, Wolbank[16] found that a large capacitance and a small inductance in a spark circuit prevent the interference by Al in the analysis of zinc alloys. Cholak and Hubbard[17] have reported that the effect of extraneous elements is usually small when a solution is vaporized into a flame. Using a spark source in the analysis of corrosion products, Burke[18] found no effect of acids on the intensity ratios. Hasler and Kemp[19] showed that the effect of extraneous elements upon the intensity ratios can be eliminated to a considerable extent by the proper choice of circuit constants for the source unit.

The most common means of reducing or correcting for the effect of an extraneous element is to add this element or some other "buffer" to the sample in excess. Other special techniques

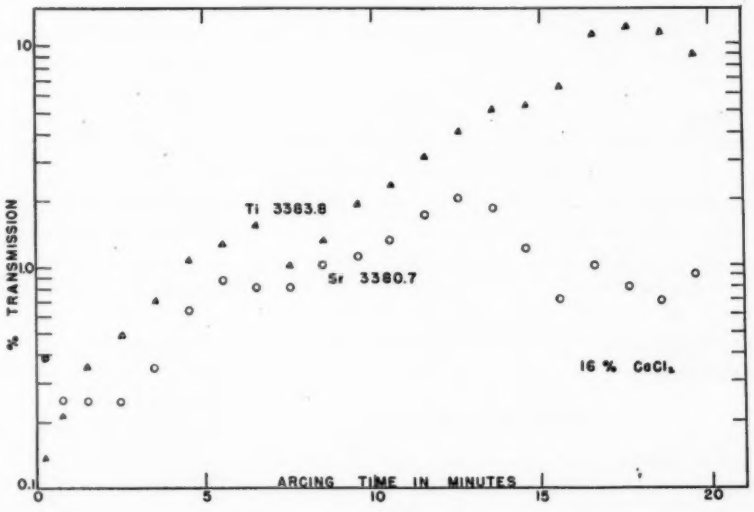

FIG. 1. Effect of 16 percent $CaCl_2$ upon the intensities of Sr 3380.7 and Ti 3383.8A at different times after the arc was started. The ordinate is the logarithm of the minimum percent transmission of the lines.

[8] R. Q. Parks, J. Opt. Soc. Am. **32**, 233 (1942).
[9] O. S. Duffendack, K. B. Thomson, H. C. Lee, and O. G. Koppius, J. Biol. Chem. **126**, 1–7 (1938).
[10] C. N. McCarth, B. F. Scribner, M. Lawrenz, and B. S. Hopkins, Ind. Eng. Chem. Anal. Ed. **10**, 184 (1938).
[11] W. R. Brode and R. W. Silverthorn, *Sixth Summer Conference on Spectroscopy and Its Applications* (John Wiley and Sons, Inc., New York, 1939), pp. 60–65.
[12] W. R. Brode and J. L. Appleton, *Seventh Summer Conference on Spectroscopy and Its Applications* (John Wiley and Sons, Inc., New York, 1940), pp. 36–41.
[13] W. R. Brode and E. S. Hodge, J. Opt. Soc. Am. **31**, 58–63 (1941).
[14] G. O. Langstroth and K. B. Newbound, Can. J. Research **20A**, 39–47 (1942).
[15] G. O. Langstroth and D. R. McRae, Can. J. Research **16A**, 61–74 (1938).
[16] F. Wolbank, Zeits. Metallkunde **33**, 272 (1941).
[17] J. Cholak and D. M. Hubbard, Ind. Eng. Chem. Anal. Ed. **16**, 728 (1944).
[18] S. A. Burke, Trans. Faraday Soc. **33**, 309 (1937).
[19] M. F. Hasler and J. W. Kemp, J. Opt. Soc. Am. **34**, 21–32 (1944).

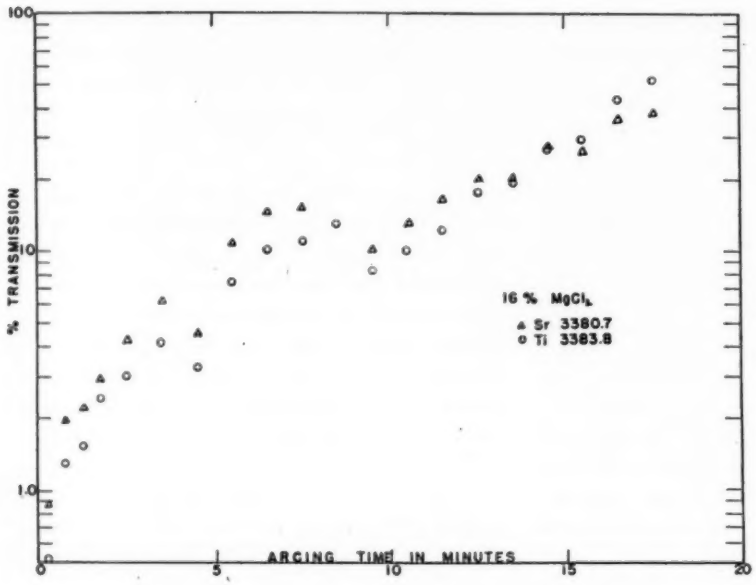

FIG. 2. Effect of 16 percent $MgCl_2$ upon the intensities of Sr 3380.7 and Ti 3383.8A at different times after the arc was started.

have been reported by Zehden[20] and by Post, Schoffstall, and Hurley.[21]

The present investigation originated in an attempt to develop a method of quantitative spectrographic analysis for oil-field waters. These usually contain alkali and alkaline earth salts in considerable and greatly varying amounts. Strontium was selected for special study because of its favorable spectrum and wide occurrence and because it is not determined in the usual chemical water analysis, although its presence in oil-field waters is often of considerable practical importance.

EXPERIMENTAL

The source used was a high voltage a.c. arc supplied by a 5-kva transformer giving about 2300 volts. The arc current was limited to about 2.1 amperes by a variable inductance in series with the primary of the transformer. This arrangement was found to give somewhat more reproducible results than when a resistor was used in the secondary. An analysis of the circuit showed that the variation in arc voltage during a cycle was qualitatively the same as that found by Sawyer and Vincent[22] with a resistor in the secondary, whereas the arc current was stabilized by the inductance.

At first the previously described multiple-electrode arc stand was used.[23] However, it was found that the reproducibility could be increased by cooling the electrodes. Water-cooled electrode holders, similar to those described by Scribner and Corliss,[24] were therefore substituted. They were used in all the work to be reported here.

In addition to giving more reproducible intensity ratios, water-cooling of the electrodes increased the intensities of the lines used here. This is in accord with the finding of Schmidt[25] and of Hemsalech and de Gramont[26] that such cooling enhances the spark lines but decreases the intensities of arc lines.

Previous experience with oil-field waters had shown that best results can be obtained by evaporating the waters to dryness, powdering the dry salt residue, and mixing it thoroughly

[20] W. Zehden, J. Soc. Chem. Ind. **59**, 236 (1940).
[21] C. B. Post, D. G. Schoffstall, and G. Hurley, Ind. Eng. Chem. Anal. Ed. **17**, 412 (1945).
[22] R. A. Sawyer and H. B. Vincent, *Sixth Summer Conference on Spectroscopy and Its Applications* (John Wiley and Sons, Inc., New York, 1939), pp. 54–59.
[23] R. C. McReynolds and W. D. Owsley, Rev. Sci. Inst. **13**, 342 (1942).
[24] B. F. Scribner and C. H. Corliss, J. Opt. Soc. Am. **33**, 515 (1943).
[25] R. W. Schmidt, Zeits. f. Physik. **107**, 35–48 (1937).
[26] G. A. Hemsalech and A. de Gramont, Phil. Mag. **43**, 287–306 and 834 (1922).

with a buffer of fine graphite dust. This procedure was therefore followed with the synthetic salt mixtures used in the present investigation. All the salts were dried at 110°C until constant weight was attained. From the loss of weight it was concluded that no water of hydration remained except in the case of $SrCl_2$ and $MgCl_2$, which retained one and two molecules of water, respectively. Titanium was used as internal standard. A mixture of $SrCl_2$ and TiO_2 in the ratio of 2:1 by weight made up 2 percent by weight of all the samples prepared. After addition of the desired amounts of salts of the extraneous elements to be studied, graphite dust was added to make up the proper total amount. While the amount of graphite varied, it never made up less than half of the sample by weight. The weighed materials were ground together to form a homogeneous mixture and were placed in cupped electrodes made of $\frac{1}{4}$-inch rods of special spectrographic graphite obtained from the National Carbon Company. The prepared electrodes were kept at 110°C in a drying oven until just before they were to be arced.

A condensing lens focused the light from the arc approximately at the collimator lens of a Hilger E 1 large Littrow-type quartz spectrograph. Eastman Spectrum Analysis No. 1 plates were used in practically all of the work. They were processed in the usual manner in Eastman D-19 developer and Eastman F-5 fixer. An ARL-Dietert densitometer-comparator[27] served to determine the line intensities. Each plate was calibrated separately by means of a set of iron lines, the relative intensities of which had been previously determined by the use of a step sector.

A number of exposures were made at different times after the arc was started. The exposure time was usually 50 seconds, and an interval of 10 seconds was allowed to reposition the plate. When this gave too opaque lines on the plate, the exposure time was shortened or the intensity of the light entering the spectrograph was reduced by a variable rotating sector. Except when the sample was consumed quickly 20 to 24 exposures were made on each plate. In no case was the arc interrupted until all the exposures were made.

The strontium line and the internal standard were chosen with great care. A survey of the strontium spectrum showed that the lines Sr II 3380.7A and Sr II 3464.5A would be most suitable. Most of the other strontium lines that might be considered lie either in the region of the cyanogen bands or in the visible region where the plate contrast changes rapidly with wavelength. Moreover, since the Sr II lines are not caused by transitions terminating in the ground state of the neutral atom, they will usually not

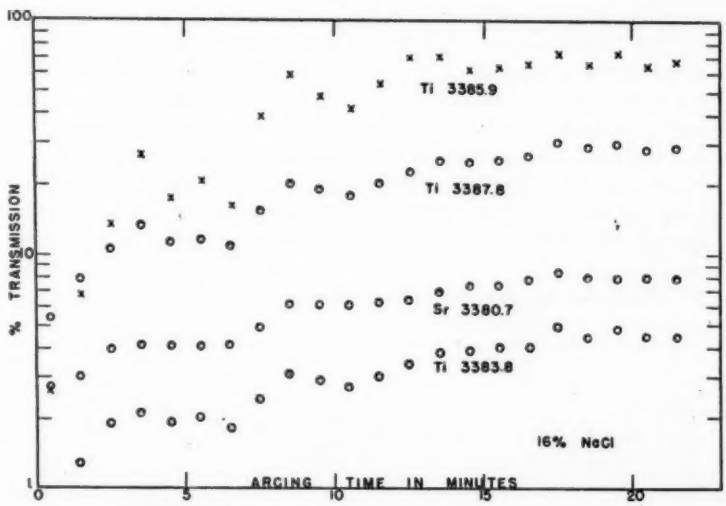

FIG. 3. Effect of 16 percent NaCl upon Sr 3380.7 and three titanium lines at different times after the arc was started.

[27] H. W. Dietert and J. Schuch, J. Opt. Soc. Am. **31**, 54 (1941).

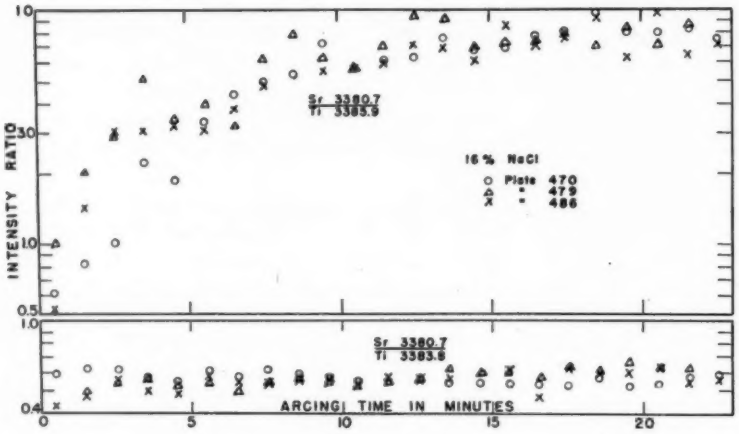

FIG. 4. Effect of 16 percent NaCl upon the intensity ratios Sr 3380.7/Ti 3383.8 and Sr 3380.7/Ti 3385.9 at different times after the arc was started.

show self-reversal. Although Sr II 3464.5 is the stronger, Sr II 3380.7 has less background. The latter line was therefore used in all the work. Its excitation potential (measured from the ground state of the neutral atom) is 12.3 volts.

In searching for a suitable internal standard all the elements (except those whose effect as extraneous elements was to be studied) were considered. On the basis of the available information, titanium was chosen as the most suitable. Singly ionized titanium has several lines including Ti II 3383.8A and Ti II 3387.8A which lie close to Sr II 3380.7 and have a common excitation potential of 10.46 volts, fairly close to that of the strontium line. Since the intensity of Ti 3387.8 is roughly one-fifth that of Ti 3383.8, a given concentration of Ti will be satisfactory for a wide range of concentration of Sr. The titanium is readily available in the form of TiO_2 which has fairly satisfactory physical properties. The ratio of $SrCl_2$ to TiO_2, 2:1 by weight, was chosen so as to make the intensity of the strontium line lie between those of the titanium lines.

Consideration was also given to cadmium as an internal standard. It has the advantage that it can be used in the form of a chloride like all the other elements used. However, the excitation potential of its most suitable line Cd I 3403.7A is only 7.3 volts.

RESULTS

In a series of experiments 16 percent of a salt of a single extraneous element was added to the Sr-Ti-graphite matrix. Figure 1 shows the results obtained with 16 percent of $CaCl_2$. The ordinate is the logarithm of the minimum percent transmission as determined by the densitometer for the lines Sr 3380.7 and Ti 3383.8. This is the negative of the maximum opacitance (or "optical density") of these lines as they appear on the photographic plate with a 50-sec. exposure. The abscissa is the time from the starting of the arc to the midpoint of the exposure. It will be noticed that the opacitance of the strontium line first decreases with time of arcing and then, after about 12 minutes, begins to increase. This would indicate that the rate at which strontium is volatilized and excited in the arc reaches a minimum about 12 minutes after the arc is

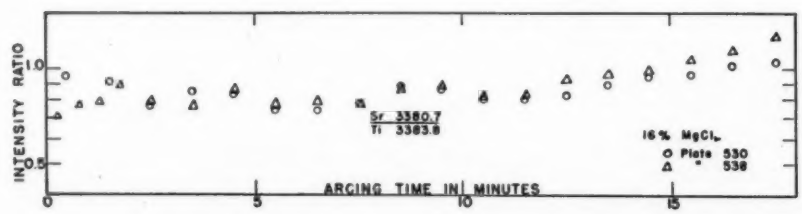

FIG. 5. Effect of 16 percent $MgCl_2$ upon the intensity ratio Sr 3380.7/Ti 3383.8 at different times after the arc was started.

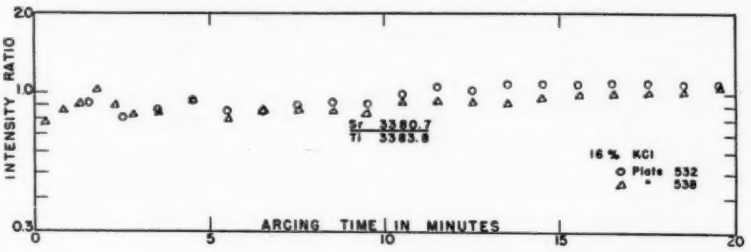

FIG. 6. Effect of 16 percent KCl upon the intensity ratio Sr 3380.7/Ti 3383.8 at different times after the arc was started.

started. On the other hand, the opacitance of the titanium line produced by a 50-sec. exposure seems to decrease steadily with arcing time.

In Fig. 2 are shown the results of similar experiments with 16 percent of $MgCl_2$ as the extraneous substance. The opacitances of the Sr 3380.7 and Ti 3383.8 lines decrease rapidly with increasing arcing time, but they follow nearly the same curve, indicating that the ratio between the rates at which Sr and Ti volatilize in the arc remains essentially constant over the entire arcing time during which observations were made. Figure 3 gives similar results obtained with 16 percent of NaCl added. It appears that in this case the rate of volatilization becomes nearly constant, both for Sr and Ti, after the first few minutes of arcing. The line Ti 3385.9 is an arc line of only 3.7 volts excitation potential. $BaCl_2$, in comparable concentration, gave results similar to those found with $MgCl_2$, and KCl gave results similar to those with NaCl.

In spectrographic analysis it is the intensity ratio for a line pair, rather than the intensity or opacitance of a single line, that is of interest. In Fig. 4 the intensity ratio Sr 3380.7/Ti 3383.8, as evaluated from 50-second exposures with 16 percent NaCl as extraneous substance, has therefore been plotted on a logarithmic scale against the time elapsed since the arc was started. Results are given for three different sets of exposures on different plates. It will be noted that this intensity ratio remains nearly constant during arcing. On the other hand, the intensity ratio Sr 3380.7/Ti 3385.9, plotted in the upper part of Fig. 4, varies greatly. This shows that the line Ti 3385.9 is unsuited to serve as a standard line, as was to be expected from its low excitation potential.

In Figs. 5 and 6 the intensity ratio Sr 3380.7/Ti 3383.8 is plotted against arcing time when the extraneous substance is 16 percent $MgCl_2$ and KCl, respectively. In these and other cases the fluctuations in the observed ratio are greatest during the first couple of minutes after the arc is started, after which the ratio remains fairly constant for a time. Its value depends greatly upon the added substance.

Data like those presented were obtained with each of the extraneous substances NaCl, KCl, $CaCl_2$, $BaCl_2$, and $MgCl_2$ added in concentrations ranging up to 48 percent. With $BaCl_2$, especially when present in high concentration, there was observed an initial maximum in the intensity ratio which then became constant 6 to 8 minutes after the arc was started. Least constancy in the intensity ratio was observed with $CaCl_2$ as extraneous substance. However, the curves obtained in repeated experiments were in fair qualitative agreement. They showed an initial sharp rise, then a constant value, and finally

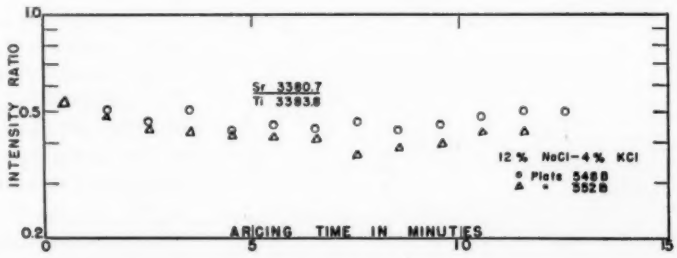

FIG. 7. Effect of 12 percent NaCl and 4 percent KCl upon the intensity ratio Sr 3380.7/Ti 3383.8 at different times after the arc was started.

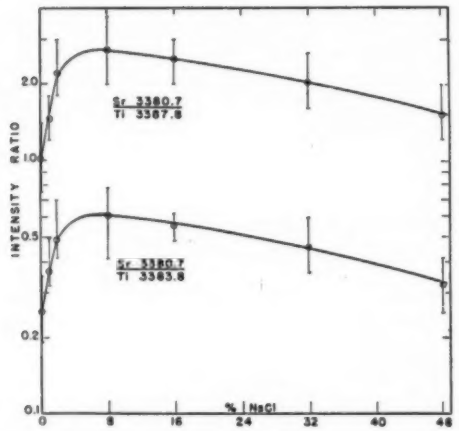

FIG. 8. Average values of the intensity ratios Sr 3380.7/Ti 3383.8 and Sr 3380.7/Ti 3387.8 for samples containing different amounts of NaCl as extraneous substance. The short vertical lines indicate the maximum spread of the points from which the average intensity ratios were computed.

another sharp increase. With KCl at a concentration of 48 percent, a small drift toward lower values was found during the first 6 to 8 minutes of arcing.

In another series of experiments mixtures of NaCl and KCl and of NaCl and $CaCl_2$ were added as extraneous substances. The total concentration was 16 percent by weight in all cases, but the relative amounts of the two components were varied. Fig. 7 shows the intensity ratio *vs.* arcing time curve obtained with 12 percent NaCl and 4 percent KCl added. A gradual small decrease in the intensity ratio during the first 8 or 10 minutes was observed for all mixtures

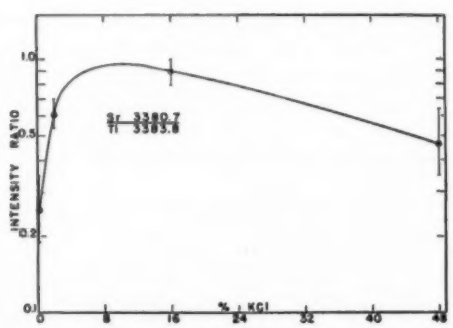

FIG. 9. Average value of the intensity ratio Sr 3380.7/Ti 3383.8 for different amounts of KCl as extraneous substance.

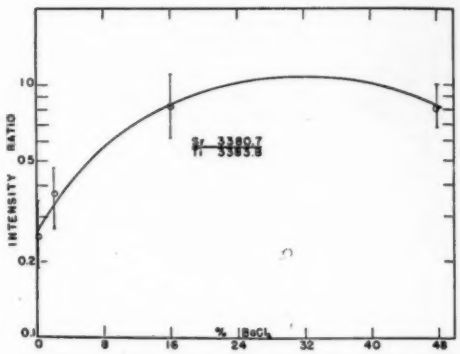

FIG. 10. Average value of the intensity ratio Sr 3380.7/Ti 3383.8 for different amounts of $BaCl_2$ as extraneous substance.

containing both NaCl and KCl. With NaCl and $CaCl_2$ added an initial rise in the intensity ratio was observed, but the reproducibility was not good.

The information which is of principal interest is the dependence of the Sr/Ti intensity ratio upon the concentration of the extraneous substance. This was obtained in the following way from data such as those presented in Figs. 4 to 7. Since the intensity ratio was generally most nearly constant during the interval of 8 minutes following the first two minutes of arcing, the weighted average over this interval was taken to be representative for each mixture. The weighting was done on the basis of the over-all picture presented by the ratio *vs.* time curves obtained with the mixture.

In Fig. 8 are shown the average values of the ratios Sr 3380.7/Ti 3383.8 and Sr 3380.7/Ti 3387.8 obtained in this manner for samples containing different amounts of NaCl as extraneous substance. The short lines parallel to the ordinate indicate the maximum spread of the points from which the average intensity ratios were computed. It will be noted that both intensity ratios have a low value when the extraneous substance is absent, increase to a maximum for a certain concentration of the NaCl, and then decrease slowly as the concentration of the added NaCl is increased. In Figs. 9 to 12 similar results are given for KCl, $BaCl_2$, $CaCl_2$, and $MgCl_2$ as extraneous substances. In all cases, except with $MgCl_2$, the intensity ratio attains a maximum value for some intermediate concentration of the

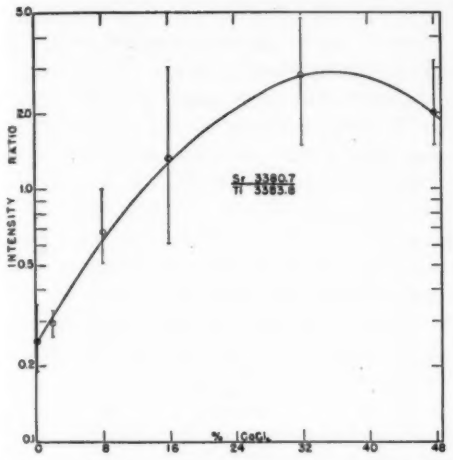

FIG. 11. Average values of the intensity ratio Sr 3380.7/Ti 3383.8 for different amounts of $CaCl_2$ as extraneous substance.

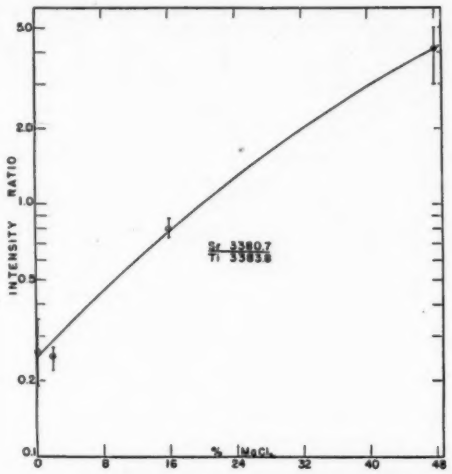

FIG. 12. Average value of the intensity ratio Sr 3380.7/Ti 3383.8 for different amounts of $MgCl_2$ as extraneous substance.

extraneous substance. Even with $MgCl_2$ there is evidence that a maximum is being approached at the highest concentration used. The effects of the two alkali salts are similar in that the intensity ratio shows an initial sharp rise to a maximum at a rather low concentration of the extraneous substance. With the alkaline earth salts the rise in the intensity ratio is more gradual, and the maximum lies at higher concentration of the extraneous substance. However, the maximum effect is much greater with the alkaline earths than with the alkalis. The results indicate that for the alkaline earths the effect decreases with the atomic weight, whereas it increases with the atomic weight for the alkalis. When an alkaline earth is added, the concentration at which the maximum change is produced in the Sr/Ti intensity ratio decreases with the atomic weight. The alkalis seem to show the opposite behavior. The magnitude of the effect is very great. With NaCl added the Sr 3380.7/Ti 3383.8 intensity ratio has a maximum value which is twice as great as when no extraneous element is present. With 48 percent $MgCl_2$ added the observed intensity ratio is about 16 times as great as when no $MgCl_2$ is present, and it appears that the effect would be still greater if more $MgCl_2$ were added.

Figure 13 shows the manner in which the intensity ratio Sr 3380.7/Ti 3383.8 varies with the composition of the extraneous substance when this is a mixture of NaCl and KCl making up 16 percent of the total sample. The dotted curve gives the intensity ratio computed from the data obtained with NaCl and KCl separately under the assumption that the effects of the extraneous substances are additive. The great difference between the two curves shows that this assumption is not valid. Figure 14 gives similar curves for mixtures of NaCl and $CaCl_2$ as extraneous substance. It will be noted that in this case the deviation from additivity is in the opposite direction.

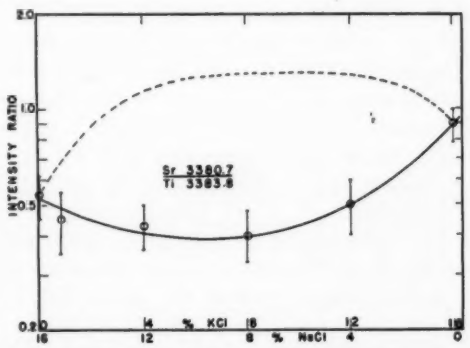

FIG. 13. Variation of the intensity ratio Sr 3380.7/Ti 3383.8 with the composition of a mixture of NaCl and KCl as extraneous substance. The dotted curve is computed on the assumption that the effects of the extraneous substances are additive.

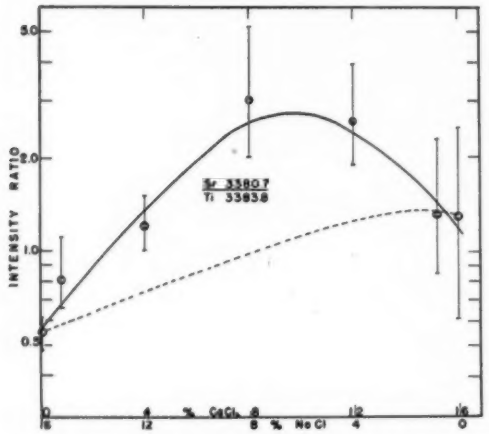

FIG. 14. Variation of the intensity ratio Sr 3380.7/Ti 3383.8 with the composition of a mixture of NaCl and $CaCl_2$ as extraneous substance. The dotted curve is computed on the assumption that the effects of the extraneous substances are additive.

DISCUSSION

A detailed explanation of the observed results is hardly possible at the present time. According to Prokof'ev[28] the intensity of a spectral line depends primarily upon the partial pressure of the emitting element in the source, the temperature of the discharge, and collisions of the second kind with extraneous atoms. In the present work the total amounts of strontium and titanium were always the same. Moreover, a buffer was chosen, and the electrodes were water-cooled, so as to make the excitation conditions in the arc, and hence the temperature, nearly the same in all the experiments. It is therefore natural to look to collisions of the second kind for an understanding of the observed effects. The energies required to ionize the Sr and Ti atoms correspond to 45 926 and 55 138 cm^{-1}, respectively. The excitation energies required to bring the ions to the initial levels of Sr II 3380.7, Ti II 3383.8 and Ti II 3387.8 correspond to 53 267, 29 544, and 29 734 cm^{-1}, respectively. The initial and final levels for the strontium line are doublet levels, whereas the initial and final levels for the titanium lines are quartets. A search for transitions in the extraneous atoms, which would result in energy changes nearly equal to those involved in the emission of any one of the Sr or Ti lines in question, and which would not change the spin, gave the following results. NaI has two pairs of levels which may make possible an enhancement of the Ti lines and one pair of levels which would have the opposite effect. KI has five pairs of levels which may result in enhancement and four pairs of levels which may cause a decrease in the intensity of the titanium lines. For MgI we find two types of collisions which would lead to a decrease in the intensity of the Sr line. For CaI there is at least one type of collision which would enhance the Ti lines, and for Ca II there is one which would decrease the intensity of the Sr line. For BaI we find one type of collision which would enhance the Ti lines. Thus, while collisions of the second kind undoubtedly influence the intensities of the spectral lines emitted when a mixture of elements are present in the arc, no explanation of the observed results can be given in terms of the collision mechanisms which can be predicted on the basis of our present knowledge of atomic energy levels. The failure to account for the large enhancement of the Sr/Ti intensity ratio observed with magnesium as extraneous element is particularly striking.

The rate at which $SrCl_2$ and TiO_2 vaporize in the arc and the partial pressures of the metallic vapors produced by their dissociation may well depend to a considerable extent upon the presence of extraneous salts. However, no data are available from which such effects may be estimated.

Although considerable effort has been made to choose the most favorable conditions for the determination of strontium in oil-field waters, the results reported here show that this problem is beset with great difficulties.

The writers wish to express their sincere appreciation to the Halliburton Oil Well Cementing Company for the grant of a fellowship in support of the investigation reported in part in the present paper.

[28] V. K. Prokof'ev, Bull. Acad. Sci. U. R. S. S., Ser. Phys. 4, 5–8 (1940).

The Reflection of Light from Glass with Double and Multiple Films

ANTONIN VAŠIČEK
The Beneš Technical University, Brno, Czechoslovakia

(Received July 18, 1946)

For the reflection of light from a thin film on glass, that is, from two boundary surfaces, the generalized Fresnel equations are:

$$r_p e^{i\delta_p} = \frac{r_p' + r_p'' e^{-ix}}{1 + r_p' r_p'' e^{-ix}}, \quad r_s e^{i\delta_s} = \frac{r_s' + r_s'' e^{-ix}}{1 + r_s' r_s'' e^{-ix}}.$$

This also can be interpreted as a reflection from a single surface of a hypothetical medium, the reflected components having amplitudes r_p and r_s and phases δ_p and δ_s. Similarly, the reflection from two thin films on glass, that is, from three boundaries, can be reduced to the case of a single film which in turn can be reduced to the reflection from a single surface. This process can be carried for any number of thin films on glass. The normal incidence problem is considered for one, two, and several films and limiting cases of interest in optical practice are calculated. The reflection formulae are simplified if multiple reflections in the films are disregarded. In conclusion the results for two thin films on glass are given. These may be used in practice to decrease or completely extinguish reflection, as well as to increase it.

1. THE REFLECTION OF LIGHT FROM GLASS WITH ONE THIN FILM

THE reflection of light from *glass with no film* is given by Fresnel's relations

$$r_p = \frac{R_p}{E_p} = \frac{\tan(\varphi - j)}{\tan(\varphi + j)}, \quad r_s = \frac{R_s}{E_s} = -\frac{\sin(\varphi - j)}{\sin(\varphi + j)}, \tag{1}$$

where E_p and E_s are the amplitude components of Fresnel's vector in plane polarized light. Usually $E_p = E_s = 1$. Similarly, R_p and R_s are the amplitude components of the reflected light. The p-component lies in the plane of incidence; the s-component is normal to it. The light is incident from air with refractive index 1 on the glass with refractive index n. In Eqs. (1) φ indicates the angle of incidence, j the angle of refraction calculated by Snell's law

$$n = \frac{\sin\varphi}{\sin j}. \tag{2}$$

Figure 1a represents the reflection of light from one refracting medium I. The amplitude of each component of the incident light is assumed equal to 1, in the reflected light the amplitude is designated by r instead of r_p and r_s.

For the reflection of plane polarized light from *glass with one thin film* the following generalized Fresnel's formulae were deduced:

$$r_p e^{i\delta_p} = \frac{r_p' + r_p'' e^{-ix}}{1 + r_p' r_p'' e^{-ix}}, \quad r_s e^{i\delta_s} = \frac{r_s' + r_s'' e^{-ix}}{1 + r_s' r_s'' e^{-ix}}. \tag{3}$$

These relations take into account multiple reflections in the film.* The amplitude components r_p' and r_s' of the reflected light from the boundary I, air-film, and r_p'', r_s'' reflected from the boundary II, film-glass, are given by the formulae

$$r_p' = \frac{\tan(\varphi - j_1)}{\tan(\varphi + j_1)}, \quad r_s' = -\frac{\sin(\varphi - j_1)}{\sin(\varphi + j_1)},$$
$$r_p'' = \frac{\tan(j_1 - j)}{\tan(j_1 + j)}, \quad r_s'' = -\frac{\sin(j_1 - j)}{\sin(j_1 + j)}, \tag{4}$$

where j_1 is the angle of refraction in the film. This angle is, according to the Snell's law,

$$n_1 = \frac{\sin\varphi}{\sin j_1}, \tag{5}$$

where n_1 is the refractive index of the film. The optical path difference x between the rays reflected from the boundaries I and II

$$x = \frac{2\pi}{\lambda} 2 n_1 d \cos j_1; \tag{6}$$

λ is the wave-length of the incident monochromatic light, d the thickness of the film.

* A. Vašiček, J. Opt. Soc. Am. **37**, 145 (1947).

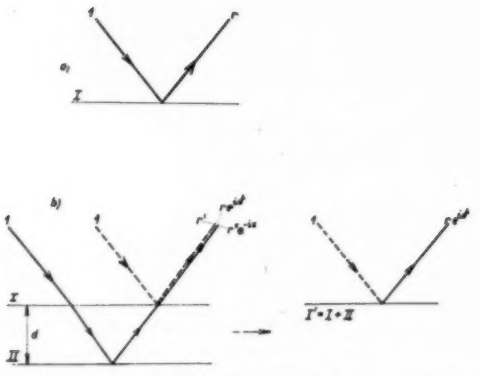

FIG. 1. The schematical illustration of the reflection of light: (a) on a clean glass with no film, (b) on glass with one thin film.

The multiple reflections in the film being neglected, Eqs. (3) are simplified to:

$$r_p e^{i\delta_p} = r_p' + r_p'' e^{-ix}, \quad r_s e^{i\delta_s} = r_s' + r_s'' e^{-ix}. \quad (3')$$

Let us notice that the denominator in Eqs. (3) arises from the sum of the infinite geometrical series.

Figure 1b represents schematically the reflection of light from glass with a thin film. No distinction has been made between the p- and s-components. The reflected ray from the boundary II represented by the full line and the reflected ray from the boundary I, dashed line, combine to $r''e^{-ix}$. The amplitudes of the light reflected on the boundary I, r_p' and r_s', and on the boundary II, $r_p''e^{-ix}$ and $r_s''e^{-ix}$, are called *the basic amplitudes*.

According to the Eqs. (3) we can replace the reflection on glass with one thin film by the reflection on a hypothetical medium which reflects the light with the amplitudes r_p and r_s and phases δ_p and δ_s. In this way we reduce the problem of the reflection on the optical boundaries I and II to the reflection on a single boundary I. Schematically the previous results may be illustrated as follows:

(a) Considering multiple reflections in the film,

$$\left.\begin{matrix} I\ r_p' \\ II\ r_p''e^{-ix} \end{matrix}\right\rangle r_p e^{i\delta_p} = \frac{r_p' + r_p'' e^{-ix}}{1 + r_p' r_p'' e^{-ix}};$$

$$\left.\begin{matrix} I\ r_s' \\ II\ r_s''e^{-ix} \end{matrix}\right\rangle r_s e^{i\delta_s} = \frac{r_s' + r_s'' e^{-ix}}{1 + r_s' r_s'' e^{-ix}};$$

(b) Neglecting multiple reflections,

$$\left.\begin{matrix} I\ r_p' \\ II\ r_p''e^{-ix} \end{matrix}\right\rangle r_p e^{i\delta_p} = r_p' + r_p'' e^{-ix};$$

$$\left.\begin{matrix} I\ r_s' \\ II\ r_s''e^{-ix} \end{matrix}\right\rangle r_s e^{i\delta_s} = r_s' + r_s'' e^{-ix}.$$

This circumstance, that the reflection from optical boundaries I and II, which have a separation $d < \lambda$, is reduced to the reflection of the light from a single optical boundary I, enables one to deduce the formulae for reflection from glass with two and more films. Thus the reflection from glass with two thin films, i.e., the reflection from three boundaries, may be reduced to the reflection from two boundaries, i.e. to the reflection from glass with one thin film. In a similar manner it is possible to reduce successively the reflection from several boundary surfaces to the reflection from a single surface which is optically equivalent to the combination of all the boundary surfaces.

2. THE REFLECTION OF LIGHT FROM GLASS WITH TWO AND MORE THIN FILMS

On glass with refractive index n let there be two thin homogeneous films of refractive indices n_1 and n_2, the former in contact with air, the latter with the glass. The refractive index of air is assumed to be 1. Indicate the angle of incidence of the light by φ, the angles of refraction in films 1 and 2 by j_1 and j_2, and the angle of refraction in the glass by j. These angles are calculated from Snell's law

$$n_1 = \frac{\sin\varphi}{\sin j_1}, \quad n_2 = \frac{\sin\varphi}{\sin j_2}, \quad n = \frac{\sin\varphi}{\sin j}. \quad (6)$$

For the reflection of the light on the boundary I, air-film 1, Fresnel's equations are:

$$r_p' = \frac{\tan(\varphi - j_1)}{\tan(\varphi + j_1)}, \quad r_s' = -\frac{\sin(\varphi - j_1)}{\sin(\varphi + j_1)} \quad (7)$$

similarly for the boundary II, films 1 and 2:

$$r_p'' = \frac{\tan(j_1 - j_2)}{\tan(j_1 + j_2)}, \quad r_s'' = -\frac{\sin(j_1 - j_2)}{\sin(j_1 + j_2)}, \quad (8)$$

and for the boundary *III*, film 2-glass:

$$r_p'''=\frac{\tan(j_2-j)}{\tan(j_2+j)},\quad r_s'''=-\frac{\sin(j_2-j)}{\sin(j_2+j)}. \tag{9}$$

Indicating by d_1 and d_2 thicknesses of the films 1 and 2, the path difference in the film 1 is:

$$x_1=\frac{2\pi}{\lambda}2n_1d_1\cos j_1, \tag{10}$$

and in the film 2

$$x_2=\frac{2\pi}{\lambda}2n_2d_2\cos j_2. \tag{10'}$$

The multiple reflection of the light from glass with two thin films is represented in Fig. 2. According to Fig. 2, the optical state in point D_0, where the rays S_0', S_1', S_2', etc., are reflected or refracted back in the air, is determined by the rays which come to this point after multiple reflections in the film 1 and after combination multiple reflections in both films 1 and 2. In the calculation we consider the amplitude and the phase of the p-component.

(a) The ray S_0 is reflected in the point D_0 as a ray S_0' with the amplitude r_p'.

(b) The ray S_1 arrives at point D_0 as a ray $S_1D_1E_1D_0$ and is refracted at the point D_0 as a ray S_1' with the amplitude $r_p''(1-r_p'^2)$ and with the path difference x_1; therefore the complex amplitude of the ray S_1' is given in the form $r_p''(1-r_p'^2)e^{-ix_1}$.

(c) The ray S_2 arrives at the point D_0 in two different ways, namely:

(1) as the ray $S_2D_2E_2D_1E_1D_0S_2'$ (i.e., the three times reflected ray in the film 1) with the amplitude $r_p'r_p''^2(1-r_p'^2)$ and with the path difference $2x_1+\pi$; the complex amplitude of this ray may be written in the form

$$r_p'r_p''^2(1-r_p'^2)e^{-i(2x_1+\pi)}=-r_p'r_p''^2(1-r_p'^2)e^{-i2x_1};$$

the negative sign is connected with the change of phase at reflection in the point D_1;

(2) as the ray $S_2D_2E_2F_2E_1D_0S_2'$ (i.e., once reflected ray in the both films) with the amplitude $r_p'''(1-r_p'^2)(1-r_p''^2)$ and with the path difference x_1+x_2; the complex amplitude of this ray may be written in the form $r_p'''(1-r_p'^2)\times(1-r_p''^2)e^{-i(x_1+x_2)}$.

If we take afore-mentioned rays only, the optical state in point D_0 is given in the form

$$r_pe^{i\delta_p}=r_p'+r_p''(1-r_p'^2)e^{-ix_1}-r_p'r_p''^2(1-r_p'^2)e^{-i2x_1}+r_p'''(1-r_p'^2)(1-r_p''^2)e^{-i(x_1+x_2)}, \tag{11}$$

and similarly the s-component

$$r_se^{i\delta_s}=r_s'+r_s''(1-r_s'^2)e^{-ix_1}-r_s'r_s''^2(1-r_s'^2)e^{-i2x_1}+r_s'''(1-r_s'^2)(1-r_s''^2)e^{-i(x_1+x_2)}. \tag{11'}$$

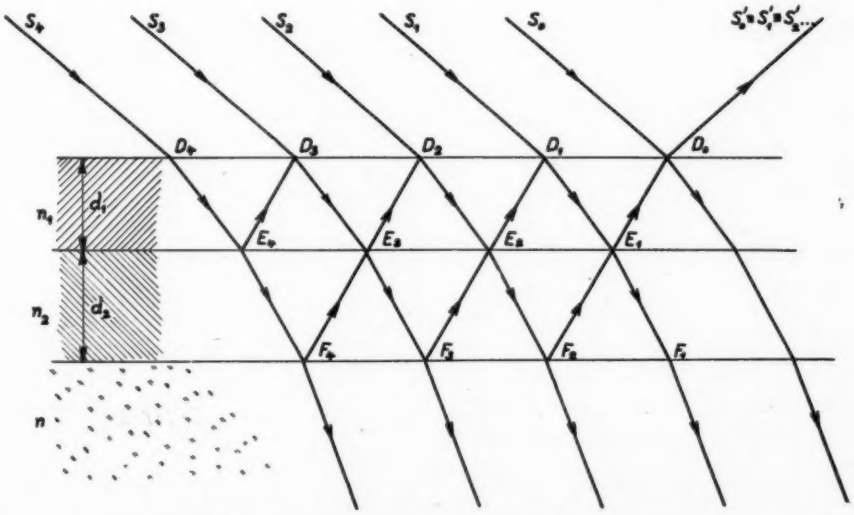

FIG. 2. The reflection of the light on glass with two thin films.

If we take more rays S_3, S_4, etc. we obtain very complicated expressions. In each case it is very difficult to deduce the formulae for the reflection of the light on glass with the two thin films. We can, however, solve the problem by reducing the reflection from *two* thin films, i.e., from *three* optical boundaries, to the reflection from *one* thin film, i.e., from *two* optical boundaries, as stated in the previous chapter. In Fig. 3 only simple reflections are represented. The subscripts p and s have been omitted. The reflected ray on the boundary II (dotted in Fig. 3a) has the path difference

$$x_1=\frac{2\pi}{\lambda}2n_1d_1\cos j_1 \tag{10}$$

with respect to the reflected ray on the boundary I (dashed line). Similarly the ray reflected on boundary III (solid line) and the ray reflected on the boundary I have the path difference

$$x_1+x_2=\frac{2\pi}{\lambda}(2n_1d_1\cos j_1+2n_2d_2\cos j_2). \tag{10''}$$

Then the *basic amplitudes* are: for boundary I.....r_p', for boundary II.....$r_p''e^{-ix_1}$, and for boundary III.....$r_p'''e^{-i(x_1+x_2)}$. According to Fig. 3a the reflection on the boundaries I and II may be replaced by the reflection on the single boundary I', as follows:

$$r_{1,p}e^{i\delta_{1,p}}=\frac{r_p'+r_p''e^{-ix_1}}{1+r_p'r_p''e^{-ix_1}}. \tag{12}$$

In this way the problem of reflection from two thin films, i.e., from three boundaries, is reduced to the reflection from the boundaries I' and III. The amplitude and the phase of the p-component of the light reflected from two thin films are then calculated by writing in Eq. (3) $r_{1,p}e^{i\delta_{1,p}}$ instead of r_p'

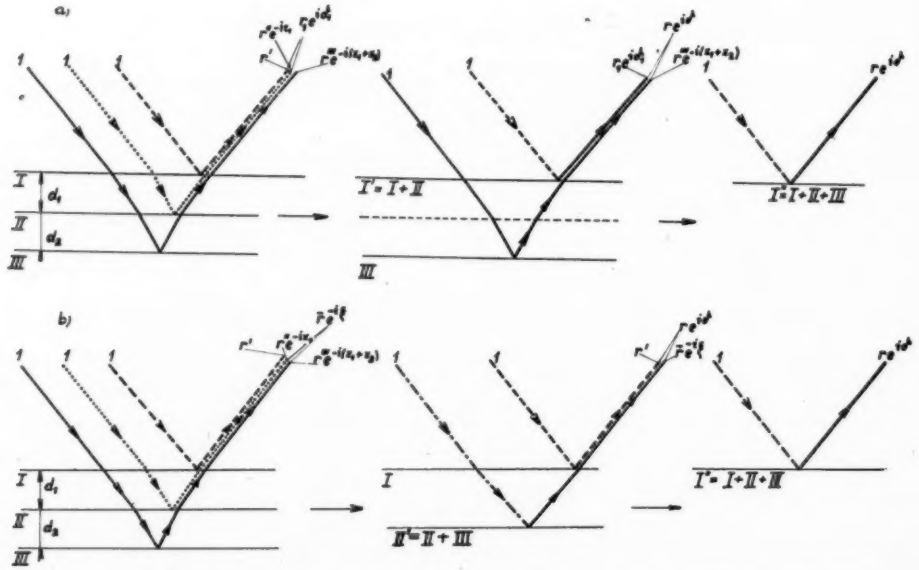

FIG. 3. The schematical illustration of the reflection of the light from glass with two thin films.

and replacing $r_p''e^{-ix_1}$ by $r_p'''e^{-i(x_1+x_2)}$, as follows:

$$r_p e^{i\delta_p}=\frac{r_{1,p}e^{i\delta_{1,p}}+r_p'''e^{-i(x_1+x_2)}}{1+r_{1,p}r_p'''e^{-i(x_1+x_2-\delta_{1,p})}}=\frac{\dfrac{r_p'+r_p''e^{-ix_1}}{1+r_p'r_p''e^{-ix_1}}+r_p'''e^{-i(x_1+x_2)}}{1+\dfrac{r_p'+r_p''e^{-ix_1}}{1+r_p'r_p''e^{-ix_1}}r_p'''e^{-i(x_1+x_2)}}$$

$$=\frac{r_p'+r_p''e^{-ix_1}+r_p'''e^{-i(x_1+x_2)}+r_p'r_p''r_p'''e^{-i(2x_1+x_2)}}{1+r_p'r_p''e^{-ix_1}+r_p'r_p'''e^{-i(x_1+x_2)}+r_p''r_p'''e^{-i(2x_1+x_2)}}. \quad (13)$$

The *s*-component may be written similarly. Schematically the foregoing results may be written as follows:

$$\begin{matrix} I\ r_p' \\ II\ r_p''e^{-ix_1} \\ III\ r_p'''e^{-i(x_1+x_2)} \end{matrix} \Big\rangle r_{1,p}e^{i\delta_{1,p}} \Big\rangle r_p e^{i\delta_p}; \qquad \begin{matrix} I\ r_s' \\ II\ r_s''e^{-ix_1} \\ III\ r_s'''e^{-i(x_1+x_2)} \end{matrix} \Big\rangle r_{1,s}e^{i\delta_{1,s}} \Big\rangle r_s e^{i\delta_s}.$$

We find the same result if we replace the reflection of light on the boundaries *II* and *III* by the reflection on the single boundary *II'* according to Fig. 3b:

$$\bar{r}_p e^{-i\xi_p}=\frac{r_p''e^{-ix_1}+r_p'''e^{-i(x_1+x_2)}}{1+r_p''r_p'''e^{-i(2x_1+x_2)}}, \quad (14)$$

and for the reflection of light on the boundaries *I* and *II'* we obtain

$$r_p e^{i\delta_p}=\frac{r_p'+\bar{r}_p e^{-i\xi_p}}{1+r_p'\bar{r}_p e^{-i\xi_p}}=\frac{r_p'+\dfrac{r_p''e^{-ix_1}+r_p'''e^{-i(x_1+x_2)}}{1+r_p''r_p'''e^{-i(2x_1+x_2)}}}{1+r_p'\dfrac{r_p''e^{-ix_1}+r_p'''e^{-i(x_1+x_2)}}{1+r_p''r_p'''e^{-i(2x_1+x_2)}}}=\frac{r_p'+r_p''e^{-ix_1}+r_p'''e^{-i(x_1+x_2)}+r_p'r_p''r_p'''e^{-i(2x_1+x_2)}}{1+r_p'r_p''e^{-ix_1}+r_p'r_p'''e^{-i(x_1+x_2)}+r_p''r_p'''e^{-i(2x_1+x_2)}}$$

in accordance with the Eq. (13). We hold Eq. (13) as more precise than Eq. (11).

The auxiliary amplitude $r_{1,p}$ and phase $\delta_{1,p}$ are calculated as follows:**

$$r_{1,p}e^{i\delta_{1,p}}=\frac{r_p'+r_p''e^{-ix_1}}{1+r_p'r_p''e^{-ix_1}}=\frac{r_p'+r_p''\cos x_1-ir_p''\sin x_1}{1+r_p'r_p''\cos x_1-ir_p'r_p''\sin x_1}=\frac{\alpha_1-i\beta_1}{\alpha_2-i\beta_2}=\frac{(\alpha_1-i\beta_1)(\alpha_2+i\beta_2)}{\alpha_2^2+\beta_2^2}; \quad (12)$$

then

$$r_{1,p}\cos\delta_{1,p}+ir_{1,p}\sin\delta_{1,p}=\frac{(\alpha_1\alpha_2+\beta_1\beta_2)+i(\alpha_1\beta_2-\alpha_2\beta_1)}{\alpha_2^2+\beta_2^2}, \quad (12')$$

where

$$\begin{aligned} \alpha_1&=r_p'+r_p''\cos x_1, \quad & \beta_1&=r_p''\sin x_1, \\ \alpha_2&=1+r_p'r_p''\cos x_1, \quad & \beta_2&=r_p'r_p''\sin x_1. \end{aligned} \quad (15)$$

Then by equating the imaginary and real parts and by dividing

$$\tan\delta_{1,p}=\frac{\alpha_1\beta_2-\alpha_2\beta_1}{\alpha_1\alpha_2+\beta_1\beta_2} \quad (16)$$

** These calculations and the calculations of the quantities accessible to optical measurements (the azimuth ψ and the phase difference $\Delta=\delta_p-\delta_s$) are presented in the author's paper in J. Opt. Soc. Am. **37**, 145 (1947). The calculations for two and more films can be made similarly.

and multiplying Eq. (12) with its complex conjugate $r_{1,p}e^{-i\delta_{1,p}}$, we get

$$r_{1,p}=\left(\frac{\alpha_1^2+\beta_1^2}{\alpha_2^2+\beta_2^2}\right)^{\frac{1}{2}}. \tag{17}$$

The multiple reflections in the both films 1 and 2 being neglected, Eq. (13) is simplified as follows:

$$r_p e^{i\delta_p}=r_p'+r_p''e^{-ix_1}+r_p'''e^{-i(x_1+x_2)}. \tag{18}$$

For *three thin films on glass*, i.e., for four boundaries, we write schematically

$$\begin{array}{l} I\ r_p' \\ II\ r_p''e^{-ix_1} \\ III\ r_p'''e^{-i(x_1+x_2)} \\ IV\ r_p''''e^{-i(x_1+x_2+x_3)} \end{array} \Big\rangle r_{1,p}e^{i\delta_{1,p}} \Big\rangle r_{2,p}e^{i\delta_{2,p}} \Big\rangle r_p e^{i\delta_p}.$$

We get then for boundaries I and II

$$r_{1,p}e^{i\delta_{1,p}}=\frac{r_p'+r_p''e^{-ix_1}}{1+r_p'r_p''e^{-ix_1}}, \tag{19}$$

and for boundary III

$$r_{2,p}e^{i\delta_{2,p}}=\frac{r_{1,p}e^{i\delta_{1,p}}+r_p'''e^{-i(x_1+x_2)}}{1+r_{1,p}r_p'''e^{-i(x_1+x_2-\delta_{1,p})}} \tag{20}$$

and taking the boundary IV we get the final formula

$$r_p e^{i\delta_p}=\frac{r_{2,p}e^{i\delta_{2,p}}+r_p''''e^{-i(x_1+x_2+x_3)}}{1+r_{2,p}r_p''''e^{-i(x_1+x_2+x_3-\delta_{2,p})}}. \tag{21}$$

When multiple reflections in films are neglected, we obtain

$$r_p e^{i\delta_p}=r_p'+r_p''e^{-ix_1}+r_p'''e^{-i(x_1+x_2)}+r_p''''e^{-i(x_1+x_2+x_3)}. \tag{22}$$

In this way the foregoing results may be generalized for any arbitrary number of thin films on glass.

When a plane polarized light is incident on glass with two and more thin films, the reflected light is in general *elliptically* polarized. Only in the limiting cases, when $x_1=x_2=\cdots k(\lambda/2)$, and k is an integer, is the reflected light strictly *plane* polarized light.

3. THE NORMAL INCIDENCE OF LIGHT ON GLASS WITH TWO AND MORE THIN FILMS

For the normal incidence of light *on glass with no film* the Fresnel's formulae (1) are simplified, as follows:

$$r_p=\frac{n-1}{n+1},\quad r_s=-\frac{n-1}{n+1}=-r_p. \tag{23}$$

Both amplitude components are equal, but they differ in the sign, i.e., $\delta_p=\delta_s\pm 180°$. Therefore the subscripts p and s may be omitted.

The reflecting power of glass with no film is given as the ratio of the reflected and incident intensity

$$\rho=\left(\frac{n-1}{n+1}\right)^2. \tag{24}$$

For the normal incidence of light on *glass with one thin film* the Fresnel's relations (4) have the form

$$\begin{aligned} r_p'&=-r_s'=\frac{n_1-1}{n_1+1}=A_1, \\ r_p''&=-r_s''=\frac{n-n_1}{n+n_1}=A_2. \end{aligned} \tag{25}$$

The formula (3) for the reflection of light on glass with one thin film has the following form

$$Ae^{i\delta}=\frac{A_1+A_2e^{-ix}}{1+A_1A_2e^{-ix}}. \tag{26}$$

Multiplying Eq. (26) with its complex conjugate $Ae^{-i\delta}$, we get the reflecting power of glass with one thin film

$$\begin{aligned} \rho=A^2&=\frac{A_1^2+A_2^2+2A_1A_2\cos x}{1+A_1^2A_2^2+2A_1A_2\cos x} \\ &=\frac{(A_1+A_2)^2-4A_1A_2\sin^2\frac{1}{2}x}{(1+A_1A_2)^2-4A_1A_2\sin^2\frac{1}{2}x}. \end{aligned} \tag{27}$$

We obtain the *limiting cases*, when $x=k(\lambda/2)$, where k is an integer. For k even Eq. (27) becomes

$$\rho'=\left(\frac{A_1+A_2}{1+A_1A_2}\right)^2=\left(\frac{n-1}{n+1}\right)^2. \tag{28}$$

This case gives *the maximum* of the reflected intensity when $n_1<n$, and *the minimum* when $n_1>n$. The reflecting power is the same as if *no film* were on the glass at all.

For an odd k Eq. (27) has the following form:

$$\rho''=\left(\frac{A_1-A_2}{1-A_1A_2}\right)^2=\left(\frac{n_1^2-n}{n_1^2+n}\right)^2. \qquad (29)$$

This case gives *the minimum* of the reflected intensity for $n_1<n$ and *the maximum* for $n_1>n$ and is the most important for the technical practice, as it enables complete extinction of reflected light from glass surface when Strong's condition $n_1^2=n$ is fulfilled and when $n_1d=\lambda/4$.

For the normal incidence of light on *glass with two thin films* Fresnel's relations are simplified as follows:

$$r_p'=-r_s'=\frac{n_1-1}{n_1+1}=A_1,$$

$$r_p''=-r_s''=\frac{n_2-n_1}{n_2+n_1}=A_2, \qquad (30)$$

$$r_p'''=-r_s'''=\frac{n-n_2}{n+n_2}=A_3.$$

The formula (12) has the form

$$Be^{i\delta_1}=\frac{A_1+A_2e^{-ix_1}}{1+A_1A_2e^{-ix_1}}. \qquad (31)$$

The auxiliary amplitude B may be calculated by multiplying Eq. (31) with its complex conjugate. Then

$$B^2=\frac{A_1^2+A_2^2+2A_1A_2\cos x_1}{1+A_1^2A_2^2+2A_1A_2\cos x_1}=\frac{(A_1+A_2)^2-4A_1A_2\sin^2\frac{1}{2}x_1}{(1+A_1A_2)^2-4A_1A_2\sin^2\frac{1}{2}x_1}. \qquad (32)$$

The final formula for the reflection of light on glass with two thin films may be written

$$Ae^{i\delta}=\frac{Be^{i\delta_1}+A_3e^{-i(x_1+x_2)}}{1+BA_3e^{-i(x_1+x_2-\delta_1)}}. \qquad (33)$$

Multiplying with its complex conjugate $Ae^{-i\delta}$ we get the reflecting power of glass covered with two thin films as follows:

$$\rho=A^2=\frac{B^2+A_3^2+2BA_3\cos(x_1+x_2+\delta_1)}{1+B^2A_3^2+2BA_3\cos(x_1+x_2-\delta_1)}=\frac{(B+A_3)^2-4BA_3\sin^2\frac{1}{2}(x_1+x_2+\delta_1)}{(1+BA_3)^2-4BA_3\sin^2\frac{1}{2}(x_1+x_2-\delta_1)}. \qquad (34)$$

If we take the final formula (13) for the reflection of light from glass with two thin films, we obtain the formula for the reflecting power in the following longer form:

$$\rho=\frac{\begin{array}{l}A_1^2+A_2^2+A_3^2+A_1^2A_2^2A_3^2+2A_1A_2(1+A_3^2)\cos x_1+2A_2A_3\cos x_2\\ \qquad +2A_1A_3(1+A_2^2)\cos(x_1+x_2)+2A_1^2A_2A_3\cos(2x_1+x_2)\end{array}}{\begin{array}{l}1+A_1^2A_2^2+A_1^2A_3^2+A_2^2A_3^2+2A_1A_2(1+A_3^2)\cos x_1+2A_1^2A_2A_3\cos x_2\\ \qquad +2A_1A_3(1+A_2^2)\cos(x_1+x_2)+2A_2A_3\cos(2x_1+x_2)\end{array}}. \qquad (35)$$

The last equation contains no auxiliary amplitude B or phase δ_1, which means an advantage for the calculation.

The *limiting cases* may be obtained when $x_1=x_2=k(\lambda/2)$, where k is an integer. Then the auxiliary phase $\delta_1=0$.

Case 1

Let $x_1=180°$, and $x_2=180°$ or $n_1d_1=n_2d_2=\lambda/4$. Then formula (32) has the form

$$B=\frac{A_1-A_2}{1-A_1A_2}=\frac{n_1^2-n_2}{n_1^2+n_2}, \qquad (36)$$

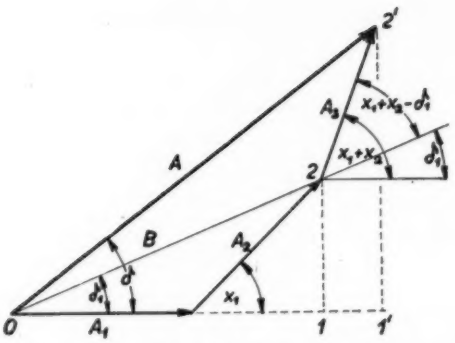

FIG. 4. The vector addition of the amplitudes A_1, A_2, A_3 with the path differences x_1, x_1+x_2.

and because $\cos x_1=-1$; with respect to $\cos(x_1+x_2)=+1$ we get

$$\rho=A^2=\left(\frac{B+A_3}{1+BA_3}\right)^2=\left(\frac{n_1^2n-n_2^2}{n_1^2n+n_2^2}\right)^2. \quad (37)$$

The reflected light from glass with two thin films may be extinguished, $\rho=0$, when

$$n_1^2n=n_2^2. \quad (38)$$

This case is the most important for the technical practice and will be solved in a special section.

Case 2

Let $x_1=360°$, $x_2=360°$, or $n_1d_1=n_2d_2=\lambda/2$. Then $\cos x_1=+1$ and formula (32) gives the following result:

$$B=\frac{A_1+A_2}{1+A_1A_2}. \quad (39)$$

Since $\cos(x_1+x_2)=+1$, we get for the reflecting power

$$\rho=A^2=\left(\frac{B+A_3}{1+BA_3}\right)^2=\left(\frac{n-1}{n+1}\right)^2. \quad (40)$$

The reflecting power is the same as if *no films 1 and 2 were* produced on glass surface at all.

Case 3

Let $x_1=180°$, $x_2=360°$, or $n_1d_1=\lambda/4$, $n_2d_2=\lambda/2$; then $\cos x_1=-1$; the formula for B is the same as in the case 1. Since $\cos(x_1+x_2)=-1$, the formula (33) for the reflecting power has the form

$$\rho=A^2=\left(\frac{B-A_3}{1-BA_3}\right)^2=\left(\frac{n_1^2-n}{n_1^2+n}\right)^2. \quad (41)$$

The reflecting power is the same as if *no film 2* were on glass at all—the problem is reduced to one thin film on glass. The similar result we obtain *for case 4*, when $x_1=360°$ and $x_2=180°$, but the reflecting power is the same as if no film 1 were on glass surface at all. The general deduction is: When the glass surface is covered with one or more films and when the path difference in any film is λ, 2λ, $3\lambda,\cdots$, then the reflecting power is the same as if this film were not present. This is true not only, for the normal incidence of light, but for an arbitrary angle of incidence as well.

Similarly we can deduce the condition for the non-reflecting glass surface covered with *three thin films* in the following form:

$$n_1^2n_3^2=n_2^2n \quad \text{and} \quad n_1d_1=n_2d_2=n_3d_3=\frac{\lambda}{4}. \quad (42)$$

This condition may be generalized for an *even number k of films*

$$n_1^2n_3^2n_5^2\cdots n_{k-1}^2n=n_2^2n_4^2n_6^2\cdots n_k^2, \quad (43)$$

and for *an odd number k of films*

$$n_1^2n_3^2n_5^2\cdots n_k^2=n_2^2n_4^2n_6^2\cdots n_{k-1}^2n, \quad (44)$$

where

$$n_1d_1=n_2d_2=n_3d_3=\cdots=n_kd_k=\frac{\lambda}{4}. \quad (45)$$

4. THE SIMPLE REFLECTIONS OF LIGHT IN TWO AND MORE THIN FILMS ON GLASS

For the simple reflection of light from glass with two thin films we have written for the p-component the following formula:

$$r_pe^{i\delta_p}=r_p'+r_p''e^{-ix_1}+r_p'''e^{-i(x_1+x_2)}; \quad (18)$$

then

$$r_p\cos\delta_p+ir_p\sin\delta_p=r_p'+r_p''\cos x_1+r_p'''\cos(x_1+x_2)-i[r_p''\sin x_1+r_p'''\sin(x_1+x_2)]. \quad (18')$$

By equating the imaginary and real parts we get

$$r_p \sin\delta_p = -[r_p'' \sin x_1 + r_p''' \sin(x_1+x_2)],$$
$$r_p \cos\delta_p = r_p' + r_p'' \cos x_1 + r_p''' \cos(x_1+x_2); \tag{46}$$

then

$$\tan\delta_p = \frac{-[r_p'' \sin x_1 + r_p''' \sin(x_1+x_2)]}{r_p' + r_p'' \cos x_1 + r_p''' \cos(x_1+x_2)}. \tag{47}$$

Multiplying the formula (18) with its complex conjugate $r_p e^{-i\delta_p}$ we obtain

$$r_p^2 = r_p'^2 + r_p''^2 + r_p'''^2 + 2r_p' r_p'' \cos x_1 + 2r_p'' r_p''' \cos x_2 + 2r_p' r_p''' \cos(x_1+x_2). \tag{48}$$

The last formula (48) can be deduced also in the following way. We introduce the auxiliary amplitude $r_{1,p}$ and phase $\delta_{1,p}$, as follows:

$$r_{1,p} e^{i\delta_{1,p}} = r_p' + r_p'' e^{-ix_1}; \tag{49}$$

for the auxiliary amplitude we get

$$r_{1,p}^2 = r_p'^2 + r_p''^2 + 2r_p' r_p'' \cos x_1, \tag{50}$$

and formula (48) may be written in the form

where

$$r_p^2 = r_{1,p}^2 + r_p'''^2 + 2r_{1,p} r_p''' \cos(x_1+x_2+\delta_{1,p}),$$
$$r_{1,p} \cos(x_1+x_2+\delta_{1,p}) = r_p'' \cos x_2 + r_p' \cos(x_1+x_2). \tag{51}$$

In this way the theory of the reflection of light from glass with one thin film is generalized into the theory of the reflection of light on glass with two thin films.

For normal incidence we write again

$$r_p' = -r_s' = \frac{n_1-1}{n_1+1} = A_1, \quad r_p'' = -r_s'' = \frac{n_2-n_1}{n_2+n_1} = A_2, \quad r_p''' = -r_s''' = \frac{n-n_2}{n+n_2} = A_3$$

and Eq. (47) has then the form

$$\tan\delta = \frac{-[A_2 \sin x_1 + A_3 \sin(x_1+x_2)]}{A_1 + A_2 \cos x_1 + A_3 \cos(x_1+x_2)}, \tag{52}$$

and

$$\rho = A^2 = A_1^2 + A_2^2 + A_3^2 + 2A_1A_2 \cos x_1 + 2A_2A_3 \cos x_2 + 2A_1A_3 \cos(x_1+x_2). \tag{53}$$

Equations (52) and (53) can be deduced directly from Fig. 4 (the phase δ_1 and δ are indicated with opposite signs). From the right-angled triangles 0 1 2, 0 1′ 2′, we obtain

$$\tan\delta_1 = \frac{-A_2 \sin x_1}{A_1 + A_2 \cos x_1}, \tag{54}$$

$$\tan\delta = \frac{-[A_2 \sin x_1 + A_3 \sin(x_1+x_2)]}{A_1 + A_2 \cos x_1 + A_3 \cos(x_1+x_2)}, \tag{55}$$

and from the vector triangles A_1A_2B, BA_3A, we get

$$B^2 = A_1^2 + A_2^2 + 2A_1A_2 \cos x_1, \tag{56}$$

$$\rho = A^2 = B^2 + A_3^2 + 2BA_3 \cos(x_1+x_2+\delta_1). \tag{57}$$

For the simple reflection of light from *glass with three thin films* we have written Eq. (22)

$$r_p e^{i\delta_p} = r_p' + r_p'' e^{-ix_1} + r_p''' e^{-i(x_1+x_2)} + r_p'''' e^{-i(x_1+x_2+x_3)}.$$

The phase δ_p may be calculated as follows:

$$\tan\delta_p = \frac{-[r_p'' \sin x_1 + r_p''' \sin(x_1+x_2) + r_p'''' \sin(x_1+x_2+x_3)]}{r_p' + r_p'' \cos x_1 + r_p''' \cos(x_1+x_2) + r_p'''' \cos(x_1+x_2+x_3)}. \tag{58}$$

The foregoing theory for the reflection of light from *glass with three and more films* may be generalized this way:

For the simple reflection on the boundaries I and II we have

$$r_{1,p} e^{i\delta_{1,p}} = r_p' + r_p'' e^{-ix_1}, \tag{59}$$

then we take the boundary III

$$r_{2,p} e^{i\delta_{2,p}} = r_{1,p} e^{i\delta_{1,p}} + r_p''' e^{-i(x_1+x_2)}, \quad \text{where} \quad \tan\delta_{1,p} = \frac{-r_p'' \sin x_1}{r_p' + r_p'' \cos x_1}, \tag{60}$$

and the boundary IV

$$r_{3,p} e^{i\delta_{3,p}} = r_{2,p} e^{i\delta_{2,p}} + r_p'''' e^{-i(x_1+x_2+x_3)}, \quad \text{where} \quad \tan\delta_{2,p} = \frac{-[r_p'' \sin x_1 + r_p''' \sin(x_1+x_2)]}{r_p' + r_p'' \cos x_1 + r_p''' \cos(x_1+x_2)}, \tag{61}$$

etc.

The formulae for the normal incidence on *glass with three thin films* can be deduced from Fig. 5. From the right-angled triangles 0 1 2, 0 1′ 2′, 0 1″ 2″, we obtain successively

$$\tan\delta_1 = \frac{-A_2 \sin x_1}{A_1 + A_2 \cos x_1}, \tag{62}$$

$$\tan\delta_2 = \frac{-[A_2 \sin x_1 + A_3 \sin(x_1+x_2)]}{A_1 + A_2 \cos x_1 + A_3 \cos(x_1+x_2)}, \tag{63}$$

$$\tan\delta = \frac{-[A_2 \sin x_1 + A_3 \sin(x_1+x_2) + A_4 \sin(x_1+x_2+x_3)]}{A_1 + A_2 \cos x_1 + A_3 \cos(x_1+x_2) + A_4 \cos(x_1+x_2+x_3)}, \tag{64}$$

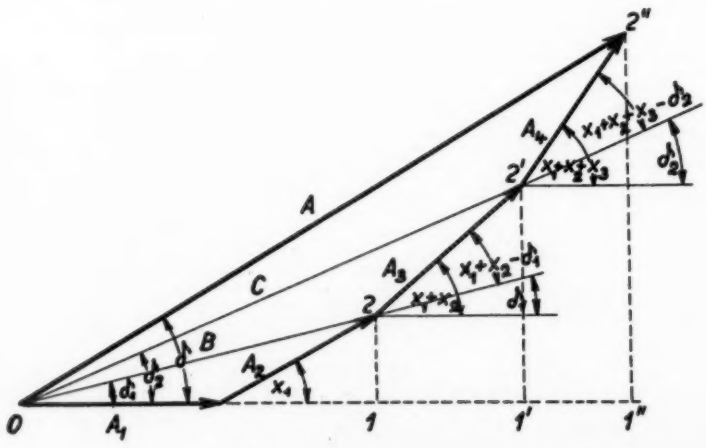

FIG. 5. The vector addition of the amplitudes A_1, A_2, A_3, A_4 with the path differences x_1, x_1+x_2, $x_1+x_2+x_3$.

and from the vector triangles A_1A_2B, BA_3C, CA_4A, it follows

$$B^2=A_1^2+A_2^2+2A_1A_2\cos x_1, \tag{65}$$

$$C^2=B^2+A_3^2+2BA_3\cos(x_1+x_2+\delta_1), \tag{66}$$

$$\rho=A^2=C^2+A_4^2+2CA_4\cos(x_1+x_2+x_3+\delta_2). \tag{67}$$

These calculations may be generalized for any arbitrary number of thin films on glass.

5. DOUBLE THIN FILMS ON GLASS IN THE OPTICAL PRACTICE

When we use only *one thin film* for the extinction of the undesirable reflecting power of the glass surface, then two conditions must be fulfilled: Strong's condition $n_1^2=n$, and the phase condition for the thickness of the film $n_1d=\lambda/4$. When the refractive index of the optical glasses lies between 1.5 and 1.7, then the refractive index of the film must be taken within the limit 1.23 to 1.30. But we have no materials with such a low refractive index. Therefore, we use materials with low refractive index—about 1.4—laid on glass as a thin film in very porous state. Then the reflecting power of the glass surface is very reduced, but in the most cases cannot be extinguished completely.

For *two thin films* on glass the following conditions for non-reflecting glass surface were deduced: for the refractive indices (38) $n_1^2n=n_2^2$, and for the thicknesses $n_1d_1=n_2d_2=\lambda/4$. The condition (38) may be fulfilled much easier than Strong's condition for one thin film. In this way new possibilities are opened for the technical practice. The author calculated the reflecting power of glass with the refractive index $n=1.6000$, which is covered with two thin films. The results for the various refractive indices of both films are arranged in the Table I. The equal values in the diagonal give the *normal reflecting power* of the *clean* glass with no films. This normal reflecting power is 5.325 percent. By convenient selection of the refractive indices of the films 1 and 2 the reflecting power of the glass surface may be controlled completely; this may be lowered or extinguished, but also can be considerably increased. Double films on glass can replace the half-silvered plates, which are used in the optical practice for dividing the intensity of the light into two parts in certain ordered ratio, with no loss.

TABLE I.

The reflecting power $\rho=\left(\frac{n_1^2n-n_2^2}{n_1^2n+n_2^2}\right)^2$ in percent

$n=1.6000$, $n_1d_1=n_2d_2=\frac{\lambda}{4}$

n_2 \ n_1	1.200	1.400	1.600	1.800	2.000	2.200	2.400	2.600
1.200	5.325	13.737	23.018	31.947	40.025	47.130	53.251	58.524
1.400	0.651	5.325	12.440	20.366	28.207	35.527	42.152	48.049
1.51789	0	—	—	—	—	—	—	—
1.600	0.277	1.023	5.325	11.482	18.367	25.312	31.947	38.097
1.77088	—	0	—	—	—	—	—	—
1.800	2.850	0.027	1.362	5.325	10.745	16.814	23.018	29.051
2.000	7.238	1.466	0.014	1.662	5.325	10.171	15.577	21.164
2.02386	—	—	0	—	—	—	—	—
2.200	12.601	4.564	0.693	0.118	1.926	5.325	9.692	14.570
2.27684	—	—	—	0	—	—	—	—
2.400	18.367	8.700	2.850	0.277	0.277	2.159	5.325	9.304
2.52982	—	—	—	—	0	—	—	—
2.600	24.169	13.411	3.623	1.741	0.075	0.460	2.363	5.325

If we consider only the simple reflections of light in films, then the glass surface with two thin films reflects no light when the following condition, deduced by B. Havelka, is fulfilled:

$$3(n_1^2n-n_2^2)+(n-1)n_1n_2$$
$$-(n_1n_2+n)(n_2-n_1)=0. \tag{68}$$

Considering multiple reflections we obtained this condition in the simple form (38) $n_1^2n=n_2^2$. If we choose the refractive indices of the glass n and of the lower film 2 n_2, we can calculate the

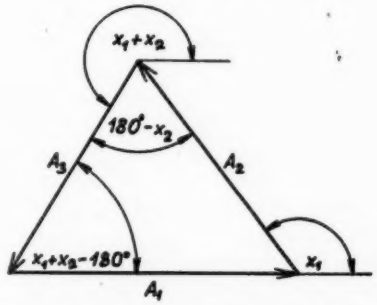

FIG. 6. The triangle of the amplitudes A_1, A_2, A_3 for solving the problem of extinguishing the reflected light from glass surface with two thin films considering the simple reflections of light in both films.

TABLE II.

The reflecting power $\rho=0$

	$n_2=1.80$		$n_2=2.00$		$n_2=2.20$	
n	n_1 simple refl.	n_1 multiple refl.	n_1 simple refl.	n_1 multiple refl.	n_1 simple refl.	n_1 multiple refl.
1.50	1.47232	1.46969	1.63887	1.63299	1.80657	1.79629
1.55	1.44798	1.44579	1.61180	1.60644	1.77681	1.76708
1.60	1.42477	1.42303	1.58593	1.58114	1.74835	1.73925
1.65	1.40260	1.40130	1.56119	1.55700	1.72108	1.71270
1.70	1.38139	1.38054	1.53750	1.53393	1.69495	1.68732
1.75	1.36109	1.36067	1.51480	1.51186	1.66990	1.66304

refractive index of the upper film n_1 from the two conditions. The results of these calculations are given in the Table II. We see that the results of these calculations are in both cases practically equal.

Taking into account the simple reflections in films, many calculations are considerably simplified. For example, we can achieve the non-reflecting power of the glass surface with two thin films not only for $x_1=x_2=180°$ and for condition (38), but in other cases as well. For the non-reflecting power of glass with two thin films according to Eq. (53) $\rho=0$; then the resultant amplitude must be $A=0$, i.e., the amplitudes A_1, A_2, A_3 give the closed triangle (Fig. 6). From this triangle we get

$$A_3^2=A_1^2+A_2^2+2A_1A_2\cos x_1, \tag{69}$$

$$\frac{\sin x_2}{\sin x_1}=\frac{A_1}{A_3}, \tag{70}$$

$$A_3=-A_1\cos(x_1+x_2)-A_2\cos x_2. \tag{71}$$

Choosing the refractive indices of films 1 and 2, n_1 and n_2, and of glass n we calculate

$$A_1=\frac{n_1-1}{n_1+1}, \quad A_2=\frac{n_2-n_1}{n_2+n_1}, \quad A_3=\frac{n-n_2}{n+n_2},$$

from Eq. (69) x_1 is calculated and substituted into Eq. (70), giving x_2. The formula (71) serves as a control of these calculations. One solution of such a calculation is given in Table III. The path differences x_1 and x_2 may deviate from 180° and the reflecting power of glass with two thin films $\rho=0$. The calculation was made for the refractive index of the glass $n=1.51824$. The thicknesses of the both films, d_1 and d_2, are calculated by

$$x_1=\frac{2\pi}{\lambda}2n_1d_1, \quad x_2=\frac{2\pi}{\lambda}2n_2d_2. \tag{72}$$

The further calculations show how the limits of the path differences x_1 and x_2 may be changed, if we try to keep the reflecting power of the glass coated with two thin films less than 0.005 or 0.01 etc. The starting formula is Eq. (53). These results are very important for the technical practice of producing such films.

TABLE III.

The reflecting power $\rho=0$

$n=1.51824$, $n_2=2.0000$

n_1	x_1	x_2	x_1+x_2
1.400	133° 04′ 17″	297° 13′ 48″	430° 18′ 05″
1.500	136° 48′ 20″	271° 15′ 00″	408° 03′ 20″
1.600	156° 00′ 30″	223° 15′ 23″	379° 15′ 53″
1.6231	180° 00′ 00″	180° 00′ 00″	360° 00′ 00″

JOURNAL OF THE OPTICAL SOCIETY OF AMERICA VOLUME 37, NUMBER 8 AUGUST, 1947

The Effect of Atmospheric Scattering Upon the Appearance of a Dark Object Against a Sky Background*

G. A. FRY, C. S. BRIDGMAN, AND V. J. ELLERBROCK
School of Optometry, The Ohio State University, Columbus, Ohio

(Received March 8, 1947)

A theoretical investigation has been made of the "ground-glass-plate effect" and the "edge effect" which are associated with the appearance of the dark object seen against a sky background. The problem has been simplified by assuming that the dark object and the observer are placed in an unbounded space filled with an atmosphere having uniform properties at all points. Rectangular and disk-shaped objects have been considered. The dark object produces its effect by intercepting the rays of light which would be transmitted directly to the observer and also rays which would be scattered one or more times between the object and the observer. In computing the distribution of brightness across that part of the field of view occupied by the object, consideration has been given to the rays which would have been transmitted directly to the eye and rays which would have been scattered once between the object and the eye, but not to scattering of a higher order. Equations for computing the brightness in a given direction with respect to the object have been developed.

INTRODUCTION

THEORETICAL and experimental investigations have been made to determine the distribution of brightness at different parts of an object, and its immediate surroundings, when it is viewed against a sky background through haze or fog.

Some investigators have considered the possibility that the size of an object affects the apparent brightness at its center and have referred to this influence as the "edge effect." There is some doubt whether this effect is sufficiently pronounced to warrant consideration.

It has also been considered that the atmosphere will make the edge of an object appear blurred. This has been referred to as the "ground-glass-plate effect."

In 1941 Middleton[1] presented a summary of the investigations of these effects which had been made up to that time. Since then Middleton[2] has presented a new paper on the theory of the subject, and more recently an experimental investigation has been reported by Duntley.[3]

The present paper represents a theoretical analysis of the "edge effect" and the "ground-glass-plate effect" for the case of a dark object surrounded on all sides by sky.

The dark object produces its effect by intercepting and absorbing rays of light that impinge upon it. Some of these rays would have been transmitted to the eye without being scattered, and their interception reduces the apparent brightness at all parts of the object but has no effect upon the appearance of the sky background.

Some of the rays, which are intercepted by the object, would have reached the eye after being scattered at one or more points in the atmosphere, and this is true for rays directed both toward the eye and also in other directions. The interception of these rays affects the apparent brightness not only at all parts of the object, but also at all parts of the sky background adjacent to the object.

In this investigation we have considered only the rays which would have been scattered once between the object and the eye. A higher degree of accuracy could be achieved by considering also the light which is scattered more than once, but calculations based on light scattered only once bring us close enough to the final answer to justify ignoring the scatterings of a higher order.

* The work described in this paper was carried out in part under Contracts OEMsr-66 and OEMsr-687 between the Office of Scientific Research and Development and The Ohio State University Research Foundation. The work has also received assistance through a grant for research in physiological optics from the Bausch and Lomb Optical Company.

[1] W. E. K. Middleton, *Visibility in Meteorology* (University of Toronto Press, Toronto, Canada, 1941), pp. 40–41, 56–57.

[2] W. E. K. Middleton, "The 'diffusing effect' of fog," J. Opt. Soc. Am. **32**, 139–143 (1942).

[3] S. Q. Duntley, "The visibility of objects seen through the atmosphere," J. Opt. Soc. Am. **36**, 359 (1946).

The real problem is whether it is necessary to consider scattering even of the first order.

FORMULATION OF THE PROBLEM

Let us consider the case of a rectangular dark object (Fig. 1) which is perpendicular to the line ET, which connects the point of observation (E) with the center (T) of the rectangle. The distance from E to T is designated by s. The distance from the center to the top edge of the rectangle is designated by y', and the distance to the lateral edge by x'.

The goal aimed at is to determine the distribution of apparent brightness (B) along the line YY' across the center of the dark object. P represents any point on the line YY' at an angular distance (μ) from the center of the rectangle.

In order to simplify the problem, it is assumed that both the observer and dark object are placed in an atmosphere which is unbounded and uniform in all of its optical characteristics at all points. It is also assumed that if it were not for the dark object, the apparent brightness measured at any point for any direction would be constant and would be equal to the general level of sky brightness (B') measured at E.

THE APPARENT BRIGHTNESS AT POINTS ABOVE AND BELOW THE OBJECT

If we pick out a point (P) which lies on the line YY' above or below the object, the apparent brightness (B) in the direction of P is determined by the light scattered toward the eye at all the points along the line EP extended to infinity.

Although the line EP passes above or below the dark object, the amount of light scattered toward the eye at any point H on the line EP is cut down by the dark object, because the object intercepts part of the light which is directed toward H and which is scattered at H toward E.

In order to determine the effect of the dark object upon the apparent brightness (B) in the direction of P, it is necessary to redefine B as equal to the general level of sky brightness (B') minus the loss in brightness produced by the object. In order to determine this loss in brightness, it is necessary to consider first of all the effect produced by a small area (ΔA) of the object which we may assume to be centered at the point (K) with coordinates (x, y).

The flux directed toward H which is intercepted by this small portion of the object is equivalent to the flux emitted by a surface having the same configuration and a brightness equal to B'.

The illumination ΔI at H is given by the following formula in which (l) is the distance between K and H, and ($\epsilon^{-l\sigma}$) is the transmission factor of the atmosphere between K and H, and β** represents the angle of incidence of the flux at the front or the back surface of the object as the case may be:

$$\Delta I = (B' \cos\beta \epsilon^{-l\sigma} \Delta A)/l^2. \tag{1}$$

Let ΔL represent the total number of lumens attenuated by a small volume of atmosphere (ΔV) at H and scattered in all directions.

$$\Delta L = \Delta V \cdot \Delta I \cdot \sigma. \tag{2}$$

In this equation σ represents the attenuation coefficient of the atmosphere. Although it is possible for part of the attenuated light to be absorbed, it is assumed in this investigation that it is all scattered.

The candlepower of the small volume of atmosphere in the direction of E, produced by light received from K and scattered toward E, is given by the following equation:

$$\Delta C = f(\phi) \cdot \Delta L. \tag{3}$$

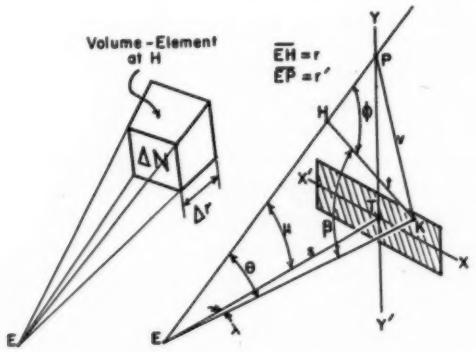

FIG. 1. Geometrical basis for calculating apparent brightness. A rectangular dark object centered at T is observed against a sky background from the point E. The figure illustrates specifically the loss in apparent brightness in the direction of P caused by the interception of light incident on the back surface of the object at K, which is directed toward H and which would have been scattered at H toward E if it had not been intercepted.

** For small values of λ it is satisfactory to assume that EK is perpendicular to the surface of the object.

In this equation $f(\phi)$ represents the scattering function which is nothing more than the ratio between the candlepower, at an angle ϕ from the direction of incidence, and the total amount of light attenuated and scattered in all directions.

For the purpose of defining the relation of the apparent brightness at P produced by the light from K which is scattered toward E, it is satisfactory to assume that the small volume of atmosphere at H has the form of a truncated cone or pyramid which has its apex at E, as shown in Fig. 1, has bases perpendicular to EP with an area (ΔN), and has a height (Δr). The volume (ΔV) is given by the following equation:

$$\Delta V = \Delta r \cdot \Delta N. \tag{4}$$

The apparent brightness (ΔB) in the direction of P is given by the following equation:

$$\Delta B = \frac{e^{-r\sigma} \cdot \Delta C}{\Delta N}. \tag{5}$$

It follows from Eqs. (1)–(5) that

$$\frac{\Delta B}{\Delta A \cdot \Delta r} = B'\sigma \frac{e^{-(t+r)\sigma} f(\phi) \cdot \cos\beta}{t^2}. \tag{6}$$

Since the quantity, $(e^{-(t+r)\sigma} f(\phi) \cdot \cos\beta)/t^2$, is a function of r, let us substitute the symbol $l(r)$ for it. Hence

$$\Delta B/(\Delta A \cdot \Delta r) = B'\sigma \cdot l(r). \tag{7}$$

If we define as B_{II} the loss in apparent brightness at P produced by the effect of the entire object upon the light scattered toward the eye at all points between E and P,

$$B_{II} = 2B'\sigma \int_{-y'}^{y'} \int_{0}^{x'} \int_{0}^{r'} l(r) dr dx dy. \tag{8}$$

By making certain approximations which are described in Appendix I, Eq. (8) reduces to,

$$B_{II} = 2B'\sigma e^{-s\sigma} f(\phi_0) \left[ZQ - \frac{2x'y'}{s} \right], \tag{9}$$

in which

$$Z = \int_0^{\frac{1}{2}\pi} \sin\phi \tan\phi \frac{f(\phi)}{f(\phi_0)} d\phi, \tag{10}$$

and

$$Q = \int_{-y'}^{y'} \int_0^{x'} \frac{dx dy}{[(y''-y)^2 + x^2]^{\frac{1}{2}}}. \tag{11}$$

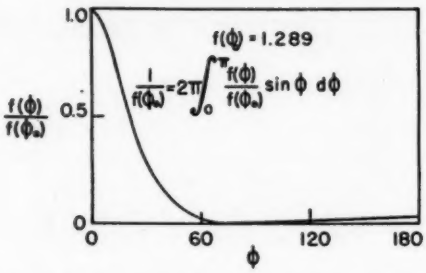

FIG. 2. Wiener's scattering function $f(\phi)$ for fog droplets.

Z is a factor whose value is determined entirely by the scattering function $f(\phi)$. Q is a factor whose value depends upon the size and shape of the object and the distance (y'') of P above or below T.

If we define B_{III} as the loss in apparent brightness at P produced by the effect of the entire object upon the light scattered toward the eye at all points on the extension of EP beyond P,

$$B_{III} = 2B'\sigma \int_{-y'}^{y'} \int_{0}^{x'} \int_{r'}^{\infty} l(r) dr dx dy. \tag{12}$$

The final equation for the apparent brightness (B) in the direction of a point P which lies on the line YY' above or below the object is:

$$B = B' - B_{II} - B_{III}. \tag{13}$$

The value of B_{III} is small with respect to that of B_{II} and hence may be dropped from Eq. (13), which reduces to

$$B = B' - B_{II}. \tag{14}$$

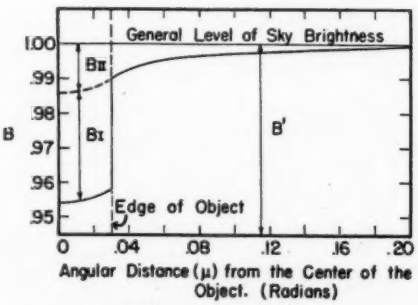

FIG. 3. Distribution of apparent brightness along the line YY' across the center of an object having an angular width of 0.06 radians.

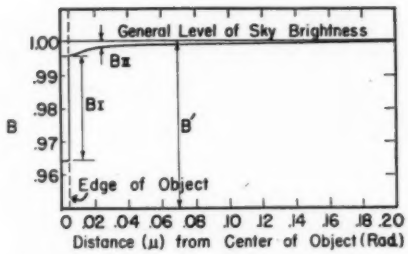

FIG. 4. Distribution of apparent brightness (B) along the line YY' across the center of an object having an angular width of 0.01 radians.

APPARENT BRIGHTNESS IN THE DIRECTION OF A POINT BETWEEN THE TOP AND BOTTOM EDGE OF THE DARK OBJECT

When P falls on the line YY' anywhere between the upper and lower border of the dark object, all of the light directed toward E originating at points on the extension of EP beyond P is intercepted by the dark object and hence in this case,

$$B = B' - B_{\mathrm{I}} - B_{\mathrm{II}}. \tag{15}$$

In this equation,

$$B_{\mathrm{I}} = B' e^{-\sigma s}, \tag{16}$$

and represents the loss in brightness produced by the interception of rays which are directed toward the eye and would have been transmitted through the atmosphere without scattering.

B_{II} represents the loss in brightness produced by the interception of light which would have been scattered toward the eye at the various points along the line EP. B_{II} in Eq. (15) is the same as in Eq. (14) and is defined by Eq. (9).

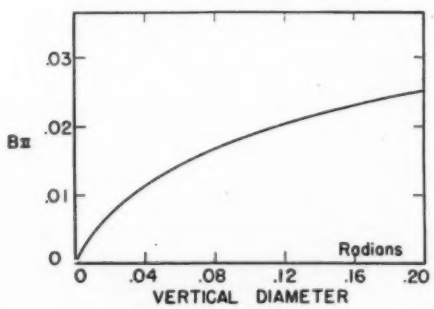

FIG. 5. Effect of varying the vertical diameter of the object on B_{II} at the center of the object.

AN EXAMPLE

Let us consider a specific case in which the dark object has a vertical angular width of 0.06 radians and a horizontal angular length of 0.12 radians. The distance (s) from the eye is 88 meters, the attenuation coefficient (σ) is 0.0391 per meter, and the $f(\phi)$ values are those given by Wiener[4] for fog droplets. (See Fig. 2.) For this set of $f(\phi)$ values, $Z = 0.3733$. The value for B' is 1 c/m^2.

In Fig. 3, the solid curve represents the distribution of brightness values (B) at points on the line YY' at various distances from the center of the object. These values have been calculated in accordance with Eqs. (14) and (15).

Figure 4, which is similar to Fig. 3, represents data for an object which has a vertical angular width of 0.01 radians, but is similar in all other respects to the object described above.

Varying the vertical angular width has no effect on B_{I} but does affect B_{II}. Figure 5 shows the effect of varying the vertical diameter of the object on the value of B_{II} at the center of the object. This constitutes the "edge effect."

If we define contrast by comparing the brightness measured at the center of the object and at a second point at a considerable distance from the object, the difference between the quantities measured corresponds to $B_{\mathrm{I}} + B_{\mathrm{II}}$. On the other hand we may define contrast in terms of the abrupt drop at the border. Since this drop at the border is equal to B_{I}, it is possible to use Eq. (16) to predict the drop from σ and *vice versa*. In order to measure the drop it is necessary to measure the brightness both of the object and of the sky at points as close as possible to the edge of the object.

The use of the drop at the edge of the object as an index of contrast is quite satisfactory in the case of small objects, because the B_{I} distribution is superposed on the relatively flat top of the B_{II} distribution. When the object is large, however, the B_{II} component is stronger in comparison with B_{I}; the edge of the object falls closer to the inflection point of the B_{II} distribution; and the gradients on the two sides of the border are more pronounced. It is conceivable that these gradients might have some effect on the appearance of the

[4] C. Wiener, Nova Acta d. k. Leop. Carol. Akad. d. Naturf. Halle **73**, 1–240 (1900); **91**, 1–292 (1909).

object and perhaps also upon the threshold of visibility. The effects of such gradients upon the appearance of the "textural quality" of color have been discussed in a previous paper.[5]

The answer to the question of the existence of the "ground-glass-plate effect" is that it is represented in the B_{II} distribution, but this "blurred-edge effect" is masked more or less by the "sharp-edge effect" of the B_I distribution, depending on the size of the object.

EFFECTS OF VARYING THE DISTANCE (s) AND THE SIZE OF THE OBJECT AND THE ATMOSPHERIC ATTENUATION (σ) ON B_I AND B_{II} AT THE CENTER OF THE OBJECT

In order to demonstrate these effects it is more convenient to use a disk-shaped object (Fig. 6) than a rectangular one. It is assumed that the disk-shaped object is perpendicular to a line TE connecting its center and the point of observation. The disk can be divided into zones Δv wide as shown in Fig. 6.

$$\text{Area of any zone} = 2\pi v \cdot \Delta v. \tag{17}$$

The apparent brightness (ΔB) at the center of the disk which is produced by a single zone is obtained by substituting $2\pi v \Delta v$ for ΔA in Eq. (7).

$$\frac{\Delta B}{\Delta v \cdot \Delta r} = 2\pi v B' \sigma l(r). \tag{18}$$

Since B_{II} is the sum of the ΔB values for all of the zones,

$$B_{II} = 2\pi B' \sigma \int_0^{v'} \int_e^{r'} l(r) \cdot v dr dv. \tag{19}$$

By making certain approximations described in Appendix I, Eq. (19) reduces to,

$$B_{II} = B' \sigma e^{-\sigma s} f(\phi_0) \cdot \pi \left(2Zv' - \frac{v'^2}{s} \right). \tag{20}$$

When the size of the object is specified in terms of radians, $v' = \theta' s$, and hence

$$B_{II} = B' \sigma s \cdot e^{-\sigma s} f(\phi_0) \cdot \pi (2Z\theta' - \theta'^2). \tag{21}$$

B_I is independent of the size and shape of the object and is given by Eq. (16). Dividing Eq. (21) by Eq. (16) we obtain

$$B_{II}/B_I = \sigma s f(\phi_0)(2Z\theta' - \theta'^2). \tag{22}$$

The ratio (B_{II}/B_I) is directly proportional to the distance (s) if the angular size of the object is kept constant. Figure 7 shows the relationship between B_{II} and B_I at various distances.

Equation (22) also shows that the ratio (B_{II}/B_I) is directly proportional to the attenuation coefficient (σ).

The angular size of the object does not affect B_I, but it does affect B_{II}. The effect on B_{II} is shown in Fig. 8.

LIMITATIONS

Although the relationships demonstrated in this analysis apply to a large variety situations, certain limitations must be recognized:

1. In order for Eqs. (9) and (16) to hold rigidly, the line of observation EP must be approximately parallel to the surface of the earth. The reason for this is that the atmosphere is not likely to be uniform at different levels above the earth's surface, and if EP is inclined, σ is not constant for the various points along EP. Furthermore the amount of solar illumination reaching the different layers of atmosphere parallel to the earth's surface varies considerably.

2. It cannot always be assumed that the

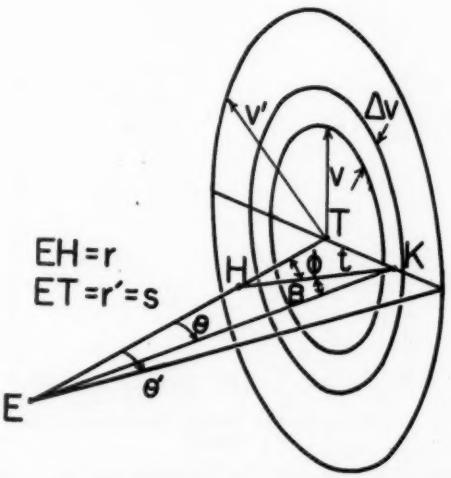

FIG. 6. Geometrical basis for calculating the apparent brightness at the center of a disk-shaped object.

[5] G. A. Fry, "The stimulus correlate of bulky color," Am. J. Psych. **43**, 618–620 (1931).

atmosphere between the object and the point of observation is uniform even though the line of observation is parallel to the surface of the earth.

3. The assumption that the illumination reaching the front or back surface of the object is uniform from all directions does not necessarily conform to reality. Particularly when the object is near the earth's surface, the light reflected from the earth's surface toward the object will be considerably less under most circumstances than the sky light above the horizon. Furthermore, sky brightness will vary at different angles of elevation, so that at least in the vertical direction the illumination reaching the front or back surface of the object is normally not uniform. In the horizontal direction there is greater chance of having uniform illumination from all directions, particularly when the sun is directly overhead.

4. Wiener's scattering data for different directions have been used in the above analysis. Wiener's data were worked out for fog droplets and are characterized by a preponderance of forward scattering. On the basis of this assumption, component B_{III} becomes negligibly small. In an atmospheric condition involving a larger amount of backward scattering, it may become necessary to take B_{III} into account.

5. It has been assumed that the attenuation is accomplished entirely by scattering. The theory could be modified to take absorption into account, merely by breaking the attenuation factor down into two components, using the sum of the two components in calculating attenuation, and using only the scattering factor in computing the total amount of light scattered by an element of volume.

6. The theory also fails to take into account the complications dependent upon the polarization and wave-length composition of sky light.

7. The object used in this investigation consisted of a small segment of a plane surface perpendicular to the line connecting its center and the point of observation. This type of object is most effective in intercepting flux directed parallel to the line of observation. It has little effect on the light flux perpendicular to the line of observation. It differs in this respect from a three-dimensional object such as a sphere which would be equally effective in intercepting light from all directions. The effect of using a surface instead of a three-dimensional object has been, therefore, to keep the B_{II} distribution more concentrated.

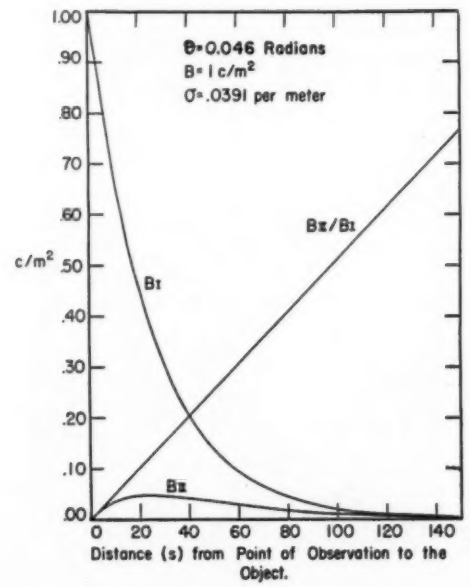

FIG. 7. The effect of distance on B_I and B_{II} at the center of a disk-shaped object when the angular size is kept constant.

APPENDIX I

Evaluation of $\int_0^{r'} l(r)dr$

This integral can be evaluated by the following method which is based on the proposition that

$$\int_0^{r'} l(r)dr = \int_{-\infty}^{r'} l(r)dr - \int_{-\infty}^{0} l(r)dr. \quad (1)$$

As long as θ is small and H falls between $-\infty$ and E, it may be assumed that

$$f(\phi) = f(\phi_0), \quad (2)$$

$$e^{-(r+l)\sigma} = e^{-s\sigma}, \quad (3)$$

$$\cos\beta = 1, \quad (4)$$

and

$$l = s - r. \quad (5)$$

Hence,

$$l(r) = \frac{e^{-s\sigma} f(\phi_0)}{(s-r)^2}, \quad (6)$$

and

$$\int_{-\infty}^{0} l(r)dr = \frac{e^{-s\sigma} f(\phi_0)}{s}. \tag{7}$$

As long as θ is small and H falls between E and P, it may be assumed that

$$e^{-(r+l)\sigma} = e^{-s\sigma}, \tag{8}$$

$$1/t = \sin\phi/v, \tag{9}$$

$$\cos\beta = \cos\phi, \tag{10}$$

and

$$dr = \frac{v}{\cos^2\phi} d\phi. \tag{11}$$

Consequently,

$$l(r) = \frac{e^{-s\sigma} f(\phi)}{v^2} \cos\phi \sin^2\phi, \tag{12}$$

and

$$\int_{-\infty}^{0} l(r) = \frac{e^{-s\sigma} f(\phi_0)}{v} \int_{0}^{\frac{1}{2}\pi} \sin\phi \tan\phi \frac{f(\phi)}{f(\phi_0)} d\phi. \tag{13}$$

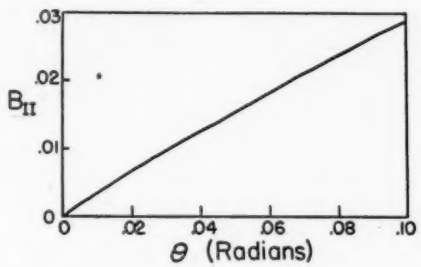

FIG. 8. The effect of changing the size of a disk-shaped object upon the value of B_{II} at the center.

It follows from Eqs. (1), (7), and (13) that

$$\int_{0}^{r'} l(r)dr = e^{-s\sigma} f(\phi_0)(Z/v - 1/s) \tag{14}$$

in which

$$Z = \int_{0}^{\frac{1}{2}\pi} \sin\phi \tan\phi \frac{f(\phi)}{f(\phi_0)} d\phi. \tag{15}$$

The value of Z is entirely determined by the scattering function $f(\phi)$.

JOURNAL OF THE OPTICAL SOCIETY OF AMERICA VOLUME 37, NUMBER 8 AUGUST, 1947

Improvements in Microscope Illumination

JAMES R. BENFORD
Bausch & Lomb Optical Company, Rochester, New York

(Received April 16, 1947)

A number of recent improvements in microscope illumination are discussed. Several applications of complex-shaped optical elements of transparent plastic are shown. A small fluorescent lamp designed for lower power microscopy is described. Two applications of movable condenser lens systems are given in which the illuminated field and aperture are concurrently varied by the lens motion. Some applications of high and low index interference films and of evaporated metallic films are described. The use of the new zirconium oxide source in microscopy is discussed.

FOR many years the two standard vertical illuminators for opaque microscope objects have been the half-aperture right-angle prism illuminator and the full-aperture thin glass plate set at 45° to the optical axis of the microscope. The prism illuminator is useful only for low power work; at the higher magnifications the illumination and image quality with half-aperture illumination are inferior. The inclined glass plate has found a wider field of usefulness, particularly in metallography, but with specimens of low reflectivity its low illuminating efficiency combined with reflected haze from the objective has limited its usefulness. The reflected haze can be very substantially reduced by low reflection films on the objective surfaces.

AN IMPROVED VERTICAL ILLUMINATOR

To increase the illuminating efficiency of the glass-plate vertical illuminator, high index films have been applied to one surface, increasing the illumination by about 2.5 times. The earliest commercially produced filmed vertical illuminators were coated with zinc sulfide[1] of index 2.3; but in recent months, with the improvement of techniques for applying titanium oxide, index 2.6, a change to the latter has been made, not only because of the increased efficiency, but also because of the greater hardness.

Unfortunately, the titanium oxide increased the reflectivity to such an extent that the multiple reflection between the filmed and unfilmed sides of the plate became strong enough to produce a faintly visible secondary image on specimens of extreme contrast. A quarter-wave film of magnesium fluoride on the second face eliminated this secondary image. A glass plate so coated with titanium oxide on one face and magnesium fluoride on the other, produces an image over 2.5 times as bright as an unfilmed plate.

Thus these filmed glass-plate vertical illuminators are beginning to approach the Foster calcite vertical illuminator[2] prism in efficiency. The Foster prism has an efficiency about four times that of an unfilmed glass plate, and is, to date, the most efficient vertical illuminator known.

LOW-POWER OBLIQUE ILLUMINATION

While these vertical illuminators have been successfully used in metallurgical microscopy, in other fields, such as botany and zoölogy, where the specimens are not truly opaque, some form of oblique or dark-field illumination has been found more useful.

For low power oblique illumination on the Greenough stereoscopic microscope the Nicholas illuminator has been widely used for some time. To increase the field of usefulness of the Nicholas illuminator, a unit having a focusable lens system has been designed. This design is capable of producing an even spot of light variable in size from 10 to 30 mm in diameter. For the higher magnifications a small intense spot is formed; for the lower powers the spot is made larger and less intense. The system employs the familiar Koehler illumination principle, the lamp con-

[1] As suggested by A. H. Pfund, J. Opt. Soc. Am. **24**, 99 (1934).

[2] L. V. Foster, "Polarizing vertical illuminator," J. Opt. Soc. Am. **28**, 124 (1938).

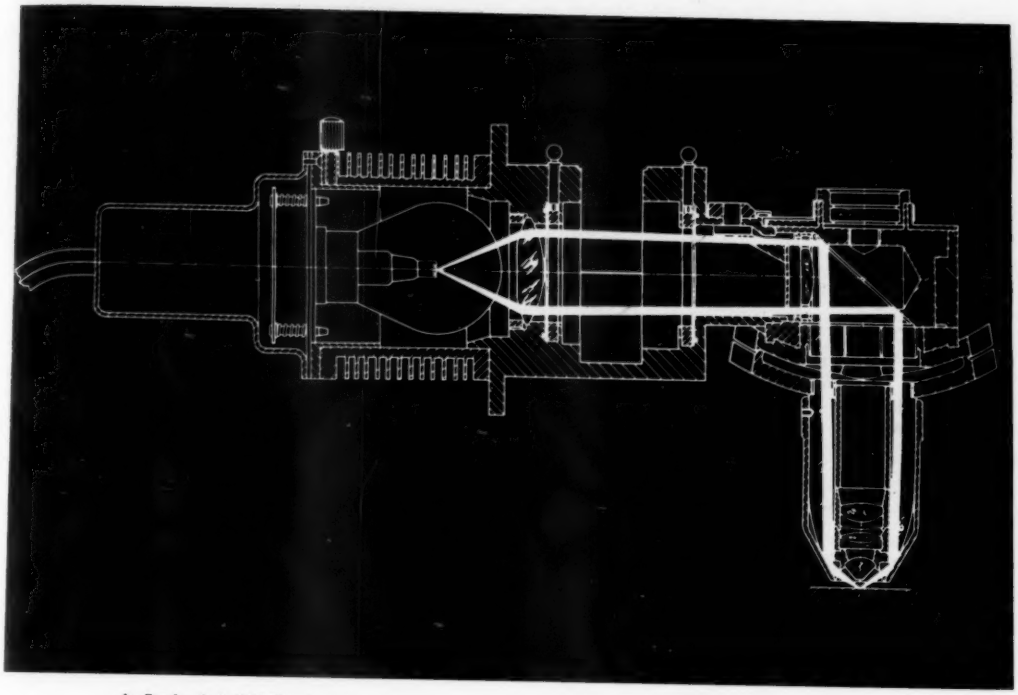

A. Set for dark-field illumination.

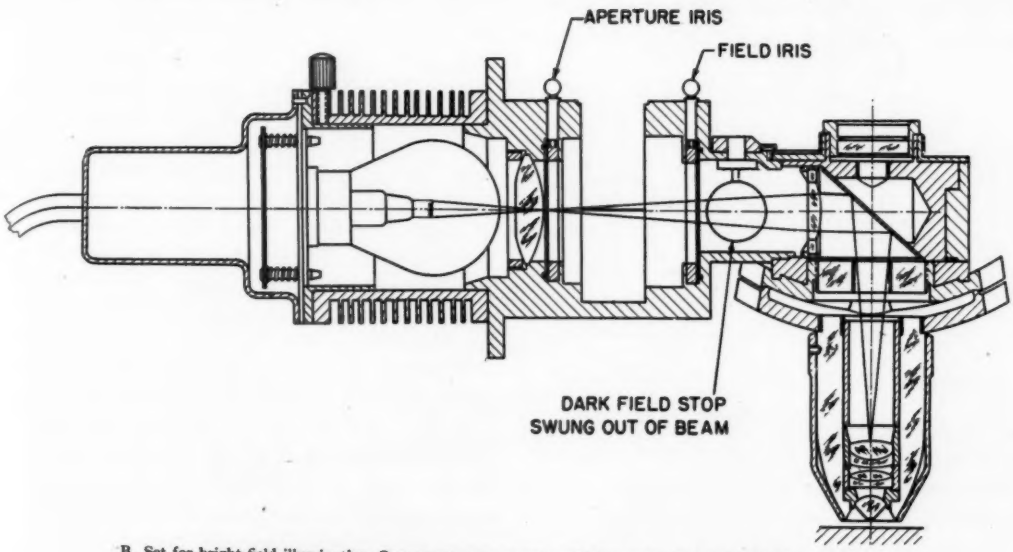

B. Set for bright-field illumination. Opaque stop swung out, and irises set for the desired field and aperture.

FIG. 1. Vertical illuminator for both bright- and dark-field illumination in reflected light.

denser being imaged on the specimen plane by the movable projection condenser. To make it possible to change the spot size without moving the whole unit, the projection condenser forms a

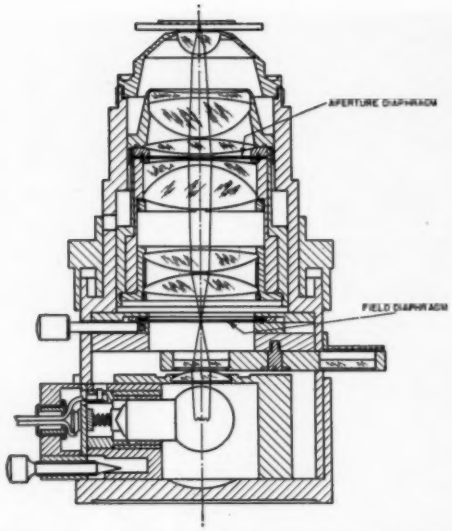

A. Low power. Movable lenses down. Aperture small. Field large.

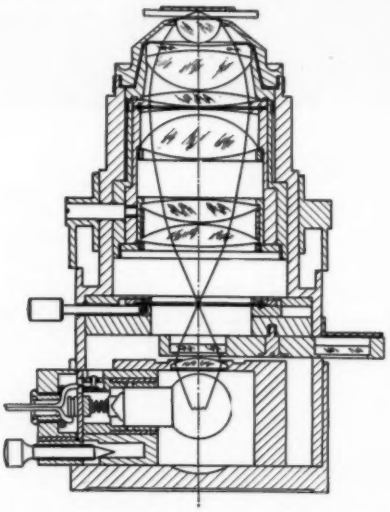

B. High power. Movable lenses up. Aperture large. Field small.

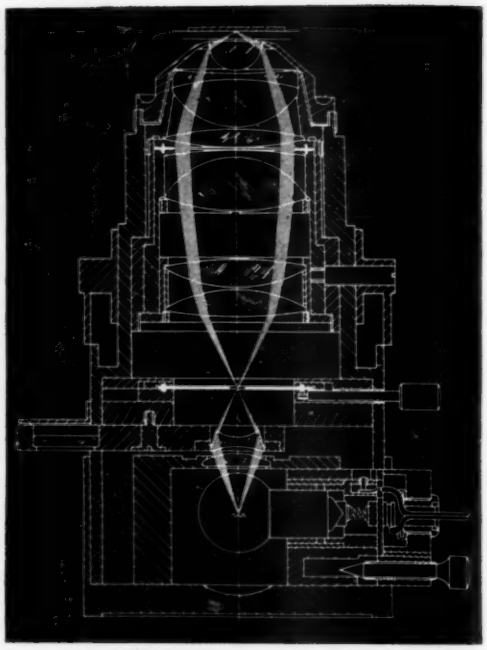

C. Dark-field. Lenses in high power position.

FIG. 2. A built-in substage illuminator. This unit fits the standard substage ring shown.

1:1 image of the lamp condenser at its mean position of travel. By this means a large magnification range without appreciable change of focus is made possible.

BRIGHT-FIELD—DARK-FIELD VERTICAL ILLUMINATOR

Figure 1 shows a unit designed for higher power bright-field and dark-field illumination of opaque and semi-opaque objects. In this unit considerable use is made of molded transparent plastic to form complex-shaped optical elements which could not well be made of glass. The objectives are mounted in cells within a transparent plastic body. The optical surfaces of the plastic body are molded, while the threads and bores are machined. The use of plastic, which can be threaded directly, permits making the objectives compact enough to go in a regular society thread multiple nosepiece, so that standard objectives can be used interchangeably.

With the dark-field stop swung out (Fig. 1B), and field and aperture irises closed down, the unit is converted to bright-field illumination. A flat diffusing spot on the condenser adjacent to the light source serves as the secondary source for bright field, while the outer (polished) portion of the lens forms the more intense dark-field beam. The vertical illuminator is a titanium oxide coated glass plate in the central bright-field portion, and is aluminized around its periphery for the dark-field illumination beam.

BUILT-IN SUBSTAGE ILLUMINATION

In the field of transmitted illumination a number of designs have been developed for built-in substage illuminators, one of which is shown in Fig. 2. The system is compact enough to fit into the standard substage ring, and employs a small 2 C.P. source, so that heat from the source is no problem. Fig. 2A is a cross section through the unit set for low power. Note the large spacing between the hemisphere and the next lower lens.

The transition from low to higher power is accomplished by a synchronous movement of internal lenses and aperture iris diaphragm. The iris controls the numerical aperture, and the lens motion controls the size of the illuminated field, the relative motion of lenses and iris being so synchronized that a correctly illuminated field is automatically obtained by setting the unit for the N.A. required by the objective. Fig. 2B shows the high power setting; the internal lenses have moved upward, and the aperture iris has fully opened up. The mechanism of this synchronous motion of iris and lenses is rather simple, being actuated by a large knurled outer ring connected to the mount of the inner lenses by a pin which passes through a helical slot in the casing. The turning motion causes the iris leaves to open and close in the normal manner, and the helical slot forces the lenses (and iris) up and down as the knurled ring is turned. The movable lenses, at the mean position of their travel, produce a 1:1 image of the field diaphragm. By this means it is possible to move the lenses through their full motion, and yet the field diaphragm stays adequately in focus, changing only in size.

In addition to controlling field and aperture, microscopists frequently require colored illumination to bring out contrast in stained or otherwise colored specimens. Polarized light is also coming to be quite universally used on microscopes for the examination of birefringent materials. Further, many types of microscopic objects are more readily seen in dark-field than in bright-field illumination. To include these various types of illumination in this instrument, a large rotatable disk containing numerous filters is mounted immediately above the lamp condenser. This disk contains red, green, blue, and daylight filters, a Polaroid disk, and a dark-field illuminator unit. All of these, except the dark-field unit, have lightly frosted surfaces to even out the illumination from the coil filament.

The dark-field unit, shown in Fig. 2C, is shaped like a biconcave lens with a polished

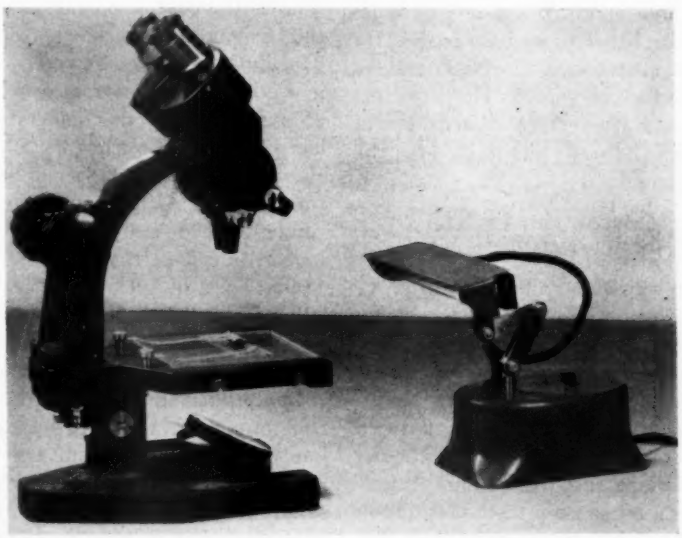

FIG. 3. A new microscope lamp employing the G. E. miniature 4-watt fluorescent tube

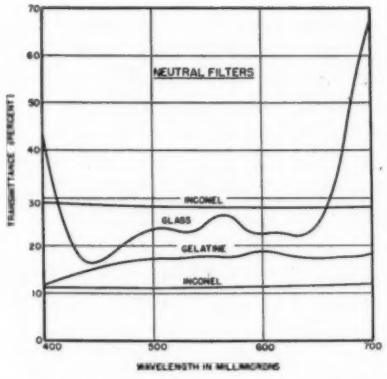

FIG. 4. Spectral-transmission curves of the Inconel film neutrals compared with glass and gelatine neutrals.

reflecting edge in the form of a surface of revolution. The central zone is blocked out by an opaque spot on the lower concave surface. This unit gives good dark-field results for objectives up to and including the 4 mm, 0.65 N.A. The field coverage is adequate for objectives as low as the 16 mm, 0.25 N.A.

MINIATURE FLUORESCENT TUBE ILLUMINATOR

In lower power microscopy the miniature 4-watt fluorescent tube (Fig. 3) has been applied as a diffuse source for the Greenough stereoscopic microscope. The source is provided with a reflector shield and mounted on a jack-knife type arm which fits either to its base or directly on the body of the microscope. The base contains the power supply for the source. The long life, cool operation, and convenient dimensions of this source make it well adaptable to the Greenough microscope.

THE ZIRCONIUM OXIDE ARC APPLIED TO PHOTO-MICROGRAPHY

Another source which undoubtedly will prove useful in microscopy is the new Western Union zirconium oxide concentrated arc. Some preliminary study has been made of the usefulness of this type of source, particularly for photomicrography. The study has taken the form of a performance comparison of the 100-watt zirconium oxide source against the common standard photo-micrographic sources, the 6-volt ribbon filament, the General Electric tungsten arc, and the 10-ampere, d.c. motor-driven carbon arc. The 100-watt zirconium source appears to be capable of providing good competition to these standard photo-micrographic sources.

The first point of comparison was brightness, and in this respect the zirconium source rated second, being about $\frac{1}{3}$ as bright as the carbon arc, about 1.4 times as bright as the tungsten arc, and about 4.3 times as bright as the ribbon filament.

From the point of view of color characteristics for natural color photo-micrography, the zirconium source appears to be about on a par with the carbon arc, and superior to the tungsten arc in which the strong mercury spectrum renders color work difficult. For convenient photoelectric color balancing and dependable exposure, however, the ribbon filament looks like the best of the four sources, because of its steady operation.

From the standpoint of source size, the zirconium arc is the poorest of the four, the largest commercially available zirconium source, the 100-watt type being smaller than the ribbon filament which already borders on being too small for convenient Koehler illumination designs. This shortcoming may be overcome, however. Mr. Buckingham of Western Union has provided us with experimental 400-watt zirconium sources of considerably larger area, and tests are under way on these sources.

To compare operating economy of the four sources the cost of operation was calculated on the basis of hours of use per dollar expenditure, distributing the original power supply, and lamp house investment over a 5000-hour total period of use and using the makers' data on average lamp life. On this arbitrary 5000-hour basis the zirconium source was about on a par with the tungsten arc for the lowest operating cost. The ribbon filament and carbon arc ran considerably higher, but since the highest cost came to only 15¢ an hour, no great emphasis is placed on this point. The ribbon filament and carbon arc can be under-volted to prolong their life, while the other two sources cannot.

In considering operating convenience, the zirconium source rates superior to the carbon arc, but less convenient than the tungsten arc or ribbon filament. The zirconium source power supply requires a brief "warm-up" period before operation. The carbon arc requires changing of carbons every 80 minutes, which is something of

a chore. The ribbon filament burns evenly and without fluctuation; the other three sources all wander and fluctuate in intensity during operation, which sometimes results in unevenly or incorrectly exposed photo-micrographs.

IMPROVED NEUTRAL FILTERS FOR PHOTO-MICROGRAPHY

In using these high intensity sources for photo-micrography, it is frequently necessary to cut down the brightness to a comfortable level for preliminary visual observations. Neutral filters are useful for this and in finding application in exposure control in photo-micrography. Dr. A. F. Turner has made an extensive study of the application of evaporated metal films for neutral filters. The best metal found was the stainless steel known as "Inconel." The standard smoke glass neutrals have never been really satisfactory because of their considerable departure from a true neutral, particularly in the higher densities. The Wratten gelatine neutrals are a somewhat better approach to neutral than the glass, but they are unable to withstand much intensity of illumination. The Inconel films can successfully withstand intense radiation and are considerably closer to a true neutral than either the glass or the gelatine, as can be seen from the spectral-transmission curves (Fig. 4).

A set of 2″ square Inconel neutrals has been designed for photo-micrography. The density value is stencilled on during the evaporation of the metal. A glass cover plate protects the metal film from abrasion. These filters should prove increasingly useful as color photo-micrography gains in popularity, as they permit controlled reduction of intensity without appreciable change in color temperature.

JOURNAL OF THE OPTICAL SOCIETY OF AMERICA VOLUME 37, NUMBER 8 AUGUST, 1947

The Most Favorable Absorption of the Phase Plate in Phase Contrast Microscopy

ARTHUR T. BRICE AND PAUL H. KECK
Ross, California

(Received April 1, 1947)

Accepting the conclusion of Zernike that phase structures in an object may be converted into apparent amplitude structures in its image by alteration of phase of portions of the light at the Fraunhofer diffraction spectrum, a simple relationship between intrinsic object contrast and optimum absorption of the phase plate is developed. For this purpose, the definition of contrast as the ratio of the brightness difference between adjacent small areas in the image to the greater brightness of the two is employed, and considered more suitable than the simple ratio of the brightest area to the darkest. The departure of biologic structures from the periodicity and grating constants characteristic of perfect object gratings is handled by means of a parameter defined as the ratio of the energy transmission by the null order of the diffraction spectrum to the total energy transmission by all orders admitted by the limited apertures of the microscope. Calculations based on the formula developed are given in the form of tables and graphs.

IN the application of the Zernike principle, now generally known as the phase contrast method, for forming images of transparent objects based on refractive index differences within such objects, and for increasing the contrast of images produced by the microscope, two means are employed—(a) phase alteration and, (b), absorption of the light transmitted by the zero-order maximum of the diffraction spectrum. It is not our purpose to deal with the subject of phase alteration, (a), in this paper, but to present some considerations with reference to absorption, (b), which have permitted us to develop a formula by means of which the approximate optimum amount of absorption to be incorporated in the "*Z*" disk or phase plate may be estimated for different structural types of objects.

Even for the simplest types of optical gratings

the calculation of energy transmission by the various orders of the diffraction spectrum presents a complicated mathematical problem. It is not our purpose to enter into the details of such a calculation, nor to discuss the theoretical considerations involved in image contrasts at interfaces, but only to give a simple calculation that yields a fairly close approximation and indicates the limits within which the precise values will fall, based on the general formula for contrast, namely, the ratio of the brightness differences between adjacent small areas to the larger brightness of the two.

It is well known that when the object consists of an ideal grating, having completely opaque strips and completely transparent slits, a Fraunhofer diffraction pattern is formed at the rear focal plane or exit pupil of the objective lens system, consisting of nicely separated maximal and minimal images of the light source, if it is not too large. Figure 1 shows some examples of the energy distribution within such a pattern for perfect grid structures of different dimensions. It is only necessary for us at present to deal with amplitude structures, as Zernike has shown that structures defined only by refractive index differences can be converted into essentially equivalent amplitude structures at the image plane by means of phase alteration as mentioned, (a) above. If the microscopic image of such a grid is a fairly good one, its contrast, K, will be about the same as that of the object, namely, 1 or 100 percent.

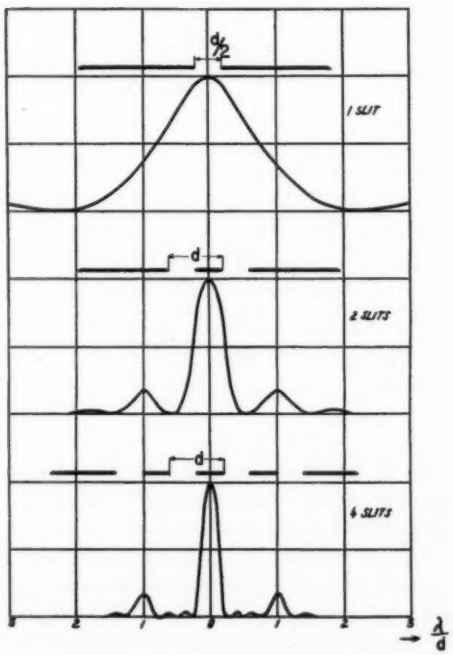

FIG. 1. Energy distribution of Fraunhofer diffraction patterns occuring from simple slit arrangements.

In order to establish a numerical relationship between the contrast and the energy transmission through the zero-order maximum, let Φ_0 be the total amount of luminous flux, expressed in lumens, which travels through the slits of the grating, then the quantity Φ_0 will again be found distributed within the maxima and minima of the diffraction pattern. Let us assume that this distribution may be described and handled mathematically by means of a parameter, α, which might be calculated according to the diffraction theory for any specified periodic object grating, but not for any much more complex object such as a biologic specimen. The precise value of α will depend on the structure of the object and the number of secondary maxima participating in the production of the image. We define this parameter as the ratio of the energy flux through the zero-order diffraction spectrum maximum to the total energy flux taking part in the production of the image by any given lens system.

α can accordingly vary between 0 and 1. Only in the case that no diffraction occurs at all, and the whole flux is through the zero-order maximum, can α become 1; and only in the case that the zero-order maximum is completely blocked in the exit pupil would α become 0. For our ideal periodic object grating, the light transmission through the zero-order diffraction spectrum maximum will be $\alpha\Phi_0$, and this value defines the essential condition for maximum attainable image contrast.

The question arises as to what relationship exists between the energy distribution within the diffraction pattern and the image contrast for values of K much smaller than 100 percent. Deterioration of contrast in the image below a theoretically attainable maximum, which results from scattered extraneous light, flare at the surfaces of lenses, and so forth, cannot be evaluated

precisely. It will depend on the skill of the microscopist and the quality of his preparations and instruments, and will differ in every instance. A certain proportion of the total deterioration of contrast, however, does result from limitations inherent in the microscope itself as heretofore designed, constructed, and used. The image is never formed by interference at the image plane between perfectly balanced distributions of light from the zero-order diffraction spectrum maximum and from all of the secondary maxima. A variable number of the latter are always eliminated from participation in the image formation by the grid characteristics of the object itself, and by the apertures and limited dimensions of the optical system, so that an excess of light from the zero maximum, which participates completely in the image formation, always overbalances the distribution from the secondary maxima. This excess covers the image plane as with a veil or luminous haze, and results in a reduction in contrast of the whole image.

If we let this excess of light from the zero-order maximum be represented by Φ_1, then assuming that we have to deal with an imperfect grating, the strips completely dark at perfect contrast before, now become illuminated by Φ_1, and the slits of the grating receive a flux of $\Phi_0+\Phi_1$, as illustrated in Fig. 2. The contrast now becomes:

$$K=(\Phi_0+\Phi_1-\Phi_1)/(\Phi_0+\Phi_1)=\Phi_0/(\Phi_0+\Phi_1). \quad (1)$$

Under these circumstances the flux through the zero-order diffraction spectrum maximum would be $\alpha\Phi_0+\Phi_1$, and to restore the original condition for maximum attainable contrast in which this value should be $\alpha\Phi_0$ it is only necessary to insert in the path of light transmission of the zero-order maximum a relative absorption A:

$$A=\Phi_1/(\alpha\Phi_0+\Phi_1). \quad (2)$$

Equations (1) and (2) may be converted into the following forms:

$$K/(1-K)=\Phi_0/\Phi_1, \quad (1a)$$

and

$$\alpha A/(1-A)=\Phi_1/\Phi_0. \quad (2a)$$

Substituting the ratio Φ_0/Φ_1, we obtain:

$$A=(1-K)/(1-(1-\alpha)K), \quad (3)$$

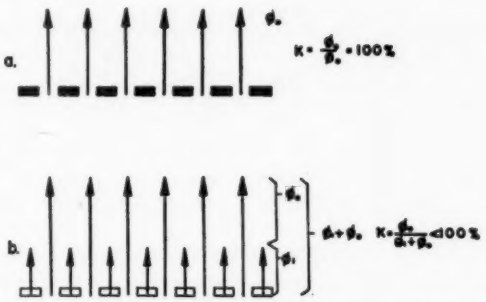

FIG. 2. Perfect amplitude grating (a) with 100 percent contrast; imperfect grating with transparent strips (b) and a contrast less than 100 percent.

which gives a simple relationship between the natural object contrast, which can be measured or estimated, and the optimum phase plate absorption. Should the absorption be increased beyond the limiting values given by this formula, (3), it would be expected that the secondary maxima would exercise a proportionately too great influence in the production of the image. The image would appear as though parts of the object were illuminated by oblique rays, and an essentially dark-field condition would be created in which reversed contrasts, i.e., dark objects appearing as bright ones, and *vice versa*, might result.

For purposes of observation of usual types of microscopic preparations, including biologic specimens for which the value of α cannot be precisely determined, it can be shown that the range within which α will reasonably lie is between 1 and $\frac{1}{2}$. The value $\alpha=1$, as has been explained, is an absolute limit that would only be reached if there were no structure at all. The other limit cannot be absolutely fixed but may be assumed to be not less than $\frac{1}{2}$ for the following reasons: Even with natural perfectly contrasty objects such as a well stained film of a single layer of erythrocytes a relatively greater amount of the total light energy will travel through the zero-order maximum than through the secondary maxima, because the field of view and optical apertures are limited as has previously been referred to; so that only a relatively small number of structure elements are effective in determining the diffraction pattern, and there is little periodicity about these, such as is the case with the ideal grating. As can be seen from

TABLE I. Absorption A.

K %	$\alpha=0$ %	$\alpha=\frac{1}{4}$ %	$\alpha=\frac{1}{3}$ %	$\alpha=\frac{1}{2}$ %	$\alpha=1$ %
90	100	25	18.2	14.3	10
75	100	50	40	33.3	25
50	100	75	66.7	60	50
25	100	90	85.7	81.8	75
10	100	96.5	94.7	93.2	90

Fig. 1 the energy of secondary maxima is decreased relatively in comparison to the zero-order maximum when this condition exists. It may further be reasoned that when the limit of resolving power of the system is called for by the nature of the object, as for example to visualize the metachromic granules of a diphteria bacillus or the hooks on ends of leptospira ichterohemorhagica spirals, the number of secondary maxima participating in the image formation is small and the transmission by the zero-order maximum relatively great, as established by Abbe's theory. It therefore is reasonable to conclude that in general the effect of the zero-order maximum transmission will be greater than the combined effects of all secondary maxima included, and that α will lie above $\frac{1}{2}$ in value for the vast majority of objects for microscopy. We therefore recommend for incorporation in the "Z" disk or phase plate absorption values not in excess of those indicated for that range of α by formula (3).

Table I gives a calculation of absorption values for different values of natural contrast of objects. It appears that the approximate values of optimum absorption do not differ very much in dependence on the object structure—within the recommended range. Table II shows the limits of absorption recommended for incorporation in phase plates designed for particular structures of determined natural contrast. Figure 3 presents the same calculation in graphic form, the optimal range being indicated by the shaded area. It is true that by application of the Zernike phase principle images of purely amplitude structures can be converted into phase structures and rendered invisible in the same sense that purely phase modifying structures can be converted to amplitude structures to be made visible, and that, therefore, when both phase and absorption controls are applied, microscopic structures or portions of them may be eliminated from the image by the phase control incorporated into the system, leaving nothing upon which the absorption control might operate to improve that contrast. It is also true that our formula and tables do not take this theoretically possible effect into account in any way. It is, however, unlikely that any natural object for microscopic observation may have the characteristic of a pure amplitude structure, i.e., exert no phase influence whatever. Such a theoretical ideal is only approached in very meticulously prepared artificial object gratings. Natural objects will in general exert some phase modifying influence at the same time as the amplitude modifying influence on the transmitted light. But let us assume that such an effect might be caused by some particular microscopic preparations. The result for all practical purposes would simply be to elevate the object to a position of lower natural contrast in our formula or table, calling for higher absorption values to attain maximum possible improvement of its image. The formula and table may therefore justly be claimed to incorporate an additional safety factor against the danger of too great absorption and reversed contrasts, provided the natural contrast to enter the table may have been determined by the usual bright field method.

In conclusion, it may again be pointed out that living biologic preparations for the observation of which the Zernike phase contrast method is outstandingly superior to all others, may never be expected to have the optical characteristics of perfect gratings for which only these calculations are strictly valid. It is quite reasonably certain, however, that all such preparations will fall within the limits recommended, and, if such limits are strictly observed, that reversed

TABLE II.

Natural object contrast K in %	Optimum phase plate absorption A in %
1	99–99.5
2	98–99
5	95–97
10	90–95
25	75–86
50	50–67
75	25–40
90	10–18

contrast will not occur as a result of the absorption value of the phase plate alone.

As to the desirability of constructing phase plates with absorption values up to such limits, however, for biologic work we must remember that living micro-organisms are generally quite photo-sensitive, and that if we include a high absorption value in the phase plate we must increase the intensity of illumination of the object accordingly. A standard "soft" plate with relative absorption/transmission ratio between 50/50 and 75/25 would be suitable for prolonged observation of living photo-sensitive specimens or time-lapse photography. A standard "hard" plate of ratio between 90/10 and 95/5 is to be recommended for maximum contrast and short visual inspections for purposes of identification of unknowns. In such work the problem of reversal of contrasts is of little practical importance to the microscopist who knows his specimens and the thickness of his preparations.

We desire, further to point out that it does not follow from any considerations touched upon in this paper, such as the natural contrast of objects, that we recommend either a phase and absorption control specifically designed to suit the character of the object under investigation, or a completely flexible system of phase and absorption control. Under such conditions the microscopist would be faced by a complexity of variables in both his instruments and its objects. When images are produced, as by the Zernike system, which are resultant of differences of a fraction of the wave-length of the light, the thickness of the preparations as well as their refractive indices introduces variable elements of proportionately far greater effect and significance than the limits of phase and absorption control that are possible. It will, therefore, be more practical to use fixed values of phase and absorption alteration which are known to be most sensitive over a wide range, and vary the thickness of the preparations, than to attempt to hold the thickness of preparations constant while varying the phase and absorption controls.

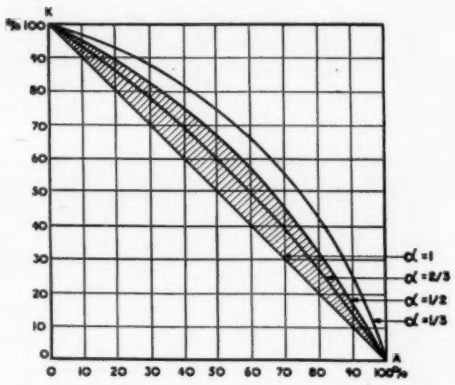

FIG. 3. Representation of Eq. (3): $A=(1-K)/(1-(1-\alpha)K)$. Absorption A *versus* contrast K.

BIBLIOGRAPHY

K. Bratuschek, Zeits. wiss. Mikroskopie **9**, 145–160 (1892).
Deutsches Reichspatent Nr. 636, 168, Klasse 42h, Einrichtung zur Verdeutlichung optischer Abbildungen, Gruppe 610 (1936).
F. Zernike, "Diffraction Theory of the Knife-Edge-Test and Its Improved Form. The Phase Contrast Method," M. N. R. A. S. **94**, 377 (1934).
F. Zernike, Physika **1**, 689 (1934).
F. Zernike, Zeits. f. tech. Physik **16**, 454 (1935).
F. Zernike, Physica **9**, 686, 974 (1942).

JOURNAL OF THE OPTICAL SOCIETY OF AMERICA VOLUME 37, NUMBER 8 AUGUST, 1947

The Nature of the Light Emitter in Photo-Flash Lamps

FRANK G. BROCKMAN
Philips Laboratories, Inc., Irvington-on-Hudson, New York
(Received June 13, 1947)

On the basis of experimental evidence, it is concluded that the light emitter in wire-filled photo-flash lamps is an incandescent vapor. In the course of this study the relative spectral energy distribution curves of two common types of photo-flash lamps were obtained.

INTRODUCTION

ALTHOUGH photo-flash lamps have become commonplace since their introduction[1] and although their characteristics have been the subject of a certain amount of investigation,[2] the question as to the nature of the light emitter has been left unanswered. By implication, Forsythe and Easley[2] look upon the emission as thermal radiation from a solid, since they refer to the emissivity of the aluminum oxide which is the product of the combustion in the lamps studied by them. Because the nature of the process poses questions of fundamental interest, an investigation was undertaken, the chief purpose of which was to attempt to explain the nature of the emitter.

This paper contains a description of the experiments which were performed, an analysis of the experimental results, and a statement of the conclusions to which they lead. In all cases, the lamps studied were of the wire-filled type, in which the filling was either aluminum or aluminum-magnesium alloy wire, with oxygen gas at about 50 cm of mercury pressure. Included in the results are the spectral-energy distribution curves of two common types of photo-flash lamps.

From three of the various experimental approaches tried, it is possible to draw a conclusion regarding the nature of the emitter. The conclusion common to these three is that the emitter is an incandescent gas.

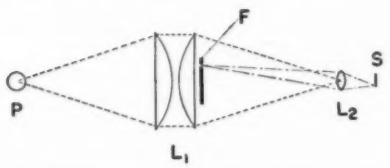

FIG. 1. Experimental arrangement for recording the variation of the spectrum during the flash:

P Photo-flash lamp under study
L_1 Condensing lens, 16.7-cm diameter, 12.5-cm focal length
F Focal plane shutter of camera, slot travel 8 cm from top of diagram to bottom, slot width 0.32 cm, slot length 10.7 cm
L_2 Anastigmat lens, 5 cm focal length, *f*:1.9, attached to lens board of camera
S Slit of medium quartz spectrograph, length 2 cm

THE VARIATION OF THE SPECTRUM DURING THE FLASH

Forsythe and Easley,[2] as well as van Liempt and DeVriend,[2] have photographed the spectra from photo-flash lamps, but in both cases the exposures were made over the full time of the flash. By means of the experimental arrangement of Fig. 1, it has been possible to record the spectrum as a function of time throughout the entire duration of the flash, and to draw some conclusions as to the nature of the emitter from these results.

In the assembly schematically shown in the figure, the lens, L_2, is carried on the lens board of a camera equipped with a focal plane shutter, *F*. The lens, L_2, serves to focus an image of the slot in *F* upon the slit, *S*, of the spectrograph. As the slot moves downward its image is thus made to scan the slit of the spectrograph. The condensing lens, L_1, is large enough to cover the focal plane shutter and is used to focus the light from the photo-flash lamp in the center of the lens L_2.

The time of travel of the shutter slot was found to be 30 milliseconds for the 8-cm distance. This calibration was made by photographing a discharge lamp operating on 60 c.p.s. a.c. The time for the slot to traverse a distance equal to its width was thus about 1 millisecond. The image

[1] The photo-flash lamp was introduced in 1931 as a sealed glass bulb charged with aluminum foil about 0.00004-cm thick. This was superseded in 1936 by the wire-filled lamp of the design now common.

[2] Forsythe and Easley, J. Opt. Soc. Am. **21**, 685 (1931); Forsythe and Easley, *ibid.* **24**, 195 (1934); van Liempt and DeVriend, Philips Tech. Rev. **1**, 289 (1936).

Wave-length (Angstroms $\times 10^{-2}$)

Early part of flash

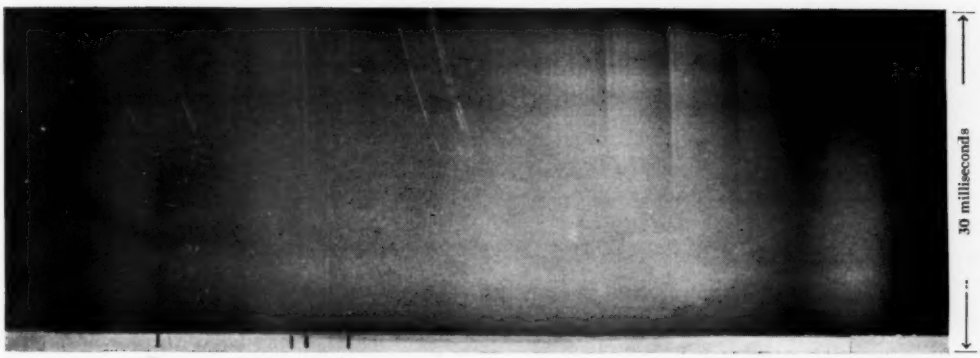

Early and middle parts

Middle and end parts

FIG. 2.

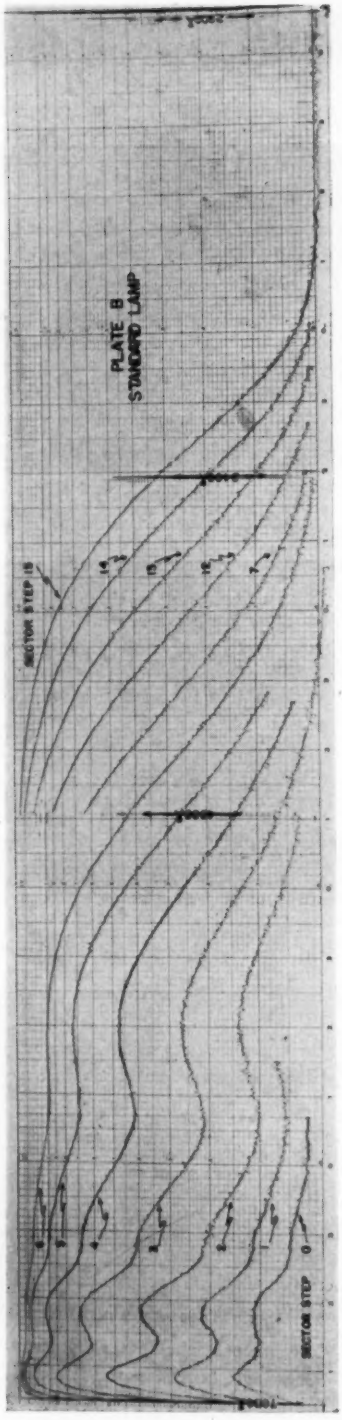

FIG. 3. Microphotometer density record for standard lamp. The wave-length scale on Fig. 4 applies to this record.

of the slot traversed the spectrograph slit in a time which was about one-half the time for the complete flash of the bulbs studied here. By suitable synchronization, however, it has been possible to record the beginning, the middle portion, and the end of the flash, though of course from different bulbs.

The outstanding characteristics of spectrograms obtained in this manner are the following:

(a) A band spectrum from about 5400A to 4400A, identified as the spectrum of AlO.

(b) Aluminum lines at 3944A and 3961A. These lines invariably broaden as the flash progresses and have been observed to reverse during the latter part of the flash.

(c) A broad reversed line at about 3720A. This is due to the absorption of the unresolved three most sensitive lines of the arc spectrum of iron.

(d) A line at 4045A which broadens and reverses as the flash progresses. This is from the unresolved third and fourth most sensitive lines of the arc spectrum of potassium.

(e) A broad absorption about 50A wide at about 5000A. Since this absorption did not appear in the spectra from lamps charged with aluminum but only from those with aluminum-magnesium alloy, we have tentatively ascribed this to a reversal caused by MgO, since the strongest bands of the MgO emission spectrum appear at 5007A.

(f) A line due to the unresolved yellow sodium doublet.

Figure 2 is a reproduction of three typical spectrograms. The one at the top was synchronized so that the early part of the flash was recorded, that in the middle is a record during the early and middle part, and the one at the bottom records the spectra during the middle and end of the flash. The reversals of the Al and K lines are to be seen at the bottom of the middle record. The reversal of the Fe lines is evident in all three.

From the observations recorded above, we may conclude that a substantial portion of the radiative process takes place from substances which are in the vapor phase. This conclusion can be based on the behavior of the aluminum lines alone. In the early part of the flash, when the vapor pressure is relatively low, the lines are sharp. As the flash progresses these lines are broadened. This broadening can be attributed to increasing vapor pressure. The reversal observed occasionally indicates that the combustion process is, in these cases, occurring in a region such that the radiation traverses a path of aluminum vapor not yet involved in the combustion. At the end of the flash, when the visible radiation has

diminished to a low value, the pressure-broadened lines again become sharp as the vapor pressure diminishes. The presence of the bands of aluminum oxide throughout the entire duration of the flash demonstrates the presence of aluminum oxide in the vapor phase.

The presence of elements other than aluminum and magnesium is due to the ignitor and to impurities from the lead-through wires and the glass.

SPECTRAL ENERGY DISTRIBUTION AND THE EQUIVALENT BLACKBODY TEMPERATURE

Forsythe and Easley[2] have determined the spectral energy distribution of aluminum foil photo-flash lamps and have estimated an equivalent blackbody temperature of 3500°K for these lamps.

Since it has been reported[3] that aluminum-magnesium alloy photo-flash lamps have a greater actinic effect than comparable aluminum lamps, we have determined the relative spectral energy distribution of two sizes of commercial aluminum-magnesium wire-filled bulbs.

Forsythe and Easley[2] used a monochromator equipped with a photo-cell at the exit slit. The total amount of light energy at a chosen wave-length was computed from the throw of a ballistic galvanometer connected in the photo-cell circuit.

Because of the comparative experimental simplicity of the photographic procedure, this method of obtaining the energy distribution was chosen for the present work. The simplification in experimental technique is, however, offset by the tedious analysis of the data.

The procedure that was used consisted in recording, through a logarithmic step-sector, two exposures of a standard tungsten lamp calibrated at the Electrical Testing Laboratories, New York City, for a color temperature of 2850°K. The two exposure times were in the ratio of about 1 to 17, so that a full range of densities was recorded at all wave-lengths of interest. The third exposure on each plate was that of two photo-flash bulbs fired consecutively, also through the step-sector. The sector was rotated at 5000 r.p.m. and the disk had steps on each semicircle, so that the complete range of the sector was traversed every 6 milliseconds. This was considered to be sufficiently fast for

[3] U. S. Patent 2,037,101.

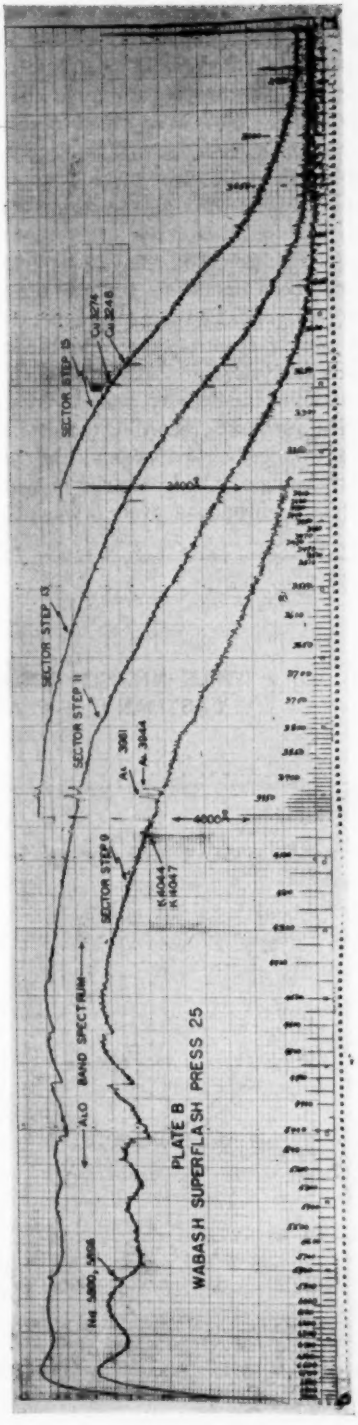

FIG. 4. Microphotometer density record for photo-flash lamp. The wave-length scale at the bottom of this record was obtained by scanning the scale as photographed on the plate. The density data of both Figs. 3 and 4 are from exposures on a single photographic plate.

the duration of the flashes studied here, which was about 120 milliseconds for the two bulbs. The wave-length scale of the spectrograph was printed on the top and bottom of each plate. Several reference lines were ruled across the plates at chosen wave-lengths. The accuracy of the wave-length scale was tested against 31 known spectral lines through the region 3000 to 7000A and was found to have an average error of +11A. As high precision was not required, no attempt has been made to correct the scale readings in this work. The spectrograph used was a medium quartz spectrograph, and the plates used for this analysis were Eastman 103-F.

The densities of the exposed plates were determined with an automatic recording densitometer* in which the recording paper and the photographic plate being scanned were run in synchronism. By this synchronous feature it was possible to record the wave-length scale and the densities of the various steps in accurate register so that densities could be determined at chosen wave-lengths with ease. Figures 3 and 4 are reproductions of such density records.

The procedure in the analysis of the data was as follows:

I *Standard Lamp Spectrogram Densities*

(a) Densities at 100A intervals from 3300A to 7000A for each sector-step recorded were tabulated.

(b) Using the relative exposure factors for the step sector, gamma-curves were plotted from the data of (a). These were composite curves constructed from data taken over a limited spectral region. From the rate at which the gamma changed, it was decided that 5 different curves would adequately cover the range 3000A to 7000A.

(c) From (a) and (b) it was then possible to tabulate relative exposures at 100A intervals. By the use of the gamma-curves, densities were converted into relative exposures. This operation was performed for each step which

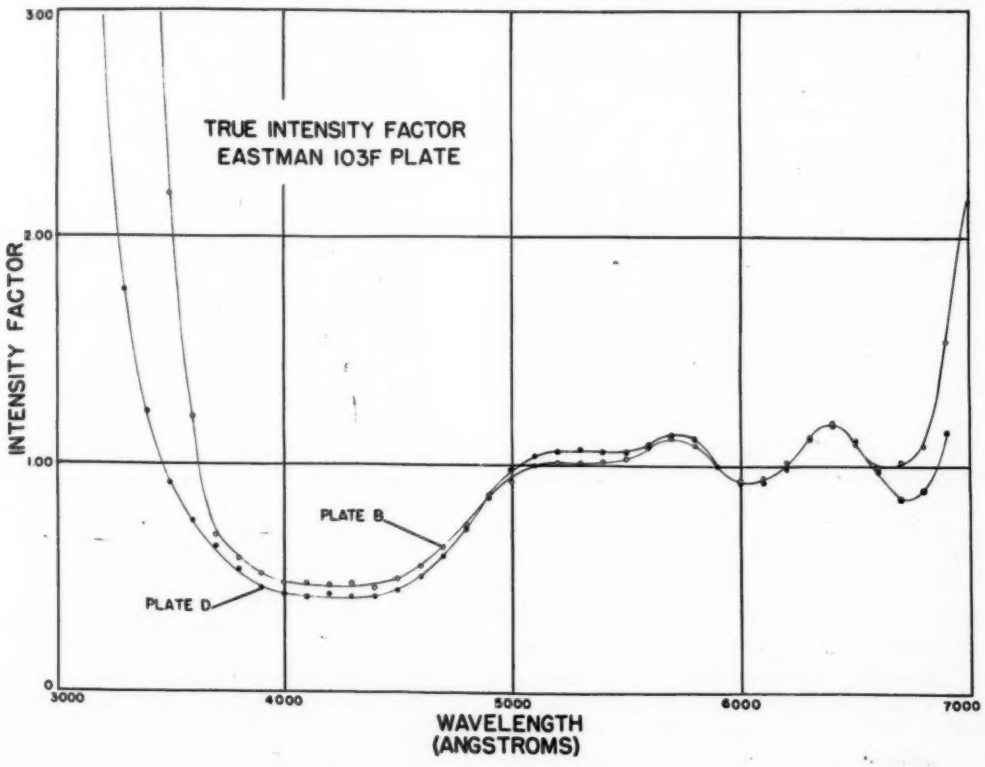

FIG. 5.

* Acknowledgment is made of the courtesy of the Socony-Vacuum Research Laboratories in permitting the use of their microphotometer for these measurements.

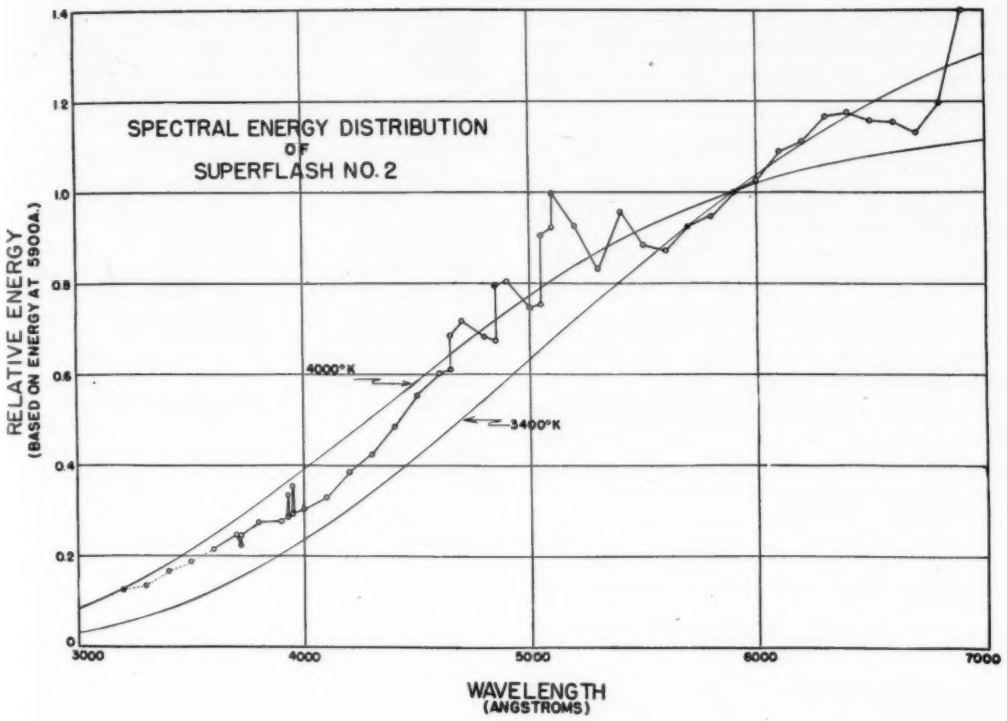

FIG. 6.

gave useful densities. When the step-relative exposures were adjusted to an effective common basis by multiplying each exposure by the corresponding sector factor, an average relative exposure for that wave-length was obtained. Since each gamma-curve has as abscissae only relative exposures which were arbitrarily chosen, it was necessary to reduce all data to some common basis. Accordingly, the data from each gamma-curve were carfully overlapped by making 10A (or 50A, depending upon the region) readings of densities and exposures for short overlapping regions. Ratios so obtained permitted the data to be reduced to a final common-basis relative exposure.

(d) Assuming reciprocity between exposure and intensity, relative photographic intensities, corresponding to the spectral distribution of the standard lamp intensity, were next tabulated at 100A intervals. These relative photographic intensities were taken so that the intensity at 5900A was unity.

(e) Finally, a factor which is here referred to as a "true intensity factor" was obtained at each wave-length. This factor is the 2850°K blackbody relative intensity** (intensity at 5900A as unity) divided by the relative photographic intensity of (d).

The steps (a) to (e) were performed to supply a working curve by which it is possible to correct for the variation of sensitivity of the photographic plate with wave-length. Figure 5 is a reproduction of "true-intensity factor" curves obtained by two different experiments. The agreement between the two is good, especially when the difficulties of the photographic process as a means for quantitative measurement are considered.

The steep rise in these curves below 3800A cannot be attributed to the photographic emulsion, but is the result of a decrease in transmittance of the standard-lamp glass envelope. In the absence of accurate quantitative information on this effect, the analysis of the results presented in this paper is based on the assumption that the photographic sensitivity is relatively constant from 3000A to 3800A and equal to that at 3800A.

** These data are contained in the Bureau of Standards Miscellaneous Publication No. 86, "Tables of Spectral Energy Distribution and Luminosity for Use in Computing Light Transmissions and Relative Brightness from Spectrophotometric Data," by J. F. Skogland.

For this reason the curves in Figs. 6 and 7 are drawn as dashed lines below 3600A to indicate the fact that the reliability of those points is not high.

II *Photo-flash Lamp Spectrogram Densities****

Steps (a)–(d) were the same as with the standard lamp.

(e) True relative intensity at each wave-length was obtained by multiplying the relative photographic intensity at that wave-length by the true intensity factor for this same wave-length.

The spectral energy distributions determined in this manner for two types of flash lamps are reproduced in Figs. 6 and 7. In Fig. 6 the distribution curves for a blackbody at 3400°K and 4000°K are included, and it is seen that the experimental curve for the flash bulb in general lies between the blackbody curves for these two temperatures. The experimental curve in Fig. 6 applies to a commercial photo-flash lamp with a rating of 70,000 lumen-seconds output and 3,500,000 lumens peak.

Figure 7 is a similar illustration of the experimental curve for a commercial lamp rated at 25,000 lumen-seconds output and 1,400,000 lumens peak.

It is observed that the experimental data of Figs. 6 and 7 are in good agreement, that the deviations of the spectra from a blackbody spectrum are chiefly due to the energy in the AlO band spectrum and that the equivalent blackbody temperature approaches 4000°K.

Two questions may be raised at this point. The first asks how the continuous spectrum is produced; the second,

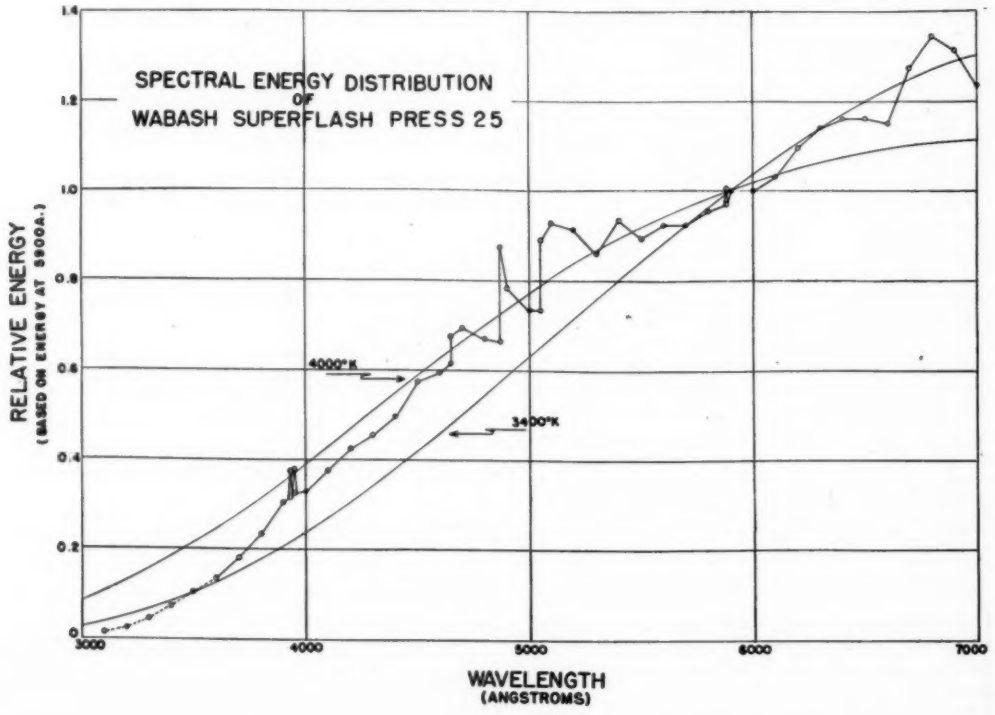

FIG. 7.

*** In analyzing these data it was found that, as regards the determination of the relative exposures for the various sector-steps at single wave-lengths, the gamma-curves prepared from the standard lamp exposures did not yield as consistent values for the unknown lamp exposure as for the standard. This was true even though each plate carried standard lamp calibration exposures. For this reason composite gamma-curves were also prepared from the densities at various sector-step exposures for the flash lamp. Relative exposures for this lamp were then obtained from these curves. This behavior was not investigated further, but it may be a manifestation of departure from the reciprocity law, since the ratio of the exposure times for the unknown and the standard was as great as 1:2000.

whether it can be compared with blackbody radiation at all, since blackbody radiation presupposes some kind of thermal equilibrium. Thermal equilibrium, of course, is not attained in this process.

The first question can be answered by recalling that in combustion processes great quantities of free electrons and ions are produced. The recombination process and other processes which can occur in a high temperature mixture of electrons, ions, and neutral molecules will produce a continuous spectrum.

With respect to the second question, the experimental curves of Figs. 6 and 7 show, in the regions free of bands, the shape of blackbody-radiation curves for the temperatures as indicated in the diagram. If some constant emissivity is assumed, then the temperature must be at least as great as those indicated.

As regards the departure from a blackbody-emission curve, the added flux caused by the AlO band spectrum is about 3 percent of the total flux in the region from 3000 to 7000A. However, the relative actinic effect of the added flux is considerably greater than this percentage figure would indicate, since these bands lie in the blue and green portions of the spectrum.

The fact that the equivalent radiation temperature that is attained approaches 4000°K leads us again to the conclusion that the radiator is a body of luminous vapor. As nearly as one can predict from the data[4] available, all reactants and products within the bulb are in the vapor phase at the equivalent temperatures indicated by the radiation curves and the probable pressures existing during the flash.

[4] Landolt-Boernstein Tables (Julius Springer Verlagsbuchandlung, Berlin, 1923), Vol. 1; Int. Crit. Tab. 3 (1928).

PRODUCTS OF THE REACTION

The oxide residue within the bulb has been examined microscopically, and in all cases the form of the particles is spherical. Analysis by x-ray diffraction shows the particles to be aluminum oxide or aluminum-magnesium oxides, depending upon the character of the filling. The spherical shape of the products of combustion must be attributed to the fact that the particles form by condensation from the vapor.

CONCLUSION

Because the spectrum of the emitted light shows spectral line reversal, because the temperature attained in the flash is probably above the boiling point of all the products and reactants, and because the residue after the flash consists of spherical particles which appear to have condensed from the vapor, it is concluded that the radiant source is an incandescent vapor.

ACKNOWLEDGMENT

The author gratefully acknowledges the constant interest and advice throughout the course of this work of Dr. O. S. Duffendack, President and Director of Research of Philips Laboratories, Inc.

In addition, the author has profited by a discussion regarding the radiation process with Dr. J. G. Black, Professor H. B. G. Casimir, and Professor G. E. Uhlenbeck.

Infra-Red Filters and Cells of Unpolished Salt Crystals

J. J. McGovern
Koppers Company, Inc., Coal Products Analysis Fellowship, Mellon Institute, Pittsburgh, Pennsylvania

AND

R. A. Friedel
U. S. Bureau of Mines, Synthetic Liquid Fuels Research and Development Division, Pittsburgh, Pennsylvania

(Received May 1, 1947)

Transmission characteristics of NaCl and KBr plates, ground with various abrasives or etched by a solvent, have been investigated between 2 and 25 microns for use as infra-red filters and absorption cell windows. Low transmissions are obtainable with these plates in the high energy region of the blackbody maximum without appreciable decrease in their transparency at longer wave-lengths. Simple, dry grinding with the finer abrasives produces windows for absorption cells, which, in spite of visible scratches, are as transparent in the infra-red as windows tediously prepared on the usual pitch or cloth lap.

INTRODUCTION

IN infra-red work it is occasionally noticed that a salt window, which is visually fogged, still possesses some infra-red transmission. This observation suggested that such a window might serve as a filter for effectively reducing scattered light in a spectrometer. Also it was felt desirable to ascertain whether repolishing fogged cell windows is necessary.

It is well known that a relationship exists between the wave-length of the light incident on a matt surface and the amount of light reflected, refracted, or transmitted. If the particles of the matt surface are much larger than the wave-length of the incident light, namely, $\rho \gg \lambda$, then the transmission is very low as a result of refraction of the radiation within the particles or reflection from their surfaces. On the other hand, if $\lambda \gg \rho$, the energy losses are due mainly to Rayleigh scattering and true absorption. For transparent particles the transmission under these conditions will be high. A region of transition from low to high transmission is to be expected if the particle size is approximately equal to the wave-length of the incident light. Hence a filter dependent upon scattering for its effectiveness should possess a surface of particles roughly equal in size to the lower limit of the region to be transmitted.

The advantage of eliminating the higher intensity radiation from the region of the blackbody maximum, when working at longer wave-lengths, has received the attention of several investigators. Most of the work in the infra-red region has been carried out by Pfund,[1,2] Barnes,[3] and Plummer,[4] on filters for isolating the far infra-red. However, selenium[2,3] and various powders,[1,3] principally magnesium oxide, have been studied as filters for the near infra-red. Vaporized selenium layers display sufficiently sharp filter characteristics, but the ordinary backing used, a nitrocellulose film, possesses a spectrum. In addition, preparation of these films involves the usual tedious vacuum technique. Magnesium oxide films can be easily applied to a transparent backing material, but the powder itself absorbs

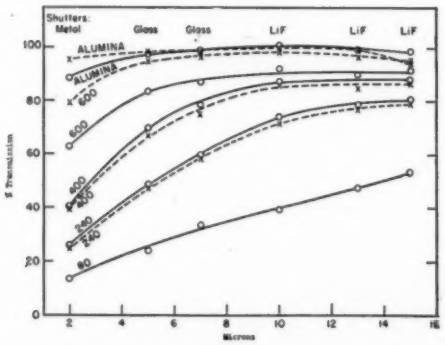

FIG. 1. Rocksalt filters; one side ground; grinding mesh indicated on curves; Globar source; ○—○ fine to coarse grit; ×—× coarse to fine grit.

[1] A. H. Pfund, Phys. Rev. **36**, 71 (1930).
[2] A. H. Pfund, J. Opt. Soc. Am. **23**, 375 (1933).
[3] R. B. Barnes and L. G. Bonner, J. Opt. Soc. Am. **26**, 428 (1936).
[4] J. H. Plummer, J. Opt. Soc. Am. **26**, 434 (1936).

radiation beyond ten microns. It was thought that a salt plate, which had been appropriately surface-ground, fogged, or etched, might prove to be a filter that would be both easily prepared and free of any additional absorbing material.

EXPERIMENTAL PROCEDURE AND RESULTS

A Perkin-Elmer infra-red spectrometer was used for most of this investigation. The instrument was equipped with the standard amplifier and recorder. Sodium chloride and potassium bromide prisms, and opaque, glass, lithium fluoride, and sodium chloride shutters were employed.

Surface-Ground NaCl Plates

Most of the filters were prepared by grinding the salt plates with various abrasives rather than by fogging or etching, because the former technique was thought to be more readily controlled. Two commercially polished rocksalt plates of identical size and transparency were chosen for sample and comparison blank. The sample specimen was ground on one side, first with powdered alumina, then, respectively, with 600, 400, 240, and 80-mesh Carborundum. The grinding operations were carried out manually on an ordinary sheet of paper lying on a desk top. The transparency of the sample after each grinding was compared with the polished blank at 2, 5, 7, 10, 13, and 15 microns. The results shown in Fig. 1 were obtained with a Globar source and shutters as indicated. The curves indicate a definite filtering effect, but the transmission cut-offs are not sharp because of heterogeneity of effective particle size produced by surface grinding. As might be expected, the over-all transparency of the filters varies inversely as the grit size used in grinding. Then, starting with 80-mesh Carborundum, the order of grinding was reversed and the transmission measurements repeated. The curves, with the exception of the one obtained with the 600-mesh material, agree quite well with the original traces. The lack of reproducibility in working with the finer grades of abrasives will be discussed later.

Filter characteristics of plates with both sides ground also were investigated. As shown in Fig. 2, grinding both sides of a plate with the various grades of abrasives resulted in decreased per-

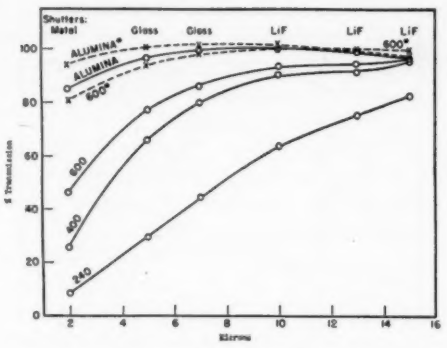

FIG. 2. Rocksalt filters; both sides ground; grinding mesh indicated on curves; Globar source; O—O normal grinding; X—X extended grinding.

centage transmissions at shorter wave-lengths, but did not appreciably affect the transmission at longer wave-lengths. It was noted, however, that continued grinding with the same portion of either 600-mesh Carborundum or alumina resulted in a general increase in transparency. The magnitude of this effect is probably due to a decrease in the effective particle size of the abrasive upon continued use. Grinding the two sides with different combinations of abrasives permitted, in the case of the coarser grades, the construction of filters with intermediate characteristics.

The effect of the nature of the source in the experiments dealing with both surfaces ground was also ascertained. Comparison of Fig. 3 with Fig. 2 indicates that the filter characteristics of the ground plates varied somewhat if a Nernst

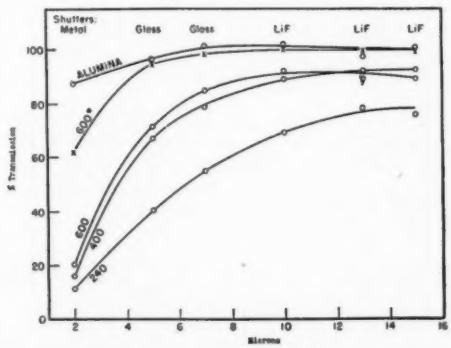

FIG. 3. Rocksalt filters; both sides ground; grinding mesh indicated on curves; Nernst glower source; O—O normal grinding; X—X extended grinding.

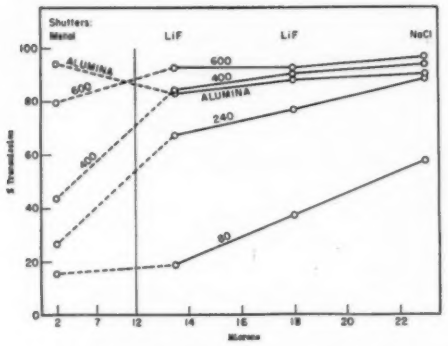

FIG. 4. Potassium bromide filters; both sides ground; grinding mesh indicated on curves; Globar source.

glower was substituted for a Globar. Curves obtained with the former source have greater slopes and hence indicate a better filtering action. A direct check on this finding was obtained by alternately comparing one specimen (one side, 400 mesh; other side, 600 mesh) with the two sources. The resulting curves were almost identical at longer wave-lengths, but at the blackbody maximum the relative transmission with the Globar was 39 percent compared to 20 percent with the glower.

Surface-Ground KBr Plates

Filtering out the intense, short wave-length radiation is especially desirable for measurements in the low energy KBr region. Accordingly, one of the KBr plates of a matched pair was ground and tested for transmission at 2, 13.5, 18, and 23 microns with a Globar as the source (Fig. 4). Appropriate shutters were used as indicated. As for the NaCl filters, grinding with various grades of Carborundum resulted in much lower transmissions in the high energy region at two microns than at the longer wave-lengths. Alumina grinding, however, produced a slightly higher transmission at two microns than at 13.5, probably because of strongly absorbing alumina particles[5] which become imbedded in the comparatively soft KBr surface.

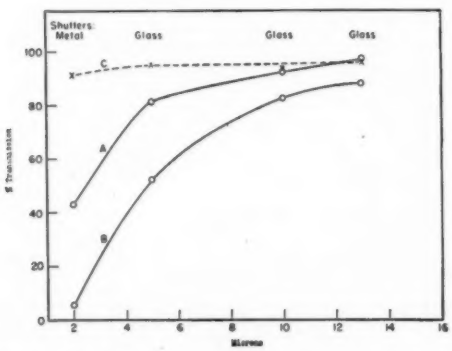

FIG. 5. Rocksalt filters; solvent etching by immersion in methanol: curve *A*, 3 minutes; curve *B*, 7 minutes; curve *C*, oil films on both sides of specimen *B*.

Solvent-Etched NaCl Plates

An additional series of tests was run to determine the effect of etching rocksalt with a solvent, using a Nernst glower as the source. Figure 5 shows that even after three minutes of immersion the plate still retained 93 percent of its original transparency at 10 microns. Immersion for four additional minutes in methanol resulted in a filter that passed only about 5 percent of the energy at the blackbody maximum but still transmitted 83 percent of the incident energy at 10 microns and 88 percent at 13 microns. The third curve in Fig. 5 is the result of an incidental experiment in which high transmission was regained by simply applying a thin film of mineral oil to the etched surfaces of the salt plate.

Absorption Cell Windows of Surface-Ground or Etched Plates

The high transmissions obtained for salt windows ground with dry alumina, or even 600 Carborundum, indicate that it is not necessary to lap infra-red absorption cell windows to a high visible polish. Elimination of this tedious operation, which is usually carried out on special pitch or cloth laps, represents a considerable saving in time, money, and patience.

Without extensive lapping of the windows, the absorption cell itself might serve as the filter for decreasing stray radiation. The four salt surfaces of the cell windows may be ground or etched in various ways so that the resulting combination will give the most advantageous filtering effect and still maintain high transmission at long wave-

[5] W. W. Coblentz, *Supplementary Investigation of Infra-red Spectra, Part V* (Carnegie Institution of Washington, Washington, D. C., 1908).

lengths. For example, a liquid cell with the two inner surfaces ground with alumina or 600 Carborundum, and the two outer surfaces ground with 400 Carborundum, should be satisfactory for many infra-red quantitative techniques. Other filters, even though mounted on transparent backing material, as magnesium oxide on rock-salt, cause energy losses of which an appreciable part is due to reflection from the salt surfaces themselves. Use of the absorption cell windows as filters would obviate such additional optical components.

A further advantage of these comparatively rough surfaces concerns the recalibration of liquid cells for quantitative work. Gradual fogging of a cell produces slightly decreasing transmission and therefore shifting calibration, which requires repeated checking. It is common practice to dismantle the cell eventually in order to repolish the inner surfaces, thus completely destroying the calibration. The present work would indicate that some initial fogging is even advantageous. Further, it is believed that if the surfaces are sufficiently roughened when the cell is originally assembled, water vapor in the air or moisture in the sample would have little further effect on the transmission of the cell. Hence, the time between recalibrations should be materially increased.

Further results on the solvent-etching of salt plates will be reported later. We wish to acknowledge the helpful suggestions of Dr. D. S. McKinney.

Erratum: On the Theory and Computation of an Aspherical Surface

[J. Opt. Soc. Am. **36**, 423 (1946).]

A. E. GLANCY
Research Laboratory, American Optical Company, Southbridge, Massachusetts

THE equation

$$L_2Q_2/L_1Q_1=(AP_3)_z/(AP_3)_{Az}$$

is in error.

Since the angular size of the object is also inversely proportional to the object distance AP_1, the corrected equation is:

$$L_2Q_2/L_1Q_1=\frac{(AP_3)_z}{(AP_3)_{Az}}\frac{(AP_1)_{Az}}{(AP_1)_z}.$$

Therefore

$$K_2L_2/K_2L_1=\frac{(AP_3)_z}{(AP_3)_{Az}}\frac{(AP_1)_{Az}}{(AP_1)_z},$$

where $(AP_3)/(AP_1)=-\sin\omega_1/\sin\omega_3$.

Subtracting unity from both sides of the equation, we find the condition for no coma for small objects on the axis is:

$$\text{Sph Ab}=K_2L_1\left[\left(\frac{\sin\omega_1}{\sin\omega_3}\right)_z\left(\frac{\sin\omega_3}{\sin\omega_1}\right)_{Az}-1\right].$$

When the spherical aberration is zero, the condition is identical with the sine condition:

$$\sin\omega_1/\sin\omega_3=\text{constant}.$$

When the object is at infinity, the condition reduces to

$$\text{Sph Ab}=\left(\frac{\kappa_1}{\sin\omega_3}\right)_z-\left(\frac{\kappa_1}{\sin\omega_3}\right)_{Az},$$

where κ_1 is the height of the initial ray.

In the spherical system the coma is a little larger than given in Table VIII; in the aspherical system the coma is practically as given in Table IX.

An Instrument for the Measurement of the Index of Refraction of Liquids in the Wave-Length Range 200 mμ to 1000 mμ

JAMES L. LAUER AND P. H. MILLER, JR.
Randal Morgan Laboratory of Physics, University of Pennsylvania, Philadelphia, Pennsylvania

(Received April 24, 1947)

An instrument which can be used from 200 mμ to 1000 mμ with transparent liquids for the determination of the refractive index, relative to air with an error of ±.0002 is described. A cell consisting of two quartz plates and an air space is rotated in the liquid through which is passing a parallel monochromatic beam of light, and the critical angle at the quartz air interface is determined. The instrument in its present form is particularly adapted for use with a Beckman Model DU quartz spectrophotometer. Results for water and *n*-hexane are given as examples.

INTRODUCTION

THE index of refraction of liquids is structure sensitive and its measurement can be used both as an analytical tool[1] and as an aid in the study of bond types.[2–4] Several devices for measurement of the index of refraction of liquids in the ultraviolet are described in the literature.[5–8] The device herein described is believed superior to methods involving hollow prisms because it is absolute, requires no calibration, and its inherent accuracy depends only on the precision with which an angle can be measured and the parallelism and monochromaticism of the light available. Our device was developed for use with a Beckman DU spectrophotometer, and the accuracy and precision of the measurements are believed to be about ±0.0002 in refractive index.

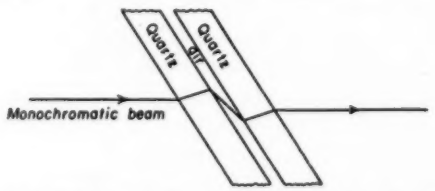

FIG. 1. Method. Turning the quartz-air sandwich slightly more in a clockwise direction will cut off the transmitted beam entirely since the critical angle will be exceeded.

APPARATUS

The basic principle of the instrument is illustrated in Fig. 1. A parallel monochromatic horizontal beam of light is allowed to transverse two plane parallel vertical quartz plates separated by a thin lead gasket. If this sandwich is rotated about a vertical axis the transmitted light intensity will drop rapidly as the critical angle between the quartz and air space is approached. This behavior which is illustrated in Fig. 2 is consistent with the Fresnel equations,[9] and in practice the knee of the curve can be determined to within 0.1 minute of arc. The critical angle, of course, depends only in the index of the liquid relative to that of the air between the quartz plates. A measurement of the index consists in determining the angle θ through which the sandwich must be rotated in going from one critical position to the other. The index n relative to air is given by

$$n = \csc\theta/2.$$

The lead gasket separating the quartz plates should not be too thick, for near the critical angle the oblique rays in the air space will strike the sides of the cell. On the other hand, if it is too thin, interference fringes and penetration through the barrier introduce disturbing effects. The former becomes important when the angular deviation ϵ, between the incident ray corresponding to the first fringe and the ray totally reflected

[1] See, for example, *International Critical Tables* (McGraw-Hill Book Company, New York, 1930), Vol. VII, pp. 1–109.
[2] H. Gilman, *Organic Chemistry—An Advanced Treatise* (John Wiley and Sons, Inc., New York, 1943), Vol. II, second edition, p. 381.
[3] N. Bauer and K. Fajans, *Physical Methods of Organic Chemistry*, ed. by B. Weissberger (Interscience Publications, New York, 1946), Vol. I, p. 653.
[4] An excellent résumé of the theoretical aspects was given by S. S. Kurtz and A. L. Ward, J. Frank. Inst. **224**, 583, 697 (1937).
[5] A. Goldet, Comptes rendus **207**, 1040 (1938).
[6] V. Holbro, Helv. Phys. Acta **10.6**, 431–454 (1937).
[7] M. Bayen, Comptes rendus **202**, 207 (1936).
[8] L. C. Martin, Trans. Opt. Soc. (England) **29**, 1–21 (1927–28).
[9] P. Drude, *Theory of Optics*, Trans. by C. R. Mann and R. A. Millikan (Longmans, Green, and Company, New York, 1939), p. 301.

at an angle α, becomes of order of magnitude of the experimental error. An elementary derivation gives $\epsilon=(\lambda^2\tan\alpha)/8t^2$ where t is the thickness of the air space and λ the wave-length of the incident light. The intensity of the light that has penetrated the barrier close to the critical angle falls to $1/e$ of its value before the barrier at a distance of $z=\lambda/2\pi(2\zeta\cot\alpha)^{\frac{1}{2}}$, where ζ is the small deviation from the critical angle α. This can be shown as follows. When the angle of incidence i exceeds the critical angle α, the transmitted beam becomes $1/e$ as intense as before at a distance $\lambda/2\pi(n^2\sin^2 i-1)^{\frac{1}{2}}$ from the boundary (reference 9, p. 299). If $i=\alpha+\zeta$ we can expand the sine function and, since ζ is small, neglect the squared term. With $\lambda\sim250$ mμ and $\zeta\sim10^{-4}$ radian, $z\sim3\mu$.

A good compromise was found in the 20μ lead foil used in packaging cigarettes. The details of the rotating sandwich and thermostated sample holder are shown in Fig. 3. Lead gaskets made from 5-amp. fuse wire were used to make the liquid holder tight and provide uniform mechanical pressure on all quartz plates. The gaskets were found to be tight to all hydrocarbons for a minimum of four hours.

The light emerging from the exit slit of the Beckman spectrophotometer was made plane parallel by reflection from a concave aluminized spherical surface of 20-cm radius of curvature and useful aperture of diameter 1 cm. The light was in turn reflected from a plane aluminized

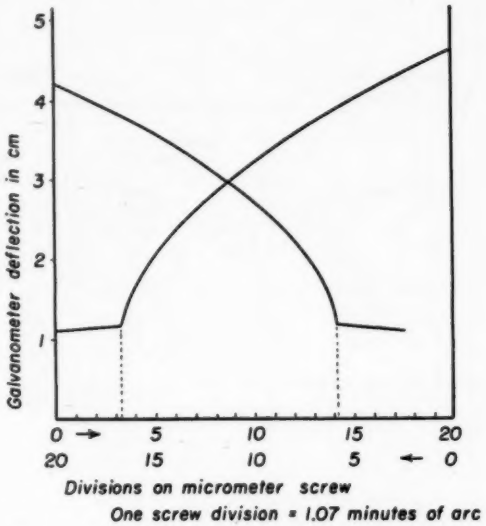

FIG. 2. A measurement of index. The critical angle is approached from both a clockwise (curve starting on the right) and a counter-clockwise (curve starting on the left) direction. The distance between the two ordinates drawn plus the angle through which the calibrating prism was turned is a measure of twice the critical angle.

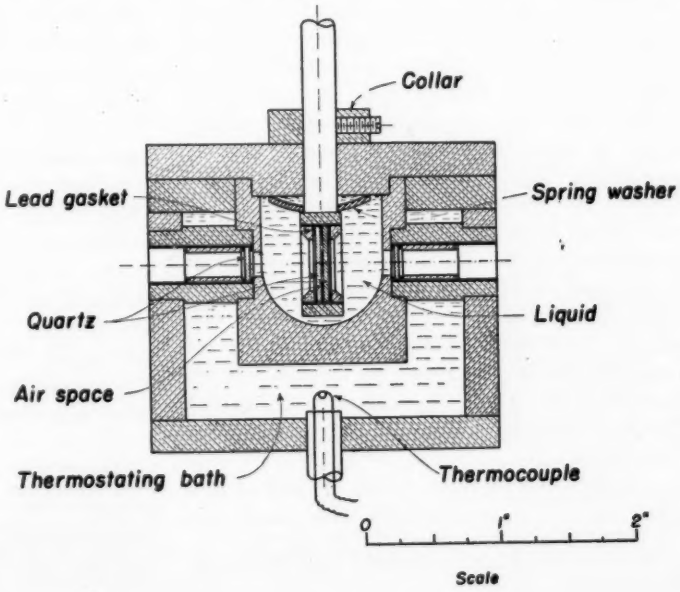

FIG. 3. Cross section through cell. The tight cover permits measurements on slightly volatile material without noticeable losses.

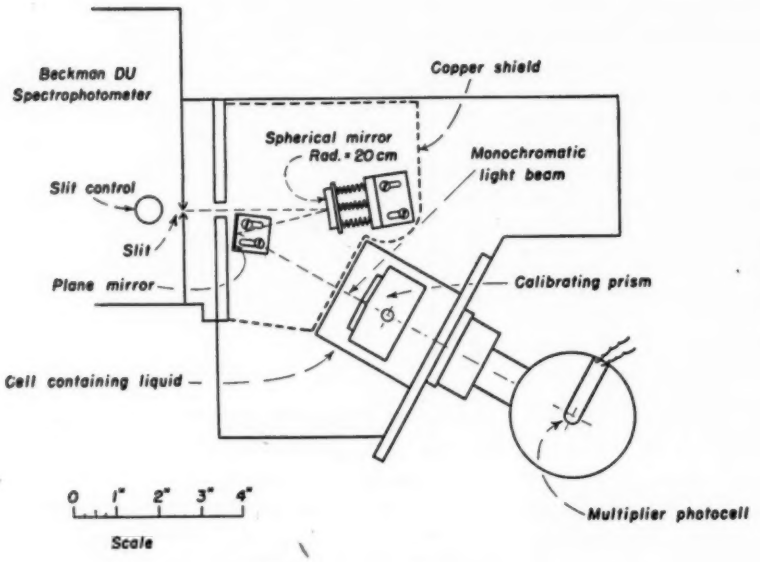

FIG. 4. Light path in the refractometer attachment. Either the housing containing the photo-multiplier or the housing containing the Beckman photo-cells can be screwed on to the plate behind the cell holder.

mirror through the sample holder and into the photo-cell (Fig. 4). Two errors are inherent in the optical system: lack of parallelism and monochromaticism in the final light beam. The latter is unimportant in liquids with a small dispersion, but becomes important near absorption bands. Even if infinitely narrow slits are employed, the straight slits and aberrations in the optical system of the Beckman DU spectrophotometer itself introduce a band width equivalent to that obtained from a .01-mm slit width.[10] Hence, if $dn/d\lambda$ of the liquid is larger than 3×10^{-5}, an uncertainty of more than 0.1 minute of arc in the critical angle is present. Lack of parallelism is introduced by finite exit slit width, vertical divergence because of slit height, and aberrations introduced by off-axis reflection from a spherical mirror. To be consistent with our 0.1 minute of arc, the slit must be narrower than 3×10^{-4} cm, its height <0.3 cm. By employing a spherical mirror of larger radius of curvature the requirements on the exit slit are less stringent and the aberrations reduced, but the light intensity in the parallel beam suffers correspondingly.

Actually, slit widths between .01 and .1 mm and 1-cm slit height were used. This contributes only a small error, since both experimental and theoretical work indicates[11] that when dispersive effects can be neglected the position of break in the intensity-angle curve (Fig. 2) is not shifted. The section to the low intensity side is no longer horizontal but is curved downward, the break becoming less sharp. There are additional factors which contribute to the variations in intensity with angle, but their angular dependence is always small in comparison with the variations in transmission near the critical angle. Stray light contributes a background whose angular dependence is small and which is symmetric with respect to the incident beam.

In order to use the minimum possible slit width 9 stage photo-multiplier tubes were used as detectors, a 1P28 in the ultraviolet and a 931 in the visible. The power supply which was regulated by VR tubes was operated at 105 volts per dynode. It was found possible to operate with a slit width of 0.1 mm from 240 mμ to 300 mμ and much narrower slits were used for longer wave-lengths. Measurements became diffi-

[10] H. H. Cary and A. O. Beckman, J. Opt. Soc. Am. 31, 682–689 (1941).

[11] Theoretically a sharp break is not obtained, only a point of inflection. The position of the apparent break for wider slit width is obtained by extrapolating both the curve some distance above and the curve some distance below the point of inflection until they meet. When this position is taken as the critical angle a much better value is obtained than by trying to use the point of inflection.

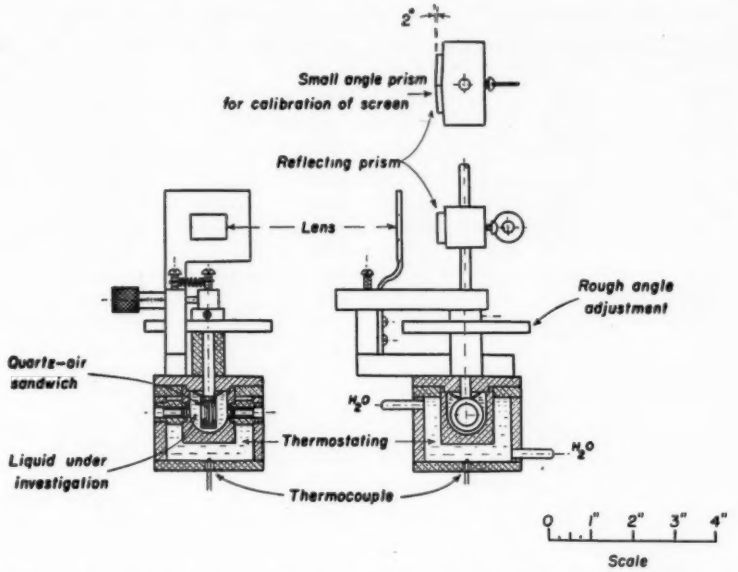

FIG. 5. Cross sections through sample holder and angle measuring attachments. Three reflecting prisms can be used interchangeably to cover a range of 2α from 70 to 140°. First the reflecting prism is set to bring an image of a thin wire into the middle of the scale (cf. Fig. 6) when the galvanometer indicates a critical position. Using the micrometer screw one of the curves of Fig. 2 is plotted. Next the micrometer screw is unlocked, and the rough angle adjustment is turned to bring the sandwich into the other critical position. The micrometer is thereupon locked in again, and the other curve of Fig. 2 is obtained.

cult when the absorption in the 2-cm light path is larger than 5–10 percent.

The sample holder was double walled and thermostated to ±0.2°C by means of the circulation of water maintained at constant temperature. The actual temperature was measured by means of the thermocouple shown in Figs. 3 and 5 to 0.01°C.

An optical lever was used to measure the angle through which the quartz-air sandwich was rotated. While somewhat cumbersome, an optical lever presents the least possible problems in mechanical design and is capable of very great accuracy. The optical arrangement is shown in Fig. 6. For each range of index two front-surfaced mirrors with an angle between their normals of approximately $2 \sin^{-1} 1/n$ were employed. Thus if one mirror reflected light near the center of the scale at one critical angle, then at the other critical position the other mirror

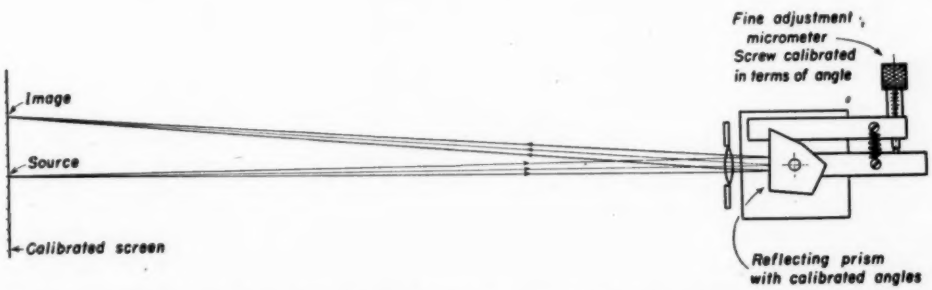

FIG. 6. Optical lever arrangement for measuring angles. The image on the screen gives one reference point. When the prism is turned so that an image is formed by the next face on the same spot, the sandwich has been turned through an angle supplementary to that between the prism faces.

TABLE I. Dispersion of water.

λ(A°)	n 20° (Holbro)	n 20° (Ducleaux)	n 20° (our)
2377	1.3845	1.3847	1.3845
2469	1.3789	1.3792	1.3788
2490	1.3778	1.3780	1.3775
2530	1.3757	1.3759	1.3758
2545	1.3750	1.3752	1.3750
2619	1.3716	1.3718	1.3714
2878	1.3622	1.3624	1.3622
2961	1.3599	1.3600	1.3599
3248	1.3534	1.3534	1.3533
3274	1.3529	1.3529	1.3527
3308	1.3523	1.3523	1.3522
3366	1.3513	1.3513	1.3513
3451	1.3500	1.3499	1.3500
3995	1.3433	1.3433	1.3432
4275	1.3409	1.3409	1.3408

would also form an image near the center of scale, and the scale readings would merely represent a correction term to the angle between the two mirrors which can be very accurately measured in a spectrometer. In practice the light flux transmitted by the sample holder was plotted against setting of the micrometer screw shown in Fig. 5. This screw which pressed against the mechanical arm provided a convenient means of imparting small rotations to the quartz-air sandwich. It in turn was calibrated by means of a special wedge consisting of two front-silvered mirrors with an angle of 2° between them and so arranged that two images were simultaneously formed on the scale.

In general each new liquid requires about two hours for the general preparation. This consists of assembling the quartz-air sandwich, the sample holder, adjusting the calibrating mirrors, etc. Each observation of the critical angle requires about 10 minutes, and the reduction of the observations about the same time.

TABLE II. Dispersion of *n*-hexane.

λ(A°)	n 20°	n 25°	n 14.7° (extrapolated)	n 14.7° (Voellmy)
2150	1.4629	1.4601	1.4657	1.4660
2200	1.4560	1.4532		
2250	1.4509	1.4471	1.4536	1.4536
2300	1.4462	1.4434		
2350	1.4420	1.4393	1.4447	1.4445
2400	1.4380	1.4353		
2450	1.4342	1.4315		
2500	1.4309	1.4282	1.4335	1.4336
2550	1.4276	1.4249		
2600	1.4250	1.4223		
2650	1.4225	1.4198		
2700	1.4200	1.4173	1.4226	1.4225
2750	1.4164	1.4137		
2800	1.4153	1.4126		
2850	1.4133	1.4106		
2900	1.4117	1.4090		
2950	1.4102	1.4075		
3000	1.4085	1.4058	1.4111	1.4110
3050	1.4070	1.4043		
3100	1.4056	1.4029		
3150	1 4040	1 4013		
3200	1.4029	1.4003	1.4055	1.4055
3500	1.3970	1.3945	1.3995	1.3996

RESULTS

Typical experimental results for water and hexane are shown in Tables I and II. The errors to be expected from the inherent limitations of the device are believed to be ±0.0002 in the value of the index of refraction. Comparison of our results on water with those of Holbro (reference 6) and those of Ducleaux and Jeantet,[12] and our results on hexane with those of Voellmy[13] indicate our estimate of errors is conservative.

Exact measurements on a number of very pure hydrocarbons are now in progress. The results of these determinations will be published elsewhere.

[12] Ducleaux and Jeantet, J. de phys. et rad. **5**, 92 (1924).
[13] Voellmy, Zeits. f. physik. Chemie **127**, 305 (1927).

Letters to the Editor

Metameric Formulation

ROBERT H. MORRIS
Color Control Department, Eastman Kodak Company, Rochester 4, New York
May 5, 1947

IN their recent paper[1] on optimum sensitivities for color reproduction, R. H. Bingham and H. Hoerlin have indicated the difficulty of formulating reflection or transmission curves which are spectrophotometrically different but colorimetrically equivalent.

A method which has been used with considerable success in this laboratory consists of finding such curves in the form of polynomials,

$$R=\sum_{k=0}^{n} a_k\lambda^k.$$

The tristimulus values of such a curve are given by

$$M=\sum_{k=0}^{n} a_k\int_0^{\infty} E\bar{m}\lambda^k d\lambda.$$

Substituting the desired tristimulus values and evaluating the integrals gives a set of three linear equations in the $n+1$ unknown a_k. This set may be augmented by imposing other conditions, such as defining points through which the curve must pass.

Figure 1 shows two curves which are metameric under Illuminant "*C*." Curve *A* is an actual curve obtained by means of a recording spectrophotometer; curve *B* is the cubic

$$R=44.1593-256.7322\lambda+488.1884\lambda^2-301.1956\lambda^3,$$

which was obtained from the above equations and the additional requirement that it pass through the point $\lambda=0.4\mu$, $R=0.3$.

The tristimulus values (Illuminant *C*) are as follows:

	X	*Y*	*Z*
Curve *A*	0.5872	0.5449	0.0943
Curve *B*	0.5879	0.5451	0.0943

If the number $(n+1)$ of terms taken is large, the determinant of the system becomes small, and special techniques must be used to obtain the solution. One such technique is described by M. Herzberger and the writer in a paper on least squares which is to be published in the *Quarterly of Applied Mathematics*.

[1] R. H. Bingham and H. Hoerlin, J. Opt. Soc. Am. **37**, 199 (1947).

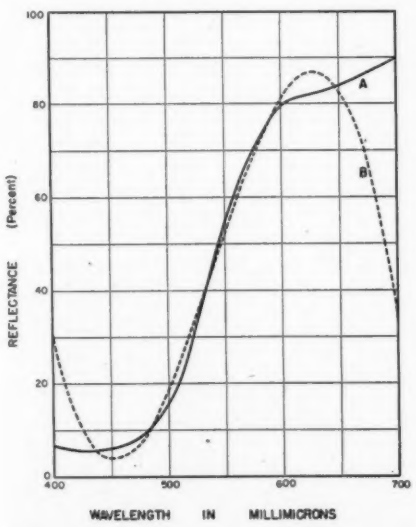

FIG. 1. Metameric reflectance curves. Curve *A*, actual spectrophotometer trace; curve *B*, polynomial reflectance curve.

On the Wright-Nelson Explanation of the Stiles-Crawford Effect

JOHN R. PLATT
Department of Physics, The University of Chicago, Chicago, Illinois
May 5, 1947

WITH the help of a model, O'Brien has recently discussed[1] the concentration of light in the outer segments of retinal cones which must follow from the Wright-Nelson explanation of the Stiles-Crawford effect.

This concentration is limited by the universal area-solid-angle relation for non-image-forming optical systems,

$$A\Omega=\text{constant},$$

which is a generalization of the Abbé sine condition.

Thus, in Fig. 1, if Ω is the average solid angle of reception by a retinal cone and *A* the entrance area, and if this flux is concentrated into tip area *a* and angle ω,

$$\Omega A=\omega a.$$

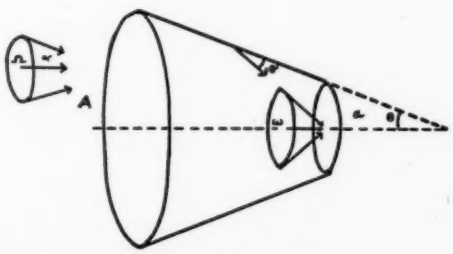

FIG. 1. Concentration of flux by a retinal cone.

Or, for solid angles much less than a hemisphere,

$$A \sin^2\alpha = a \sin^2(\theta+\theta'),$$

where α is the half-angle of the cone of reception, θ the half-angle of the retinal cone, and θ' the limiting grazing angle on the cone wall for total reflection.

$$\cos\theta' = n^*,$$

where n^* is the relative index of refraction of the surrounding medium.

Taking an average of the values used by O'Brien, $\theta = 5°$, $n^* = 0.97$, $a = 0.10$A, one derives $\theta' = 13°$ and

$$\sin\alpha = (a/A)^{\frac{1}{2}} \sin(\theta+\theta') = \sin 6°,$$

making the useful radius of the entrance pupil of the eye 1.7-mm for a 17-mm focal length. Judging from laboratory measurements on axially symmetrical non-image-forming receiving systems, this should represent approximately the radius at which the response falls to half-peak value. It is of the same order of magnitude as the half-peak-response pupil radius of 2.7 mm found experimentally for the Stiles-Crawford effect.[2]

Actually, since this experimental radius is known more accurately than any of the other parameters, the argument could well be reversed so as to compute some one of the poorly-known properties of the cones.

By a qualitative argument of a different kind, the order of magnitude of the polarization effect investigated by O'Brien may also be estimated. For a boundary between two media of relative index of refraction 0.97 the maximum difference between the perpendicular and parallel internal reflection coefficients at the most favorable angle is only 3 percent. Indeed the difference is appreciable only over a range of a very few degrees in angle of incidence. It follows that for an uncollimated beam striking a conical collector, an averaging effect will occur, and the difference in response to the two directions of polarization must become at least an order of magnitude smaller than 3 percent. This agrees with O'Brien's result on his model.

[1] J. Opt. Soc. Am. **37**, 275 (1947).
[2] See P. Moon and D. E. Spencer, J. Opt. Soc. Am. **34**, 319 (1944), for references.

Book Review

Applications of Germicidal, Erythemal and Infra-Red Energy

MATTHEW LUCKIESH. Pp. X+464. D. Van Nostrand Company, Inc., New York, 1946. Price $5.50.

This is a semi-technical book devoted primarily to the biological effects of radiation within the range of the sun's spectrum, with special emphasis upon the production of such effects by radiation from artificial sources. Following discussion of the spectral energy distribution of sunlight and skylight, the erythemal, tanning, and germicidal effects of ultraviolet radiation are discussed in some detail. Other topics covered include the fading of materials as a result of exposure to light, the relation of ultraviolet energy to plant life, the spectral energy distribution of commercial sources, the reflection and transmission properties of common materials, and the measurement of ultraviolet radiation.

The author stresses the importance of relating biological effects quantitatively to the energy and wave-length of the radiation giving rise to them. He includes many useful tables and graphs of quantitative data summarized from results obtained in his own laboratories and elsewhere.

The book stresses applications of particular commercial light sources, and, as a consequence, falls considerably short of being a general, comprehensive treatment of the biological effects of infra-red, visible, and ultraviolet radiation. Some unfortunate errors occur, as for example the reference to "microwatts of energy" on page 49. The list of references provided is neither comprehensive nor up-to-date. For example, the 1925 edition of *The Chemical Action of Ultraviolet Rays* is cited instead of the extensively revised 1941 edition.

While this book can hardly be regarded as an authoritative treatise, it includes considerable information which will be of interest to workers in the field with which it deals.

JOHN R. LOOFBOUROW
Massachusetts Institute of Technology